

UNCLASSIFIED

AD NUMBER

AD807479

LIMITATION CHANGES

TO:

Approved for public release; distribution is unlimited.

FROM:

Distribution authorized to U.S. Gov't. agencies and their contractors; Critical Technology; AUG 1966. Other requests shall be referred to Air Force Materials Laboratory, Attn: MAYA, Wright-Patterson AFB, OH 45433. This document contains export-controlled technical data.

AUTHORITY

AFSC ltr, 1 Jun 1972

THIS PAGE IS UNCLASSIFIED

THE EFFECTS OF ELECTRONIC STRUCTURE AND
INTERATOMIC BONDING ON THE SOFT X-RAY EMISSION
SPECTRA FROM ALUMINUM BINARY SYSTEMS

DAVID W. FISCHER and WILLIAM L. BAUN

TECHNICAL REPORT AFML-TR-66-191

AUGUST 1966

This document is subject to special export controls and each transmittal to foreign governments or foreign nationals may be made only with prior approval of Air Force Materials Laboratory (MAYA), Wright-Patterson Air Force Base, Ohio 45433.

AIR FORCE MATERIALS LABORATORY
RESEARCH AND TECHNOLOGY DIVISION
AIR FORCE SYSTEMS COMMAND
WRIGHT-PATTERSON AIR FORCE BASE, OHIO

NOTICES

When Government drawings, specifications, or other data are used for any purpose other than in connection with a definitely related Government procurement operation, the United States Government thereby incurs no responsibility nor any obligation whatsoever; and the fact that the Government may have formulated, furnished, or in any way supplied the said drawings, specifications, or other data, is not to be regarded by implication or otherwise as in any manner licensing the holder or any other person or corporation, or conveying any rights or permission to manufacture, use, or sell any patented invention that may in any way be related thereto.

Copies of this report should not be returned to the Research and Technology Division unless return is required by security considerations, contractual obligations, or notice on a specific document.

AFML-TR-66-191

**THE EFFECTS OF ELECTRONIC STRUCTURE AND
INTERATOMIC BONDING ON THE SOFT X-RAY EMISSION
SPECTRA FROM ALUMINUM BINARY SYSTEMS**

DAVID W. FISCHER and WILLIAM L. BAUN

This document is subject to special export controls and each transmittal to foreign governments or foreign nationals may be made only with prior approval of Air Force Materials Laboratory (MAYA), Wright-Patterson Air Force Base, Ohio 45433.

FOREWORD

This report was prepared by the Materials Physics Division. The work was initiated under Project No. 7367, "Research on Characterization and Properties of Materials," and Task No. 73702, "Physical and Chemical Methods for Material Analysis." This work was administered under the direction of the Air Force Materials Laboratory, Research and Technology Division, with D.W. Fischer and W.L. Baun acting as project engineers.

The work covered here was conducted between April 1965 and May 1966. The manuscript of this report was released by the authors June 1966 for publication as an RTD Technical Report.

This is intended as a final report summarizing data obtained from aluminum binary systems. Much of the data shown here have been or are about to be published and this report serves to consolidate the results for a better understanding of the overall influence of the bonding type on X-ray emission spectra.

The authors are grateful for measurements and specimen images made on the electron microbeam probe by Dr. Eugene White of the Pennsylvania State University.

This technical report has been reviewed and is approved.

Freeman F. Bentley
FREEMAN F. BENTLEY
Chief, Analytical Branch
Materials Physics Division
Air Force Materials Laboratory

ABSTRACT

Aluminum, magnesium and some transition metal soft X-ray emission bands from a series of aluminum binary alloys and other aluminum binary compounds were investigated using 6KV electron excitation and a flat crystal vacuum spectrometer. The overall shape of the valence electron emission band and its energy position as a function of alloy composition was determined. It appears from the data that the aluminum K band undergoes changes in shape and energy position which are dependent on the electronic configuration of the element with which the aluminum is chemically bonded. In the Al-Mg system the Al K band is not significantly changed for any composition. On the other hand, the group 1B metals (Cu, Ag and Au) cause the Al K band to split into two components. The energy separation and relative intensities of these split components are directly dependent on alloy composition. Such band changes are interpreted as indicating a change in the type of bonding between the metal atoms. In the Al-Ni system, for instance, the Al K band becomes more symmetrical and shifts to lower energy as the nickel content is increased, indicating that probably the bonding on the aluminum atoms is becoming less metallic and more covalent-like in nature as the nickel to aluminum ratio is increased. If the same atomic ratio of aluminum and another element is formed for each of the elements in a given period of the periodic table, it is found that the aluminum K band becomes lower in energy and somewhat more symmetrical in shape as we go from lower to higher atomic number in that period. Elements of the same sub-group appear to have virtually the same effect on the aluminum band but each different sub-group apparently has a different effect. The overall trend seems to indicate that the more electronegative the second component is, the greater effect it has on the aluminum spectrum.

The aluminum $K\alpha_4/K\alpha_3$ satellite line intensity ratio also varies in an orderly manner in aluminum binary compounds. In general, these satellite line changes go hand-in-hand with the K band changes. If the K band shifts to lower energy, the $K\alpha_4/K\alpha_3$ intensity ratio will always increase in value.

These orderly variations can be used not only to elucidate the valence band structure and the nature of the interatomic bond, but for analytical purposes as well. The satellite line intensity ratio and the shape and energy position of the emission band will identify the phase or phases present in a binary alloy and can also determine the exact composition of each phase without requiring the use of an internal standard.

TABLE OF CONTENTS

SECTION	PAGE
I INTRODUCTION	1
II EXPERIMENTAL PROCEDURE	2
III RESULTS	4
Aluminum-Magnesium System	4
Aluminum-Nickel System	5
Aluminum-Iron System	9
Alumirum-Copper and Related Systems	11
Aluminum-Titanium and Related Systems	14
IV CONCLUSIONS	15
V REFERENCES	19

ILLUSTRATIONS

FIGURE	PAGE
1. Aluminum K Emission Band FROM Pure Metal and Oxide (EDDT Crystal)	31
2. Aluminum $K\alpha'$, $K\alpha_3$ and $K\alpha_4$ Satellite Lines from Pure Metal and Oxide (EDDT Crystal)	32
3. Aluminum $K\alpha'$, $K\alpha_3$ and $K\alpha_4$ Satellite Lines from Al Metal as Dispersed with EDDT, PET and Quartz Crystals	33
4. Aluminum $K\alpha'$, $K\alpha_3$ and $K\alpha_4$ Satellite Lines from Al_2O_3 as Dispersed with EDDT, PET and Quartz Crystals	34
5. Magnesium K Emission Band from Pure Metal and Oxide (ADP Crystal)	35
6. Magnesium $K\alpha'$, $K\alpha_3$ and $K\alpha_4$ Satellite Lines from Pure Metal and Oxide (ADP Crystal)	36
7. Aluminum K Emission Band from Some Al-Mg Alloys (EDDT Crystal)	37
8. Aluminum $K\alpha'$, $K\alpha_3$ and $K\alpha_4$ Lines from Some Al-Mg Alloys (EDDT Crystal)	38
9. Magnesium K Emission Band from Some Al-Mg Alloys (ADP Crystal)	39
10. Magnesium $K\alpha'$, $K\alpha_3$ and $K\alpha_4$ Lines from Some Al-Mg Alloys (ADP Crystal)	40
11. Aluminum K Emission Band from Some Al-Ni Alloys (EDDT Crystal)	41
12. Al K Band Shift with Alloy Composition in Al-Ni System	42
13. Variation in Uncorrected Emission Edge Width for Al K Band in Al-Ni System	43
14. Variation in Uncorrected Half Band Width for Al K and NiL_{III} Bands in Al-Ni System	44
15. Change in Asymmetry Constants of Al K and NiL_{III} Bands with Alloy Composition in Al-Ni System	45
16. Aluminum $K\alpha'$, $K\alpha_3$ and $K\alpha_4$ Lines from Some Al-Ni Alloys (EDDT Crystal)	46
17. Variation in $Al K\alpha_4/K\alpha_3$ Intensity Ratio with Alloy Composition in Al-Ni System	47

ILLUSTRATIONS (Cont'd)

FIGURE	PAGE
18. Microprobe Scan Images of 85Al-15Ni Alloy; (A) Beam Current Image at About 500X, (B) Al K X-ray Scan, (C) Ni K X-ray Scan	48
19. NiL _{III} Emission Band from Some Al-Ni Alloys (Gypsum Crystal)	49
20. Aluminum K Emission Band from Some Al-Fe Alloys (EDDT Crystal)	50
21. Al K Band Shift with Alloy Composition in Al-Fe System	51
22. Variation in Uncorrected Half Band Width for Al K and FeL _{III} Bands in Al-Fe System	52
23. Change in Asymmetry Constants of Al K and FeL _{III} Bands with Alloy Composition in Al-Fe System	53
24. Aluminum K _{α'} , K _{α₃} and K _{α₄} Lines from Some Al-Fe Alloys (EDDT Crystal)	54
25. Variation in Al K _{α₄} /K _{α₃} Intensity Ratio with Alloy Composition in Al-Fe System	55
26. FeL _{II} and L _{III} Emission Bands from Fe, FeO and Fe ₂ O ₃ (Itaconic Acid Crystal)	56
27. FeL _{III} Emission Band from Fe, FeO and Fe ₂ O ₃ (Itaconic Acid Crystal)	57
28. FeL _{III} Emission Band from Some Al-Fe Alloys (Itaconic Acid Crystal)	58
29. FeL _{III} Band Shift with Alloy Composition in Al-Fe System	59
30. Aluminum K Emission Band from Some Al-Cu Alloys (EDDT Crystal)	60
31. Variations in Energy Difference Between High and Low Energy Components of Al K Band with Alloy Composition in Al-Cu System	61
32. Aluminum K Emission Band from 1:1 Atomic Ratios of Al-Cu, Al-Ag, and Al-Au (EDDT Crystal)	62
33. Aluminum K Emission Band from Some Al-Ag Alloys (EDDT Crystal)	63
34. Microprobe Scan Images of 50Al-50Ag Alloy; (a) Specimen Current Image ~ 500X, (b) Al K X-ray Scan, (c) Ag K X-ray Scan	64

ILLUSTRATIONS (Cont'd)

FIGURE	PAGE
35. Aluminum K Emission Band Shapes Obtained from One and Two Phase Regions of 50Al-50Ag Alloy	65
36. Magnesium K Emission Band from Some Mg-Cu Alloys (ADP Crystal)	66
37. Aluminum $K\alpha'$, $K\alpha_3$ and $K\alpha_4$ Lines from Some Al-Cu Alloys (EDDT Crystal)	67
38. Variation in Al $K\alpha_4/K\alpha_3$ Intensity Ratio with Alloy Composition in Al-Cu System	68
39. Copper L_{II} Emission Band from Metal and Oxides (NaAP Crystal)	69
40. Copper L_{II} Emission Band from Some Cu-Al Alloys (NaAP Crystal)	70
41. Copper L_{II} Band Shift with Alloy Composition in Cu-Al System	71
42. Aluminum K Emission Band from Some Al-Ti Alloys (EDDT Crystal)	72
43. Aluminum K Emission Band from Some Al-Zr Alloys (EDDT Crystal)	73
44. Aluminum $K\alpha'$, $K\alpha_3$ and $K\alpha_4$ Lines from Some Al-Zr Alloys (EDDT Crystal)	74
45. Portion of the Periodic Table Showing the Elements with Which We Have Formed Aluminum Binary Compounds for X-Ray Emission Studies	75
46. Aluminum K Emission Band From 1:1 Atomic Composition of Al-Mg and Al-Ca (EDDT Crystal)	76
47. Aluminum K Emission Band From 1:1 Atomic Composition of Al-Ti, Al-Zr and Al-Hf (EDDT Crystal)	77
48. Aluminum K Emission Band From 1:1 Atomic Compositions of Al-Fe, Al-Co and Al-Ni (EDDT Crystal)	78
49. Aluminum K Emission Band from AlP, AlAs and AlSb (EDDT Crystal)	79
50. Aluminum K Emission Band from Various Binary Systems Where Second Components Fall Progressively from Left to Right Side of Periodic Table (EDDT Crystal)	80
51. Relationship of Variation in Al K band Positions as a Function of Alloy Compositions for Several Binary Systems	81

ILLUSTRATIONS (Cont'd)

FIGURE	PAGE
52. Relationship of Variation in Al $K\alpha_4/K\alpha_3$ Intensity Ratio as a Function of Alloy Composition for Several Binary Systems	82
53. Interdependence of Al $K\alpha_4/K\alpha_3$ Intensity Ratio and Al K Band Energy Position in Aluminum Binary Compounds	83

TABLES

TABLE	PAGE
I Al K Band Measurements for Al-Mg Alloys	21
II Mg K Band Measurements for Al-Mg Alloys	21
III Aluminum and Magnesium $K\alpha_4/K\alpha_3$ Satellite Line Intensity Ratios for Al-Mg Alloys	22
IV Uncorrected Aluminum K Emission Characteristics in Al-Ni System	23
V Comparison of Al $K\alpha_4/K\alpha_3$ Intensity Ratio in the Al-Ni System Using Macro and Micro Area Excitation	24
VI Uncorrected NiL_{III} Emission Band Characteristics in Al-Ni System	24
VII Uncorrected Aluminum K Emission Characteristics in Al-Fe System	25
VIII Uncorrected FeL_{III} Emission Band Characteristics in Al-Fe System	26
IX Aluminum K Emission Characteristics in the Al-Cu System	27
X Uncorrected Aluminum K Emission Characteristics in Al-Ti System	28
XI Uncorrected Aluminum K Emission Characteristics for Some Aluminum Binary Compounds of Semi-Metals and Non-Metals not Previously Reported	29
XII Relationship of Al K Band Energy Position and Al $K\alpha_4/K\alpha_3$ Intensity Ratio to Elemental Subgroup of Second Component in Aluminum Binary Alloys.	30

SECTION I

INTRODUCTION

Although the investigation of soft X-ray emission band spectra of metals and alloys has been the subject of several previous investigations, little is really known of the effect of alloying on the electronic structure of metals. Recent publications by Appleton (Reference 1) and Thompson and Kellen (Reference 2) provide a review of most of the work done to date and the problems of interpreting the results. The reader, however, is left with the impression that little change is to be expected in the metal spectrum as a result of alloying. To be sure, this is what has been observed for most of the systems reported to date but we intend to show that there are also alloy systems in which both the band and line spectra undergo rather large changes.

An emission band such as the aluminum K band, is produced by electron transitions from the valence band to vacancy in an inner level. The shape of the band, when properly corrected for a variety of possible distortion effects, essentially reflects the average density of the electron cloud in the outermost occupied shell. Since the valence electrons are the ones most affected by chemical combination, the X-ray emission band should reflect vital information about the chemical bond. It is found that the character of the atomic interaction in compounds and alloys of aluminum has a substantial effect on the shape and position of the K emission band. Since it is the electronic structure of the atoms that determines interatomic bonding and also some of the physical and mechanical properties of the alloys, the X-ray emission band spectrum presents us with a possible method of characterizing this bonding and studying those properties which are dependent upon it.

A study of some aluminum binary alloy systems was chosen as the initial objective for a variety of reasons, not the least of which was the rather large changes which can occur in the Al K spectrum with a change in the chemical state. In addition, aluminum readily forms binary compounds with many different elements which can behave as either electron donors or electron acceptors. Also the Al K spectrum is in a wavelength region which is amenable to our experimental set-up. Fortunately the emission bands of many of the metals with which aluminum is alloyed fall in roughly the same wavelength region so that both components of the alloy can be studied simultaneously. Previously we have shown that the aluminum K spectrum, especially the K band and the $K\alpha_3$ and the $K\alpha_4$ satellite lines, change significantly between metal and oxide (Figures 1 and 2) (References 3 and 4) and other aluminum compounds (References 5 and 6) and that these changes can be grouped according to bonding type.

SECTION II

EXPERIMENTAL PROCEDURE

INSTRUMENTATION

The flat crystal vacuum spectrometer used for this study has been described previously (Reference 7). Characteristic soft X-ray emission spectra were produced by electron beam bombardment of the target material at 6kV and from 1 to 6 ma, depending on the target compositions. The dispersing crystals used depended on the particular emission band being investigated. EDDT (ethylene diamine d-tartrate, $2d=8.8030\text{\AA}$) was used for Al K; ADP (ammonium dihydrogen phosphate, $2d=10.639\text{\AA}$) was used for Mg K; Gypsum ($2d=15.207\text{\AA}$) was used for NiL; Itaconic Acid ($2d=18.498\text{\AA}$) was used for FeL. The detector was a flow proportional counter using an argon-methane (P-10) flow gas at reduced pressure (100 mm Hg). An anode accommodating four specimens was used so that spectra could be obtained under exactly the same conditions. Usual operating pressure was 10^{-6} Torr. All recording electronics including pulse-height analyzer were standard Picker equipment except for a low-noise preamplifier by Tennelec. The resultant ratemeter scans and the curves shown in the figures have a deviation of ± 2 percent.

SPECIMEN PREPARATION

Most of the alloys were prepared primarily by induction melting in an argon atmosphere. Some alloys were also prepared by arc melting in an argon atmosphere and/or by levitation melting. The X-ray diffraction patterns from any one alloy prepared by each technique proved to be identical. Also for many of the alloys, at compositions where stoichiometric compounds were formed, very fine powders were pressed into pellets and sintered. X-ray diffraction patterns were made for each alloy to check for the phase or phases present.

The specimens were usually mounted on the anode in the form of thin solid pellets or, in the case of the brittle alloys, finely powdered and spread in a thin layer on the anode surface. Four specimens were mounted at one time and, if the Al K spectrum was being studied, one of the specimens was the pure metal which was used as calibration standard. All of the band changes in the alloys, whether it be for Al, Mg, Ni, Fe, et cetera, were measured in reference to the pure metal spectrum.

CHOOSING CRYSTALS

The choice of a crystal for dispersing an emission line or band of a particular wavelength is an important aspect to consider in our experimental arrangement. We need a crystal which will provide adequate intensity on the one hand and the desired resolution on the other. Sometimes we are lucky enough to find a crystal which possesses both these qualities to a large extent and sometimes we are forced to make a compromise between the two or even abandon the attempt altogether. For the flat crystal optics which we use, the dispersion (or apparent resolution) is directly dependent on the angle at which the radiation is diffracted. The larger this angle, the better we are able to resolve two closely spaced lines and the better we are able to detect small energy shifts and band shape changes. In general, this requires that the line or band be diffracted at an angle of $130^\circ 2\theta$ or larger. This means, according to Bragg's Law, $n\lambda = 2d \sin \theta$, that we need a crystal whose $2d$ spacing is only slightly larger than some integral multiple of the wavelength of the line or band being investigated. Obviously, it would require a very large selection of crystals to be able to study all the emission bands in the soft X-ray region of interest (~ 10 to 100\AA) in this manner. For this reason there are many emission bands which we are unable to study with the required resolution.

It is also found that the crystal perfection and surface preparation play a large role in both intensity and resolution as we go to longer and longer wavelengths. For the aluminum K spectrum, for example, there are three crystals which disperse the emission lines at approximately the same 2θ angle. These crystals are EDDT (ethylene diamine d-tartrate), PET (pentaerythritol) and Quartz. The aluminum $K\alpha'$, $K\alpha_3$ and $K\alpha_4$ satellite lines from Al metal and Al_2O_3 as dispersed by our best examples of each crystal are shown in Figures 3 and 4. The amount of resolution afforded by each of the crystals is best observed by the amount of dip in the valley between the $K\alpha_3$ and $K\alpha_4$ lines. Recently the PET crystal was introduced commercially because it gives 2 to 3 times the intensity of EDDT which was previously the most popular crystal for this wavelength region. This increased intensity provides no real advantage for us, however, since the resolution provided by PET is not nearly as good as that of EDDT or quartz as can be seen in Figures 3 and 4. EDDT and quartz provide about the same resolution but EDDT gives much better intensity. For this reason the aluminum K lines and bands as shown in Figures 1 and 2 and throughout the rest of the report were obtained using an EDDT crystal. The Al K band, with this crystal, falls at about $130^\circ 2\theta$ and the $AlK\alpha_3$ and $K\alpha_4$ are at about $140^\circ 2\theta$. For these same reasons ADP was used for the magnesium K spectrum, gypsum for the nickel L spectrum and itaconic acid for the iron L spectrum. As of yet, however, we have not been able to find a crystal of the correct 2d spacing for dispersing the CuL_{III} band with high resolution for flat crystal optics.

SPECTRAL FEATURE MEASUREMENTS

Several types of band-shape measurements were made on each of the emission bands to aid in determining how the bands changed upon alloying. To avoid any confusion as to how these measurements were obtained, the following explanations are presented:

1. Half-Band Width; the full width of the band at one-half the maximum peak intensity above background.
2. Full-Band Width; the width at the base of the band from the beginning of the emission edge to the point where the low energy tail decreases to 5 percent of the maximum intensity above background. Using this rather arbitrary point on the low energy tail permits a more accurate comparison of band-width changes among the alloys since the tailing is rather extended and the limit difficult to pinpoint.
3. Edge Width; measured at the 5 percent and 95 percent points of the edge intensity.
4. Asymmetry Index; the ratio of the part of the full width at half maximum intensity lying to the long wavelength side of the maximum ordinate to the part on the short wavelength side.
5. Asymmetry Coefficient; the ratio of the low energy band slope at 5 percent and 95 percent of maximum intensity to the high energy edge width at the 5 percent and 95 percent points. This asymmetry factor gives a little better indication of the complete band shape than does the asymmetry index. For the Al K band from pure Al metal, for instance, the asymmetry coefficient is measured as 3.7 which indicates that the low energy side of the band is about four times as broad as the high energy side.

All of the values for these terms which are listed throughout the report for the different emission bands are in no way corrected for instrumental, temperature, or other broadening effects. They are simply the values measured for the as-recorded spectra and are, therefore, only relative values to be used in comparing band shapes. All of the bands are the result of two or more individual runs.

SECTION III

RESULTS

THE ALUMINUM-MAGNESIUM SYSTEM

General Discussion

Some recent results which have been published on the aluminum and magnesium L_{II, III} emission spectra from aluminum-magnesium alloys (Reference 8) do not correspond with the results obtained earlier on the K spectra from Al-Mg alloys (Reference 9). The L_{II, III} bands were shown to undergo a progressive change in shape with alloy composition but no significant changes in the band widths were observed. In contrast, Farineau showed Al and Mg K bands which progressively changed in width but which had virtually the same shape and width for any one alloy composition. K and L bands of these metals are not directly comparable in the sense that they represent different symmetry components but it is rather surprising that they show such different patterns of progressive change as the alloy composition is varied.

Some doubt has been cast on the results of Farineau not only because of the disagreement with the L spectra observations but also because they are consistent with the common valence band model (Reference 1) and results obtained from other alloy systems do not follow this model.

K Emission Bands

In terms of wavelength (or energy) shift and band shape change, the K emission band of both Al and Mg can be strongly affected by the state of chemical combination where the nature of the chemical bond is significantly affected. The largest change occurs when going from metal to oxide (References 3 and 7) as seen in Figures 1 and 5, but many other compounds also exhibit significant changes (Reference 5).

The K bands obtained for Al and Mg from the pure metals and some of the Al-Mg alloys are shown in Figures 7 and 9. Both bands are obtained with the same resolution and dispersion since the crystals used give the same rocking curves and the ADP crystal diffracts the Mg band at virtually the same 2θ angle at which EDDT diffracts the Al band. The curves shown in these figures are taken directly from ratemeter scans with no corrections applied to them. They almost surely do not represent the true band shapes, but, nevertheless, the changes which occur in them are assumed to represent real variations in band structure due to alloying.

Before pointing out these band variations, however, it should be noted that other parameters such as specimen self absorption and electron bombardment energies in excess of threshold potentials can also affect the shape of emission bands (Reference 10). All of the bands mentioned here were obtained at 6 KV so that the bombardment energy effect should be the same for all the alloys but the changing self absorption may be contributing in a small way to the changes in band shape.

The K bands from pure Al and pure Mg metals are quite similar in shape although the Mg band is much the narrower of the two. They have virtually the same asymmetry index and asymmetry coefficient. Upon alloying, the Mg K band becomes progressively broader and the Al K band becomes progressively narrower. The band measurements from the various alloys are listed in Tables I and II. In the last two columns of each table A_i represents the asymmetry index and A_c represents the asymmetry coefficient.

This broadening of the Mg band and narrowing of the Al band is, in essence, what was observed by Farineau (Reference 9) for the K bands but quite the opposite of what Appleton and Curry (Reference 8) show for the L_{II, III} bands. It should be pointed out, however, that we do not agree with Farineau on the shape of the Al K band from the pure Al metal. As mentioned previously (Reference 3) his metal target was probably contaminated with oxide.

Both Farineau and Appleton and Curry showed alloy results from only the two ordered compositions Al₃Mg₂ and Al₁₂Mg₁₇. Farineau showed that for both of these compositions the Al and Mg K bands had the same width and the same shape. We found the K bands from both constituents to have the same width in Al₃Mg₂ but not in Al₁₂Mg₁₇. The band shapes, however, were not found to be the same, having different half widths and asymmetry constants. Appleton and Curry, on the other hand, concluded that the Al and Mg L_{II, III} bands did not assume the same width or shape on alloying and that the shapes changed between pure metal and alloy but the widths did not. Apparently the Al and Mg K bands are affected in a different manner than the L_{II, III} bands when the two metals are alloyed.

Several two-phase alloys were also studied and the results listed in Tables I and II. The compositions listed are in atomic percent. The bands obtained from two-phase alloys are averages of the bands from each phase present. In the Al-Mg alloys the Al K band becomes progressively narrower as the Al content is decreased but the band shape remains the same. A few of these bands are shown in Figure 7. The Mg K band also retains the same general shape throughout the composition range but becomes broader as the Mg content is decreased as seen in Figure 9 and Table II. In our instrumental arrangement there is a lower limit in alloy composition for which we can obtain the K band with sufficient intensity for a good band profile without causing alloy decomposition. For the Al band in Al-Mg alloys this limit is about 10 atomic percent Al. For the Mg band it is about 40 atomic percent Mg.

The energy position of the intensity maximum for both the Al and Mg K bands remains virtually unchanged for all the alloys investigated.

K_α₃ & K_α₄ Satellite Lines

In studying the Al K spectrum from various Al compounds and alloy systems our observation has been that the change in the K_α₄/K_α₃ satellite line intensity ratio generally follows very closely the change in the shape and energy position of the K band (References 3, 4, 5, 6, 7, and 11). More limited observations on the Mg K spectrum suggests the same trend occurs in the Mg K_α₄/K_α₃ satellite line ratio. The largest change occurs when going from the metal to the oxide where this ratio goes from 0.48 to 0.92 for Al and from 0.58 to 1.03 for Mg as seen in Figures 2 and 6.

It is not surprising, therefore, in light of the small K band changes in the Al-Mg system to find that neither the Al K_α₄/K_α₃ nor the Mg K_α₄/K_α₃ intensity ratios change very much throughout the range of alloy compositions investigated as listed in Table III and shown in Figures 8 and 10.

THE ALUMINUM-NICKEL SYSTEM

General Discussion

Outside of the aluminum-magnesium system just discussed, there has been virtually no X-ray emission band studies made of aluminum alloy systems. Also, in most of the work that

has been done on any binary system, an effort has been made to study only the well characterized single-phase compositions. We, however, were also interested in looking at two-phase alloys and so, for the aluminum-nickel system, examined a series of alloys which differed in aluminum content in steps of about 5 atomic percent from pure aluminum down to 4Al-96Ni.

Recently, Nemnonov and Finkel'shtein (Reference 12) published the Al K band shapes from a few ordered Al-Ni alloys and Azaroff (Reference 13) and Das and Azaroff (Reference 14) reported on some nickel K absorption studies for some Al-Ni alloys and both came to the same general conclusion as we have concerning the aluminum-nickel bond as the alloy composition varies (Reference 11).

Aluminum K band

We have examined the Al K band from a large number of Al-Ni alloys, both one and two-phase structures. Figure 11 gives an indication of the changes which take place in the band as the aluminum content is varied. These curves are taken directly from rate-meter scans with no corrections applied to them.

One obvious change in the band is the shift of the intensity maximum to lower energy as the aluminum content is decreased. If one plots these energy positions as a function of alloy composition for the whole Al-Ni system a linear relationship such as seen in Figure 12 is obtained. Using an EDDT crystal, these maxima can be determined to within ± 0.1 ev. The measured positions are listed in Column 2 of Table IV.

It is also quite apparent that the shape of the K band changes considerably as the aluminum content changes. The factor contributing most to this change is the broadening of the emission edge. The uncorrected edge width is listed in the last Column of Table 4 and the variation is shown in Figure 13. This increased broadening makes the K band become more and more symmetrical about the intensity maximum as the aluminum content is decreased.

As the alloy composition varies so does the K band half width. The uncorrected values obtained are listed in Column 3 of Table IV. The band width at half-maximum intensity (half-band width) can be measured fairly accurately but the full-band width is subject to much more uncertainty because of the slow tailing off of the long wavelength side of the band. It appears, however, that the band width does not change significantly as the alloy composition is varied. In a previous report (Reference 11) we had stated that the Al K band appeared to become progressively narrower as the aluminum content decreased but a more careful study of the band indicates that this may not be true. If any narrowing does occur, it is very slight. The half-band width, however, does vary as shown in Figure 14.

This band shape change can be measured directly by the asymmetry index (A_i) and the asymmetry coefficient (A_c), the results of which are listed in Columns 5 and 6 of Table 4. A comparison of the manner in which both of these asymmetry constants vary with alloy composition in the Al-Ni system is shown in Figure 15. The asymmetry coefficient undergoes a smoother and larger variation than does the asymmetry index. In the pure aluminum metal the asymmetry coefficient of the K band is 3.7 which means that the low-energy side of the band is about four times as broad as the high-energy edge. This gives a little better indication of the band shape than the asymmetry index. In Al₂O₃ the Al K band becomes quite symmetrical with both the asymmetry index and asymmetry coefficient being equal to 1.0.

In the many different types of aluminum compounds which we have studied (References 3, 5, 6) it appears that the shape and position of the Al K band is closely allied to the type of chemical bond in which the aluminum atoms are involved. A more symmetrical band and a lower energy position is, in general, indicative of an increase in a covalent-like nature in the atomic

interaction. As can be seen in Figure 11 and as described above, our data shows that the Al K band from Al-Ni alloys becomes more symmetrical and shifts to lower energy as the Al content is decreased. The band is, in fact, tending toward the shape and position of the band obtained from aluminum oxide. Apparently in the Al-Ni alloys the electronic structure of aluminum is undergoing a pronounced change indicating that the chemical bonding of the aluminum atoms is becoming more covalent like in nature as the nickel to aluminum ratio is increased.

Nemnonov and Finkel'shtein (Reference 12) also noted that the Al K band from Al-Ni alloys occupies an intermediate position between pure Al and Al_2O_3 although their band shapes do not entirely agree with ours. The main difference is in the shape of the high energy edge for NiAl_3 and NiAl . This may be due to slightly better resolution on their part although we obtain a narrower half band width than they do. The difference could also arise from different alloy compositions or different methods of sample excitation.

As the alloy composition varies, therefore, the Al K band from Al-Ni alloys displays significant changes in energy position, half-band width, emission-edge breadth and asymmetry constants although the full band width remains virtually unchanged. This is an entirely different effect than was found in the Al-Mg alloys as mentioned earlier and reflects the different electronic structures and atomic interactions which take place in the two alloy systems.

Aluminum $\text{K}\alpha_3$ and $\text{K}\alpha_4$ Lines

Figure 16 shows the $\text{K}\alpha_4$ and $\text{K}\alpha_3$ lines obtained from a few of the alloys. As the aluminum content decreases, the intensity of $\text{K}\alpha_4$ increases with respect to $\text{K}\alpha_3$. If we make a plot of the $\text{AlK}\alpha_4/\text{K}\alpha_3$ intensity ratio versus atomic percent aluminum we obtain the linear relationship seen in Figure 17. From this, one would expect that, in the two-phase alloys, we are seeing an average aluminum content, due to the large beam size ($3/4'' \times 1/4''$). This fact was confirmed by using a microprobe beam, the results of which are listed in Table V and shown in Figure 18. A metallurgical mount was made of a few selected alloys. The single-phase alloys gave the same $\text{K}\alpha_4/\text{K}\alpha_3$ intensity ratio with both the macro area and micro area excitations. In a two-phase alloy, such as 85Al-15Ni, the microbeam probe could excite each phase selectively. Figure 18A is a beam current scan of this alloy at a magnification of about 500X. The dark areas are the Al_3Ni phase and the light areas the Al phase. It is found that each phase produces a different $\text{K}\alpha_4/\text{K}\alpha_3$ intensity ratio and that the area seen by the macro-size beam gives an average of the two ratios as seen in Figure 5. This satellite line intensity ratio is reproducible to within ± 1 percent and we have been able to use it as a quantitative tool for determining the aluminum content to within ± 2 percent (atomic) in the Al-Ni alloys. This technique may be compared to a measurement such as a lattice parameter determination in that once a curve such as that seen in Figure 17 has been obtained, it is not necessary to run standards with each sample. The $\text{K}\alpha_4/\text{K}\alpha_3$ values obtained for a series of the alloys are shown in Column 1 of Table IV. They were obtained simply by dividing the peak intensity of $\text{K}\alpha_4$ by the peak intensity of $\text{K}\alpha_3$ after correcting for background. Several of these alloys were run ten or more times and the results indicate the intensity ratios listed in Table IV have a deviation of no more than ± 0.01 .

$K\alpha_3$ and $K\alpha_4$ also shift slightly as the aluminum content is decreased. Between 100Al and 4Al-96Ni the shift is about 0.4ev to higher energy and appears to be fairly linear with composition for the entire system.

Here again, our results emphasize the fact that the changes in the $K\alpha_4/K\alpha_3$ intensity ratio go hand-in-hand with changes in the K band. As the band becomes more symmetrical and shifts to lower energies the $K\alpha_4/K\alpha_3$ ratio becomes larger and this inter-relationship appears to be quite linear.

Nickel L_{III} Band

There are two emission bands of interest in the nickel L spectrum, these being the L_{II} (or $L\beta_1$) and L_{III} (or $L\alpha$) bands at 14.280 and 14.571 Å, respectively for the pure metal (Reference 17). The largest shift observed for the L_{III} band was less than 0.20ev between Ni metal and the 10Ni-90Al alloy. The L_{III} band is about 5 times as intense as the L_{II} band in the metal and consequently our study was confined mainly to L_{III} because L_{II} was difficult to obtain with enough intensity for low nickel content in the alloys. In general, however, most of the changes discussed for the L_{III} band also apply to L_{II} .

Some of the experimental band shapes observed for NiL_{III} from Al-Ni alloys are shown in Figure 19. Here again, the curves are taken directly from rate-meter scans with no corrections applied to them. Liefeld and Chopra (References 10, 15, and 16) have shown that the shape of NiL_{III} from bulk samples is dependent to some extent on the electron beam potential and on sample self absorption. We therefore obtained all the Ni bands at the same beam potential (5KV) although the self-absorption effect, of course, changes as the alloy composition is varied. Accordingly, it must be realized that the changes observed in the L_{III} band may be due, in some small part, to this changing self absorption.

For the Al-Ni system the most obvious change in NiL_{III} occurs at the high-energy edge. As the nickel content is decreased the edge becomes broader and the intensity of the satellite band decreases considerably. The uncorrected edge width for a series of the alloys is listed in Table VI. This variation is shown in Figure 13 along with that observed for the Al K band edge. An interesting observation is that the two curves are practically mirror images of each other. As the nickel content is decreased the NiL_{III} edge broadens rather slowly down to about 60 percent nickel and then the broadening increases more noticeably as the nickel is further decreased. On the other hand, the Al K band edge increases appreciably as soon as alloying occurs and starts to level off as the aluminum content is further decreased. The net effect is that the average of the two edge widths remains fairly constant.

The NiL_{III} band width also varies with alloy composition. It is rather difficult to measure the full-band width because of the overlap of the satellite band but the half-band width can be measured rather accurately and its variation with composition is shown in Figure 14, again compared to that observed for the Al K band. Both bands display the same type of half-width variation. A rather interesting point is that the narrowest band measured for NiL_{III} is from the alloy with 60 atomic percent nickel while the narrowest band measured for Al K is at 60 atomic percent aluminum.

As with the Al K band there is also a change in the asymmetry index of the NiL_{III} band with alloy composition as can be seen in Figure 15. The measured values are given in Table VI. One difference in the two bands is that the NiL_{III} band has an asymmetry index of less than one

for low nickel concentrations. In other words, the high-energy halfwidth becomes larger than the low-energy halfwidth which we have never observed to happen for the Al K band. Because of the satellite interference, we were unable to obtain accurate asymmetry coefficients for the NiL_{III} band but this value also appears to become less than one for nickel concentrations below about 15 atomic percent.

These band changes also seem to indicate that as the aluminum to nickel ratio is increased in the alloy composition the chemical bonding on the nickel atoms tends to become more covalent-like in nature. From what was mentioned earlier concerning the Al K band, it appears that both components in the aluminum-nickel alloys show evidence of the intermetallic bonding taking on a certain amount of covalent-like character through the entire composition range.

THE ALUMINUM-IRON SYSTEM

General Discussion

One of the reasons we chose this particular system was our interest in comparing the results with those obtained from the Al-Ni system which were just discussed. In many respects, Fe is very similar to Ni; they have similar electronic structures, electronegativities, oxidation states, atomic and ionic radii, et cetera.

From our instrumental standpoint, we are able to study both the aluminum and iron emission bands and compare them to the aluminum and nickel emission bands from the Al-Ni system. Such comparisons should help elucidate the physical and/or chemical factors which determine the change in character of the interatomic bond in aluminum binary systems.

Several one- and two-phase Al-Fe alloys were prepared and studied and the results are presented here.

Aluminum K Band

The Al K bands obtained from a few of the Al-Fe alloys are shown in Figure 20. As with the other systems mentioned, these curves are taken directly from rate-meter scans with no corrections applied to them. If one compares these bands with those shown in Figure 11 for the Al-Ni system, a very strong similarity becomes apparent. In both the Al-Ni and Al-Fe systems, the Al K bands change in virtually the same manner as the alloy composition is varied. The rate of shift of the intensity maximum in the Al-Fe system, shown in Figure 21, has almost the same shape as that shown in Figure 12 for the Al-Ni system. The band shapes, too, are quite similar although the band widths are not.

For the Al-Fe system, then, the Al K band becomes more symmetrical and shifts to lower energy as the Al content is decreased. The result is a considerable broadening of the emission edge as a function of alloy composition. Column 2 of Table VII contains the energy position values for the band intensity maximum.

As the alloy composition varies, so does the Al K band half width and base width. The uncorrected values obtained for these terms are listed in Columns 3 and 4 of Table VII. Figure 22 illustrates the manner in which the half band width varies. Immediately upon alloying, the half width becomes narrower until the Fe_2Al_5 composition is reached, at which

point it starts becoming broader. This is quite different from what was observed to happen in the Al-Ni system (Figure 14). The full band width is more difficult to measure accurately because of the extended low energy tailing but it appears to be slightly smaller for the alloys than for the pure Al metal. A similar observation was noted in the Al-Ni system.

The Al K band shape change can be measured directly by the asymmetry index (A_f) and the asymmetry coefficient (A_c), the results of which are listed in Columns 5 and 6 of Table VII. A comparison of the manner in which both of these asymmetry constants vary with alloy composition in the Al-Fe system is shown in Figure 23. Both terms undergo much the same variation.

It appears, therefore, that in many ways the Al K band from the Al-Fe system is quite similar to that obtained from the Al-Ni system. The band shape and energy position tends toward the shape and position of the band obtained from the oxide, as the iron to aluminum ratio is increased. This shows that the nature of the interatomic bonding on the aluminum atoms is undergoing a pronounced change, probably due to an increase in covalent-like nature as the aluminum content is decreased.

Aluminum $K\alpha_3$ and $K\alpha_4$ Lines

The $K\alpha_3$ and $K\alpha_4$ satellite lines from a few of the Al-Fe alloys are shown in Figure 24. As the aluminum content decreases, the intensity of $K\alpha_4$ increases with respect to $K\alpha_3$. If one makes a plot of the $AlK\alpha_4/K\alpha_3$ intensity ratio versus alloy composition, a linear relationship such as seen in Figure 25 is obtained. Again, if we compare these results with those obtained from the Al-Ni system (Figures 16 and 17), we find that the two are almost identical. In both systems this satellite line intensity ratio is quite reproducible and can be used as a quantitative analysis tool. The values obtained for the Al-Fe alloys studied are listed in Column 1 of Table VII.

Both $K\alpha_3$ and $K\alpha_4$ shift slightly to higher energy as the aluminum content is decreased and this shift appears to be fairly linear with alloy composition. Once again, we would like to emphasize the fact that the satellite line intensity ratio variation goes hand-in-hand with the changes in the K band.

Iron L_{III} Band

In the iron L emission spectrum, there are two bands of interest to us, these being the L_{II} ($3d4s \rightarrow 2p1/2$) and L_{III} ($3d4s \rightarrow 2p3/2$). Our study was confined mainly to the L_{III} band because in the Al-Fe alloys the L_{II} band is quite weak and difficult to obtain a good band profile for when the iron content is below about 50 percent. When going from the metal to either of the oxides, the FeL_{III} band does change somewhat in shape and energy position as shown in Figure 27 but the change is not nearly as large as that observed for the Al K band when going from metal to oxide (Figure 1). The main effect that oxidation has on the FeL bands is shown in Figure 26. As we go from Fe to FeO to Fe_2O_3 the L_{II} band becomes more intense in relation to L_{III} (Reference 17). The L_{II}/L_{III} intensity ratio for these three materials is 0.12, 0.63, and 0.43 respectively.

The experimental band shapes obtained for Fe metal and a couple of the Al-Fe alloys are shown in Figure 28. These bands were all obtained at 5KV beam potential with no corrections applied to them, either instrumental or otherwise (References 15 and 16).

If one compares Figures 28 and 19 it can be seen that the L_{III} bands from the pure metals are quite similar in shape. They have virtually the same band widths, edge widths, and asymmetry constants. With this in mind and remembering that both Fe and Ni have the same effect on the Al K band in the Al-Fe and Al-Ni alloys, it would seem that one should expect the FeL_{III} band in the Al-Fe alloys to change in the same manner as the NiL_{III} band in the Al-Ni alloys. Well, this may be what we would expect but it sure isn't what we find. For the Al-Ni system we observed that the NiL_{III} band becomes more and more symmetrical as the nickel content is decreased and that the emission edge appears to be lost (Table VI). The FeL_{III} band, however, does not appear to change in this manner.

As the iron content is decreased in the Al-Fe system, the FeL_{III} emission edge does not become very much broader. This fact shows up in the asymmetry index and asymmetry coefficient measurements, as listed in Columns 4 and 5 of Table VIII. This is also shown graphically in Figure 23. Neither A_i nor A_c change very much for the FeL_{III} band throughout the composition range as compared to what happens for the Al K band. Even in the 95Al-5Fe alloy, the FeL_{III} edge is just as sharp as it is in the 25Al-75Fe alloy.

The energy position of the band, however, does change as shown in Figure 29 and listed in Column 1 of Table VIII. The shift does not appear to be as linear as that observed for the Al K band (Figure 21) but it is much larger than the shift observed for the NiL_{III} band in the Al-Ni alloys.

The FeL_{III} band width also varies with alloy composition as listed in Column 3 of Table VIII. As the iron content is decreased, the base width becomes smaller and appears to level off at 6.3ev at about 35 percent (atomic) iron. According to our data, then both the Al K and FeL_{III} band widths decrease on alloying in the Al-Fe system.

As the alloy composition varied, the half-band width also changes. This change is shown in Figure 22 and listed in Table VIII. From Figure 22 it can be seen that the half-width of both the Al K and FeL_{III} bands vary in much the same manner. Both bands show their narrowest half-width at the Fe_2Al_5 composition.

It was mentioned earlier that the $FeL_{II} L_{III}$ intensity ratio increased considerably when going from the metal to either of the oxides. In the Al-Fe system this ratio remains constant at 0.12, the same as obtained from the pure iron metal.

From the changes which occur in both the Al K and FeL_{III} bands in the Al-Fe system, it appears that the nature of the interatomic bond is changing with alloy composition. As was mentioned earlier for the Al K band, the predominantly metallic bond seems to be taking on a certain amount of covalent-like character as the alloy composition is varied.

ALUMINUM-COPPER AND RELATED SYSTEMS

This particular system was chosen primarily because of the unusual effect which copper (and other group 1B metals) has on the aluminum K emission band. The copper L emission band also behaves much differently than the other transition metal L bands from aluminum-transition metal binary systems.

Aluminum K Band

The Al K band from pure aluminum and some Al-Cu alloys is shown in Figure 30. The most obvious effect of alloying is the splitting of the band into two components. This is an entirely different effect than what was observed in the Al-Mg, Al-Ni and Al-Fe systems discussed in the preceding sections. The high energy component remains in approximately the same position throughout the entire composition range but the low energy component becomes more prominent and shifts to lower energies as more and more copper is added. In addition, as shown in Table IX, the uncorrected edge width remains virtually unchanged for any composition. Also, the band width is nearly constant over the entire composition range despite the band splitting. These are essentially the same results shown by Yoshida (Reference 19) in 1936 and Farineau (Reference 20) in 1939. However, in Yoshida's work, intensities were low and for Al concentrations below about 30 percent it was assumed that the short wavelength edge remained the same. The absolute energy positions of K band components are considerably different in this work compared to the curves shown by Yoshida. For instance, his low energy component in the 50-50 alloy is at about 1550ev and we report it as being at 1554.5ev. It is interesting that the shape of Yoshida's Al K band for pure Al is correct but is seldom referred to. Rather a doubled K band for pure Al as recorded by Farineau (References 9 and 20) was used as the standard band shape for years until the correct one was shown in a review by Shaw (Reference 21) in 1956. The present authors showed that Farineau's curve was a composite curve from the metal and oxide (Reference 3). Farineau (Reference 20), in addition to presenting an incorrect K band shape for Al, also shows a triplet at approximately Al_2Cu , with which we do not agree. It is likely that some of Farineau's high Al alloys also contained oxide.

Figure 31 is a plot of the energy difference between the high and low energy components of the Al K band with alloy composition in the Al-Cu system. The change in energy between the two components is nearly linear. The energy difference for a given composition is a constant and may be used in the same way that a lattice parameter is used to determine composition of an unknown alloy. This energy difference constant has the advantage that the sample need not be stress free and perfectly crystallized in order to make measurements. In a diffusion couple of Al and Cu for instance, the identity of each phase in the reaction zone could be determined using the electron microprobe. Perhaps it would even be possible to study and prove composition and structure changes at grain boundaries.

The curve of Figure 31 extrapolates to about 4.5ev for very dilute alloys (10% Al). This is an interesting result in light of calculations made by Friedel (Reference 22) based on a model having an Al atom dissolved in Cu as an Al^+ ion plus one Fermi electron having the same energy and density of states as in copper, but with an s component repelled and p, d components attracted around the Al atoms. Friedel shown that the electron which fills the positive hole during emission may come from (a) the conduction band, (b) the 3p state, or (c) the $3s^2$ shell. Transition (a) gives a strong peak superimposed at the emission edge, and (c) gives a stronger emission band shifted toward longer wavelengths by an amount equal to the excitation energy of $3s^2 \rightarrow 3s3p$ in Al^+ . This computed value by Friedel for this displacement is 4.6ev.

Because of this unusual behavior of the K band it would be desirable to observe the Al L band in Al-Cu alloys. The Al L band is beyond our wavelength capabilities, but it has been obtained by Skinner and Johnston (Reference 23). Unfortunately, their results are nearly inconclusive and cannot be compared to the K band because the Cu M band overlaps the short wavelength portions of the Al L band. However, in an alloy they list as "about 25% Al", the band is sufficiently clear to indicate that the Al L band still maintains the short wavelength edge and probably there is no doubling.

We find that the K emission band from other polyvalent elements also becomes doubled when these elements are alloyed with monovalent elements. In addition to Cu-Al we have investigated alloys of the following systems: Cu-Mg, Cu-Si, Ag-Mg, Ag-Al, Au-Al and Au-Be. The K band from each polyvalent element was doubled. In the Ag-Al system, for instance, the Al K band appears very similar to that obtained from the Cu-Al systems as seen in Figure 33. The high energy edge is retained; the band is split into two components and the low energy component shifts approximately the same amount as in the Cu-Al system. Both bands, however, are shifted almost 1ev to lower energies compared to the Cu-Al system as evident in Figure 32 where the Al K bands from 1:1 alloys of Cu-Al, Ag-Al, Ag-Al are shown. In the Au-Al alloys the high energy component occurs at the same energy as in Cu-Al, but the low energy component has shifted farther. In addition, the linear shift of the high energy component seen in Cu-Al alloys (Figure 31) does not occur in Au-Al alloys. It appears that for the same atomic composition, the low energy component of the split Al K band becomes stronger with increasing atomic number of the monovalent element.

We can show that in multi-phase Al-Cu, Al-Ag and Al-Au alloys, the Al K band shape can be used to identify the phases present. An example of this technique is shown in Figures 34 and 35. The 50Al-50Ag alloy is two-phase as seen in the microprobe images of Figure 34. In picture A the light regions are the Al rich phase and the dark regions are the Ag rich phase. The Al K band shape obtained from each phase is shown at the left side of Figure 35. If the beam size is enlarged so that both phases are excited simultaneously, the band shape on the right side of Figure 35 is obtained, which is a composite of the band shapes from the individual phases.

Doubling of the K band has been observed in many other alloys including the Al K band from alloys having more than two components such as CuNiAl and CuMgAl. The Mg K band is doubled in Mg-Cu alloys as shown in Figure 36 but the separation between bands does not appear to change predictably with composition. For instance, ΔE for Mg_2Cu is 3.48ev and for $MgCu_2$ it is 3.69ev which is not very much of a shift considering the large composition change. The Si K band splits into two components in the Cu-Si system but measurements on energy separation were not made because of poor spectral dispersion in the region in which it was diffracted. Emission band doubling has also been observed in spectra of higher atomic number elements. The Zn K band in Cu-Zn alloys behaves almost identically to the Al K band in Cu-Al alloys (Reference 23). The Zn K band doubles and the low energy component becomes dominant in the dilute alloys.

However, it appears that K band doubling may not be universal among polyvalent elements dissolved in monovalent elements. We have prepared a number of Cu-Be alloys and have not observed any band splitting in the Be K band. Skinner and Johnston (Reference 23) have reported doubling or tripling but only in very dilute alloys. One of the band components which they show for these dilute alloys occurs at the oxide position and may be due to oxide contamination. We do observe doubling in the Be K band from Au-Be alloys, however, and the low energy component occurs at the same energy position as BeK from BeO. We know that oxide is not present in our Au-Be alloys because we also scan routinely over the oxygen K region using a KAP crystal. Possibly then, the band does not split in the Cu-Be alloys except in the very dilute concentrations of Be.

The aluminum K emission band data for pure Al and eleven Cu-Al alloys are summarized in Table IX.

Aluminum $K\alpha_3$ and $K\alpha_4$ Satellite Lines

These satellite lines from a few of the Al-Cu alloys are shown in Figure 37. Here again we find that, just as in the Al-Mg, Al-Ni and Al-Fe systems, the $K\alpha_4/K\alpha_3$ intensity ratio is a

linear function of alloy composition and the relationship is shown in Figure 38. The values for these ratios from the different Al-Cu alloys investigated are listed in Table IX.

Copper L_{II} Band

Normally one would prefer to study the CuL_{III} band instead of the L_{II} , mainly from the standpoint of the much higher emission intensity of the L_{III} band. Unfortunately, though, we were unable to find a crystal with the correct 2d spacing to obtain the CuL_{III} band with the resolution we desire. The best we could do therefore, was use a second order reflection from a sodium acid phthalate crystal (NaAP; 2d=26.414 \AA). The interplanar spacing of this crystal is such that we can obtain the CuL_{II} band with very good resolution but the CuL_{III} band is too long in wavelength to obtain the second order reflection. This doesn't matter too much since the results obtained for the L_{II} band should apply equally as well to the L_{III} band.

There is not very much of a change in the CuL_{II} band when going from pure Cu to CuO or Cu_2O as seen in Figure 39. The major change is in the intensity of the overlapping high energy satellite bands. A very slight shift to lower energy occurs in the intensity maximum which is just the opposite of the direction of shift observed in the L_{II} and L_{III} bands from Ni, Co, Fe and the other transition metals when going from pure element to oxide.

The CuL_{II} band from Cu metal and some Cu-Al alloys is shown in Figure 40. As the copper content in the alloys is decreased, the satellites become a little more prominent and the band itself shifts slightly to lower energy. Here again the direction of shift is just the opposite of that observed for NiL_{III} from Al-Ni alloys or FeL_{III} from Al-Fe alloys and shows the effect of the filled 3d level in copper. We find that the energy shift of CuL_{II} is linear with alloy composition in the Cu-Al system as shown in Figure 41.

Because of the overlapping satellite structure we were unable to determine whether or not alloying causes changes in the CuL_{II} band shape or band width. Certainly we do not observe any band splitting as reported by Farineau for the CuL_{III} band in the Cu-Al alloys (Reference 20).

ALUMINUM-TITANIUM AND RELATED SYSTEMS

Aluminum K Band

Binary alloys of aluminum with titanium, zirconium or hafnium (group 4B metals) produce an Al K band which is narrower in half-width than that from any other aluminum systems which we have investigated. The experimental band shapes from a few of these alloys are shown in Figures 42 and 43. Only four different Al-Ti compositions were investigated but the results indicate that the asymmetrical shape of the Al K band is retained in the alloys as listed in the last two columns of Table X. The band shifts in energy as a linear function of alloy composition, the amount of shift being between that observed for the Al-Mg and Al-Ni systems (Figure 51).

The half width of 3.5ev for the 50-50 alloys of Al-Ti and Al-Zr represent by far the narrowest Al K bands obtained from any aluminum compounds which we have studied. Apparently the full band width becomes continually narrower as the aluminum content is decreased but not as much as in the Al-Mg system (Tables I and X). The band shapes and energy positions from the Al-Zr and Al-Hf alloys are virtually the same as those obtained from the Al-Ti alloys.

Aluminum $K\alpha_3$ and $K\alpha_4$ Lines

As was found for the other aluminum binary systems discussed previously, the $AlK\alpha_3$ and $K\alpha_4$ satellite lines from Al-Ti, Al-Zr and Al-Hf change in an orderly manner as the alloy composition is varied. As seen in Figure 44 the $K\alpha_4/K\alpha_3$ intensity ratio increases as the aluminum content is decreased. This change is linear with alloy composition and the rate of change is between that observed for the Al-Mg and Al-Ni systems (Figure 52).

Both the $K\alpha_3$ and $K\alpha_4$ lines shift to higher energy as the aluminum content is decreased.

SECTION IV CONCLUSIONS

There are several important conclusions which can be drawn from the results shown here. First of all, it is obvious from the changes which occur in the Al K emission band, that the electronic structure of aluminum is changed, sometimes in a very pronounced manner when the chemical environment of the aluminum atoms is altered. It is also evident that the nature of the interatomic interaction changes not only for each different aluminum binary system, but with varying composition within any one system as well. We have shown that this change in the character of the bond can have one or more of the following effects on the aluminum K X-ray emission spectrum:

1. a change in energy position of lines or bands
2. a change in shape of lines or bands
3. a change in the relative intensities of lines or bands
4. the appearance or disappearance of lines or bands

This, of course, raises questions as to why the spectral changes occur and whether or not these changes can be interpreted in such a way as to indicate just how the electronic structure of aluminum is altered when the aluminum atoms interact with other non-aluminum atoms. We have shown in this report, for instance, that the Al K band from Al-Mg alloys (Figure 7) is different from what is observed from the Al-Ni alloys (Figure 11) and that both, in turn, are different from what is obtained from the Al-Cu alloys (Figure 30). We now intend to show that these variations for the different binary systems can be sorted out into a rather simple systematic order. To do this we start, not surprisingly, with the periodic table of the elements. Figure 45 is a portion of the periodic table showing which elements we have combined with aluminum in binary compounds for X-ray emission studies, some of which were reported previously (References 3, 4, 5 and 6).

Figures 46 to 49 give an indication of what we find if we compare the results of binaries in which the second components belong to the same subgroup. Earlier we showed that the Al K band from the Al-Mg alloys does not shift much with a large change in alloy composition (Figure 7). The same relationship is found for Al-Ca alloys and the fact that the Al K band shape and energy position is the same for both systems is shown in Figure 46. Metals of subgroup 4B (Ti, Zr and Hf) have the same effect on the Al K band, also, as shown in Figure 47. Figure 48 shows the results obtained from the 1:1 atomic ratios of aluminum with Fe, Co and Ni. The shape of the Al K band edge is a little different for the Al-Fe, Al-Co and Al-Ni systems but the energy positions are at the same places. Perhaps the most striking comparison is shown in Figure 32. If aluminum is combined with any of the group 1B metals (Cu, Ag or Au) the K band becomes split into two components. Furthermore, Cu, Ag and Au are the only elements which we have found to cause this band splitting. Non-metals of the same subgroup also cause this band correspondence in Al binary compounds as shown in Figure 49 for AlP, AlAs and AlSb. Spectral measurements for some of the non-metal systems are given in Table XI. Other subgroup systems which are not shown in the figures are also found to display band shape and energy position correspondence.

There appears to be a slight atomic number effect in each of the subgroup binary systems. The larger atomic numbers cause a little greater shift in the Al K band. For the same alloy compositions, for instance, the Al K band from Al-Hf will be slightly lower in energy than the band from Al-Zr which in turn will be a little lower in energy than the band from Al-Ti.

Since elements of the same subgroup have similar outer electronic configurations we conclude that the electronic structure of the second component determines the nature of the interatomic bond and hence the shape and energy position of the Al K band in aluminum binary compounds.

Now we are faced with the question of how the results from each different sub-group system are related to each other and find that a comparison of curves such as seen in Figure 50 provides an answer. If we form aluminum binary compounds of the same composition for elements in each subgroup, moving from the left to the right of the periodic table, we find that the energy position of the Al K band advances in a regular manner toward lower energy. The farther to the right that a particular element lies, the greater the change it will cause in the Al K band when formed as a binary compound with aluminum. The amount of energy shift observed in the K band corresponds fairly well with the increasing electronegativity of the second component. In general, one can assume that the more electronegative the second component, the lower the energy of the Al K band. This fact is graphically shown for a few of the aluminum binary alloy systems in Figure 51.

We find that these systematic variations are observed not only in the Al K band but in the $\text{AlK}_{\alpha_4}/\text{K}_{\alpha_3}$ intensity ratio as well. This is illustrated in Figure 52 for the same binary alloys used in Figure 51. If we examine all of the aluminum binary systems investigated, we find that elements in the same subgroup will cause the AlK_{α_4} and K_{α_3} lines to have the same intensity ratio for a given aluminum content. The farther to the right of the periodic table that an element belongs, the more of a change it will cause in the $\text{AlK}_{\alpha_4}/\text{K}_{\alpha_3}$ intensity ratio. This is the same type of relationship we observed for the Al K band as mentioned in the above paragraph.

It appears, then, that we can make two general conclusions concerning the relationship of the Al K emission spectrum from Al binary systems with the position of the second component in the periodic table:

1. elements of the same subgroup each have virtually the same effect on the aluminum spectrum.

- elements of each different subgroup have a different effect on the aluminum spectrum and these effects can be correlated according to the relative positions of each of these subgroups in the periodic table.

These are important points because they illustrate that, at least for the Al K band, the chemical effect on X-ray spectra is quite periodic in nature. Just as periodic, in fact, as the Periodic Table of the Elements.

There are a couple of points concerning Figures 51 and 52 worth mentioning here. First of all, the energy shift of the Al K band and the intensity ratio change of $\text{AlK}\alpha_4/\text{K}\alpha_3$ are linear functions of alloy composition for all of the Al binary alloys which we have investigated. The Al K band always shifts to lower energy as the Al content is decreased and the $\text{AlK}\alpha_4/\text{K}\alpha_3$ intensity ratio always increases as the Al content is decreased.

We find, in fact, that the Al K band energy position and $\text{AlK}\alpha_4/\text{K}\alpha_3$ intensity ratio are very closely inter-related as shown in Figure 53. In this figure we have plotted the energy position of the Al K band against the $\text{AlK}\alpha_4/\text{K}\alpha_3$ intensity ratio for a large number of aluminum binary compounds. This graph clearly illustrates that if the Al K band shifts in energy, it is always accompanied by a corresponding change in the $\text{AlK}\alpha_4/\text{K}\alpha_3$ intensity ratio. It makes no difference whether the compound is a conductor, semi-conductor or insulator; the lowest left-hand point is from pure Al metal, the uppermost right-hand point is from Al_2O_3 and the in-between points are from aluminum binary alloys and other aluminum binary compounds such as AlP, Al_4C_3 , Al_2Se_3 , AlAs, AlSb, et cetera.

For every 1ev that the K band shifts, the $\text{K}\alpha_4/\text{K}\alpha_3$ intensity ratio changes by 0.09. The only aluminum binary compounds which do not follow this relationship appear to be those of the Al-Cu, Al-Ag and Al-Au systems in which the Al K band becomes split into two components. We have studied approximately 200 different aluminum binary compositions where the Al K band has only one intensity maximum and have not found even one which does not follow the relationship of Figure 53. Why these two spectral characteristics should be closely inter-related is not obvious to us because supposedly they represent two entirely different phenomena. The Al K band arises, of course, from an electronic transition between the valence band and the innermost (K) shell while the atom is in the state of single K ionization. The $\text{K}\alpha_4/\text{K}\alpha_3$ intensity ratio is believed to represent two different transition probabilities between the $\text{L}_{2,3}$ and K inner levels while the atom is in a state of double (KL) ionization (Reference 26).

The $\text{K}\alpha_3$ and $\text{K}\alpha_4$ satellite lines not only display a change in their relative intensities but they shift in energy position as well. This shift, however, is quite small compared to the shift in the K band. For all of the Al binary systems which we have reported here, the AlK parent and satellite lines shift to higher energy positions when going from pure metal to an alloy or compound. This is just the opposite of the direction of shift of the Al K band which we have always observed to be towards a lower energy position. These different directions of shift point out the different types of information which lines and bands provide. The shift in energy positions of inner level transitions (such as the K lines in aluminum) are determined by changes in the density of the valence electrons in the inner regions of the atom. The shape and energy position of the emission band, on the other hand, indicates the character of the atomic interaction.

For atoms which behave as electron "donors", the lines due to inner level transitions are shifted to higher energy. For electron "acceptors", these lines shift to lower energy. Since, for all of the aluminum compounds reported here, the $\text{AlK}\alpha$ lines shift to higher energy when going from pure metal to compound, we can assume that aluminum is behaving as a donor of electrons. The more electronegative the second component, the larger the shift. This is just what one would expect to take place since electronegativity is defined as the power of an atom in a molecule to attract electrons to itself.

As mentioned above, the shift of the Al K band toward lower energy indicates that the nature of the interatomic bond is undergoing a change. In pure Al metal, for instance, the bonding is almost completely metallic in nature. The resulting K emission band is quite asymmetrical in shape showing a rather sharp emission edge with the intensity maximum at 1557.3ev as seen in several of the figures. Upon alloying aluminum with metals such as iron, cobalt, nickel and most others, the Al K band starts becoming more symmetrical in shape and its intensity maximum shifts to a lower energy. The more of the second metal that is added, the greater the change in the Al K band, which now occupies an energy position which is somewhere between that obtained from pure Al and that obtained from Al_2O_3 . These changes in shape and position appear to indicate that the predominantly metallic bond present in pure Al is acquiring a certain amount of covalent-like nature in the alloys. When the valence electrons become so localized, the energy of the valence band is reduced which causes the X-ray emission band to shift to a lower energy position.

If we combine aluminum with various non-metallic elements we find the Al K band shape to remain pretty much the same as that observed from Al_2O_3 (Figure 1) but the energy position varies with the nature of the second component. The atoms in these non-metallic binary compounds are bonded by electron sharing but this sharing is usually unequal. If the shared pair spends more time near one of the atoms than the other, the covalent bond takes on an ionic ingredient. The more ionic the bond, which is just another way of saying the more electronegative the second component, the more the shift in the Al K band. This is why we were previously able to separate the Al K band position and $\text{AlK}\alpha_4/\text{K}\alpha_3$ intensity ratio from aluminum compounds according to whether the compound was a conductor, semi-conductor or insulator (Reference 5, 6, and 18).

In the case of alloys, the theoretical foundations underlying band formation are not well understood. One finds in the literature allusions to the "rigid band model", "common valence band model", and "Friedel's theory" which all attempt to explain band formation in alloys (Reference 1, 22). Each of these theories assumes either a correspondence or noncorrespondence of the emission band shapes and widths from each of the components in the binary alloy. Let us suffice here to say that, except for perhaps the Al-Mg system, we have not observed any band shape or bandwidth correspondence from the two components of the aluminum binary alloy systems which we have investigated, apparently indicating that the common valence band model does not apply.

It is important to note that the changes in the Al K band energy position and $\text{AlK}\alpha_4/\text{K}\alpha_3$ intensity ratio, for any of the binary alloy systems investigated so far, are continuous and smooth throughout the entire composition range. This smoothness is present no matter how many crystal structure changes are encountered in the system (Figures 51 and 52).

These spectral changes which occur are valuable not only from the theoretical viewpoint but can be used as a quantitative analysis tool as well. One has the capability of using the features of the aluminum K X-ray emission spectrum to identify the phase or phases present in an aluminum binary alloy and also determine the exact composition of each phase without

requiring the use of an internal standard. The shape and energy position of the Al K band and the intensity ratio of the $K\alpha_4/K\alpha_3$ satellite lines are quite reproducible and once curves such as those shown in Figures 51 and 52 have been obtained for a particular binary system, it is not necessary to run standards with each sample to obtain compositions to within ± 2 percent (atomic).

REFERENCES

1. A. Appleton, *Contemp. Phys.* 6, 50 (1964).
2. B.J. Thompson and P.F. Kellen, *Developments in Applied Spectroscopy*, Vol. 4, Plenum Press, Inc., New York (1965).
3. D.W. Fischer and W.L. Baun, *J. Appl. Phys.* 36, 534 (1965).
4. W.L. Baun and D.W. Fischer, *Phys. Lett.* 13, 36 (1964).
5. W.L. Baun and D.W. Fischer, *Nature* 204, 642 (1964).
6. W.L. Baun and D.W. Fischer, AFML-TR-64-350 (December 1964).
7. D.W. Fischer and W.L. Baun, *Spectrochim. Acta* 21, 443 (1965).
8. A. Appleton and C. Curry, *Phil. Mag.* 12, 245 (1965).
9. J. Farineau, *Ann. Phys. (Paris)* 10, 20 (1938).
10. R.J. Liefeld, *Bull. Amer. Phys. Soc.* 10, #4 549 (1965).
11. D.W. Fischer and W.L. Baun, *Phys. Rev.*, to be published.
12. S.A. Nemnonov and L.D. Finkel'shtein, *Bull. Acad. Sci. U.S.S.R., Phys. Ser.* 25, #8, 1015 (1961).
13. L.V. Azaroff, *Science* 151, 785 (1966).
14. B.N. Das and L.V. Azaroff, *Acta Metallurgica* 13, 827 (1965).
15. D. Chopra and R. Liefeld, *Bull. Amer. Phys. Soc.* 9, #4, 404 (1964).
16. R. Liefeld and D. Chopra, *Bull. Amer. Phys. Soc.* 9, #4, 404 (1964).

REFERENCES (Cont'd)

17. D.W. Fischer, *J. Appl. Phys.* 36, 2048 (1965).
18. W.L. Baun and D.W. Fischer, *Advances in X-Ray Analysis*, Vol. 8, Plenum Press, N. Y. (1965).
19. S. Yoshida, *Sci. Papers Inst. Phys. Chem. Research (Tokyo)* 28, 2431 (1936).
20. J. Farineau, *J. Phys. Rad.* 10, 327 (1939).
21. C.H. Shaw, *Theory of Alloy Phases*, Am. Soc. for Metals, 13-62 (1956).
22. J. Friedel, *Phil. Mag.* 43, 153 (1952).
23. H.W.B. Skinner and J.E. Johnston, *Proc. Camb. Phil. Soc.* 34, 109 (1938).
24. J.A. Bearden and H. Friedman, *Phys. Rev.* 58, 387 (1940).
25. D.W. Fischer and W.L. Baun, *Bull. Amer. Phys. Soc.*, Series II, 11, 331 (1966).
26. E.H. Kennard and E. Ramberg, *Phys. Rev.* 46, 1040 (1934).

TABLE I
Al K BAND MEASUREMENTS FOR Al-Mg ALLOYS

Target	Peak Position	Half-Band Width	Full-Band Width	Edge Width	A_1	A_C
pure Al	1557.3 \pm 0.1 ev	6.0 \pm 0.1 ev	12.3 \pm 0.3 ev	2.1 \pm 0.2 ev	2.7 \pm 0.2	3.7 \pm 0.2
90 Al-10 Mg	1557.1	5.8	12.2	2.1	2.0	3.7
82 Al-18 Mg	1557.1	5.7	12.0	2.3	1.9	3.4
60 Al-40 Mg	1557.0	5.3	11.3	2.3	1.7	2.9
55 Al-45 Mg	1557.0	5.2	11.1	2.3	1.7	2.9
50 Al-50 Mg	1557.0	4.9	10.9	2.3	1.7	2.9
40 Al-60 Mg	1557.0	4.6	10.2	2.3	1.7	2.9
30 Al-70 Mg	1557.0	4.6	10.2	2.3	1.7	2.9
20 Al-80 Mg	1557.0	4.6	10.3	2.3	1.7	2.9
10 Al-90 Mg	1557.0	4.5	10.3	2.3	1.7	2.9

TABLE II
Mg K BAND MEASUREMENTS FOR Al-Mg ALLOYS

Target	Peak Position	Half-Band Width	Full-Band Width	Edge Width	A_1	A_C
pure Mg	1301.8 \pm 0.1 ev	3.4 \pm 0.1 ev	7.9 \pm 0.3 ev	1.6 \pm 0.2 ev	2.8 \pm 0.2	3.4 \pm 0.2
80 Mg-20 Al	1301.6	4.9	10.8	2.0	2.4	3.6
70 Mg-30 Al	1301.5	5.1	11.0	2.1	2.4	3.6
60 Mg-40 Al	1301.4	5.5	11.1	2.2	2.2	3.3
50 Mg-50 Al	1301.4	5.1	11.2	2.2	2.0	3.3
45 Mg-55 Al	1301.4	6.0	11.2	2.2	2.0	3.3
40 Mg-60 Al	1301.4	6.6	11.4	2.2	1.9	3.3

TABLE III

Aluminum and Magnesium $K\alpha_4/K\alpha_3$ Satellite Line
Intensity Ratios for Al-Mg Alloys

Target	Al $K\alpha_4/K\alpha_3$	Mg $K\alpha_4/K\alpha_3$
pure metal	0.48 ± 0.01	0.58 ± 0.01
oxide	0.92	1.03
90 Al-10 Mg	0.49	-
82 Al-18 Mg	0.50	-
60 Al-40 Mg	0.50	0.64
55 Al-45 Mg	0.50	0.63
50 Al-50 Mg	0.50	0.63
40 Al-60 Mg	0.50	0.62
30 Al-70 Mg	0.50	0.62
20 Al-80 Mg	0.50	0.62
10 Al-90 Mg	0.50	0.60

TABLE IV
UNCORRECTED ALUMINUM K EMISSION CHARACTERISTICS IN Al-Ni SYSTEM

Target	AlK α_4 /K α_3	AlK β Position	AlK β Half Width	AlK β Rase Width	AlK β ; A ₁	AlK β ; A _c	AlK β Edge Width
100Al	0.48 \pm 0.01	0557.3 \pm 0.1 ev	6.0 \pm 0.1 ev	12.3 \pm 0.5 ev	2.7 \pm 0.2	3.7 \pm 0.2	2.1 \pm 0.1 ev
90Al-10Ni	0.52	1556.9	7.0	12.4	2.2	2.9	3.0
85Al-15Ni	0.54	1556.7	6.9	12.4	1.9	2.3	3.2
75Al-25Ni	0.58	1556.2	6.5	12.4	1.4	1.9	3.7
65Al-35Ni	0.61	1555.8	6.2	12.4	1.4	1.7	3.9
60Al-40Ni	0.63	1555.6	5.7	12.4	1.4	1.6	4.0
50Al-50Ni	0.66	1555.3	6.0	12.5	1.4	1.3	4.2
40Al-60Ni	0.70	1555.0	6.5	12.4	1.3	1.2	4.2
35Al-65Ni	0.72	1554.7	6.6	12.3	1.3	1.2	4.3
25Al-75Ni	0.76	1554.4	6.8	12.2	1.3	1.2	4.5
20Al-80Ni	0.77	1554.2	6.8	12.3	1.3	1.2	4.5
4Al-96Ni	0.84	—	—	—	—	—	—
Al ₂ O ₃	0.92	1552.9	6.4	10.8	1.0	1.0	4.0

TABLE V

COMPARISON OF Al $K\alpha_4/K\alpha_3$ INTENSITY RATIO IN THE
Al-Ni SYSTEM USING MACRO AND MICRO AREA EXCITATION

Samples	$K\alpha_4/K\alpha_3$ Macro Area Excitation	$K\alpha_4/K\alpha_3$ Microprobe
Pure Al	0.48	0.48
85Al-15Ni (2 phase)	0.54	0.50) Al rich 0.55) Ni rich
75Al-25Ni(Al ₃ Ni)	0.57	0.57
65Al-35Ni (2 phase)	0.61	0.60) Al rich 0.63) Ni rich
50Al-50Ni(AlNi)	0.66	0.66

TABLE VI

UNCORRECTED NiLIII EMISSION BAND
CHARACTERISTICS IN Al-Ni SYSTEM

Target	Half Band Width	Edge Width	Asymmetry Index
100Ni	2.43 \pm 0.08ev	1.73 \pm 0.08ev	1.74 \pm 0.04
80Ni-20Al	2.66	1.76	1.72
75Ni-25Al	2.60	1.78	1.70
65Ni-35Al	2.40	1.86	1.60
60Ni-40Al	2.31	1.93	1.50
50Ni-50Al	2.34	2.09	1.30
40Ni-60Al	2.34	2.25	1.15
35Ni-65Al	2.41	2.34	1.08
25Ni-75Al	2.54	2.67	1.00
15Ni-85Al	2.59	2.94	0.98
10Ni-90Al	2.64	3.14	0.95

TABLE VII
UNCORRECTED ALUMINUM K EMISSION CHARACTERISTICS IN Al-Fe SYSTEM

Target	Al $K\alpha_4/K\alpha_3$	Al $K\beta$ Position	Al $K\beta$ Half Width	Al $K\beta$ Base Width	Al $K\beta$; A_1	Al $K\beta$; A_c
100Al	0.48 \pm 0.01	1557.3 \pm 0.1 ev	6.0 \pm 0.1 ev	12.3 \pm 0.5 ev	2.7 \pm 0.2	3.7 \pm 0.2
95Al-5Fe	0.49	1557.1	5.9	12.2	2.5	3.2
90Al-10Fe	0.51	1557.0	5.9	12.2	2.2	3.0
80Al-20Fe	0.54	1556.8	5.7	11.8	2.0	2.6
75Al-25Fe	0.56	1556.6	5.5	11.8	1.9	2.6
72Al-28Fe	0.58	1556.4	5.2	11.4	1.8	2.4
67Al-33Fe	0.59	1556.1	5.4	11.9	1.7	2.5
50Al-50Fe	0.67	1555.4	5.7	11.8	1.5	2.1
25Al-75Fe	0.76	1554.5	6.2	11.8	1.3	1.6
10Al-90Fe	0.83	1553.7	6.2	11.7	1.2	1.4

TABLE VIII
UNCORRECTED FeI_{III} EMISSION BAND CHARACTERISTICS IN Al-Fe SYSTEM

Target	Peak Position	Half Band Width	Base Width	Asymmetry Index	Asymmetry Coefficient
100Fe	704.73 \pm 0.04 ev	2.85 \pm 0.04 ev	7.5 \pm 0.3 ev	1.7 \pm 0.2	2.9 \pm 0.2
90Fe-10Al	704.76	2.84	7.6	1.6	2.5
75Fe-25Al	704.77	2.78	7.4	1.5	2.1
65Fe-35Al	704.84	2.61	7.1	1.5	2.1
50Fe-50Al	704.90	2.51	6.8	1.5	2.1
33Fe-67Al	704.99	2.31	6.3	1.8	2.1
28Fe-72Al	705.08	2.09	6.3	1.4	2.3
25Fe-75Al	705.11	2.19	6.3	1.5	2.1
20Fe-80Al	705.16	2.23	6.3	1.5	2.1
10Fe-90Al	705.20	2.33	6.5	1.5	2.1
5Fe-95Al	705.23	2.53	—	1.5	2.1

TABLE IX
ALUMINUM K X-RAY EMISSION SPECTRA CHARACTERISTICS IN THE Al-Cu SYSTEM

Composition	Al K Band Position (high energy component) ev	Al K Band Position (low energy component) ev	Al K Band Edge Width, ev	Al $K\alpha_4/K\alpha_3$
100Al	1557.3 \pm 0.1	not doubled	2.1 \pm 0.1	0.48 \pm 0.1
90Al-10Cu	1557.4	not resolved	2.2	0.51
75Al-25Cu	1557.6	1555.2 \pm 0.1	2.1	0.53
70Al-30Cu	1557.7	1555.1	2.4	0.55
67Al-33Cu	1557.7	1555.2	2.3	0.54
49Al-51Cu	1557.7	1554.6	2.4	0.58
40Al-60Cu	1557.7	1554.4	2.4	0.60
33Al-67Cu	1557.7	1554.4	2.3	0.61
30Al-70Cu	1557.7	1554.1	2.4	0.63
25Al-75Cu	1557.7	1554.0	2.5	0.66
20Al-80Cu	1557.7	1553.8	2.5	0.67
10Al-90Cu	1557.7	1553.7	2.5	0.70

TABLE X
UNCORRECTED ALUMINUM K EMISSION CHARACTERISTICS IN Al-Ti SYSTEM

Target	Al $K\alpha_4/K\alpha_3$	Al K β Position	Al K β Half Width	Al K β Base Width	Al K β Edge Width	Al K β ; A_1	Al K β ; A_c
100Al	0.48 ± 0.01	1557.3 ± 0.1 ev	6.0 ± 0.1 ev	12.3 ± 0.5 ev	2.1 ± 0.1 ev	2.7 ± 0.2	3.7 ± 0.2
75Al-25Ti	0.51	1556.9	4.1	12.5	2.5	1.4	2.5
67Al-33Ti	0.53	1556.7	3.9	12.0	2.6	1.4	2.5
50Al-50Ti	0.56	1556.6	3.5	11.6	2.6	1.4	2.4
25Al-75Ti	0.61	1556.1	3.8	11.1	2.5	1.4	2.6

TABLE XI
UNCORRECTED ALUMINUM K EMISSION CHARACTERISTICS FOR SOME ALUMINUM BINARY COMPOUNDS
OF SEMI-METALS AND NON-METALS NOT PREVIOUSLY REPORTED.

Target	Al $K\alpha_4/K\alpha_3$	Al $K\beta$ Position	Al $K\beta$ Halfwidth	Al $K\beta$ Base Width	Al $K\beta$; A_1	Al $K\beta$; A_c
Al	0.48 ± 0.01	1557.3 ± 0.2 ev	6.0 ± 0.1 ev	12.3 ± 0.5 ev	2.7 ± 0.2	3.7 ± 0.2
Al ₂ O ₃	0.92	1552.9	6.4	10.8	1.0	1.0
Al ₄ C ₃	0.84	1553.5	6.5	12.9	0.9	1.5
Al N	0.87	$1555.1 \left\{ \begin{array}{l} \\ 1553.0 \end{array} \right. \right\}$ doublet	4.9	9.6		
Al P	0.90	1553.2	5.2	11.6	1.0	1.1
Al As	0.90	1553.4	5.1	11.5	1.0	0.9
Al Sb	0.90	1553.4	5.1	11.5	1.0	0.9
Cryolite	0.97	1552.3	6.4	11.2	1.0	1.0

TABLE XII

RELATIONSHIP OF Al K BAND ENERGY POSITION AND Al K α_4 /K α_3 INTENSITY
RATIO TO ELEMENTAL SUBGROUP OF SECOND COMPONENT IN ALUMINUM BINARY ALLOYS.

Subgroup	Alloy	AlK β , Energy Position	Al K α_4 /K α_3
II A	50Al-50Mg	1557.0 \pm 0.1 ev	0.50 \pm 0.01
	50Al-50Ca	1557.0	0.50
III B	50Al-50Y	1556.8	0.53
IV B	50Al-50Ti	1556.6	0.56
	50Al-50Zr	1556.6	0.56
	50Al-50Hf	1556.5	0.56
V B	50Al-50Nb	1556.4	0.56
	50Al-50Ta	1556.3	0.57
VI B	50Al-50Cr	1556.1	0.59
	50Al-50Mo	1556.1	0.59
VII B	50Al-50Mn	1556.2	0.59
VIII	50Al-50Fe	1555.4	0.67
	50Al-50Co	1555.4	0.67
	50Al-50Ni	1555.3	0.66

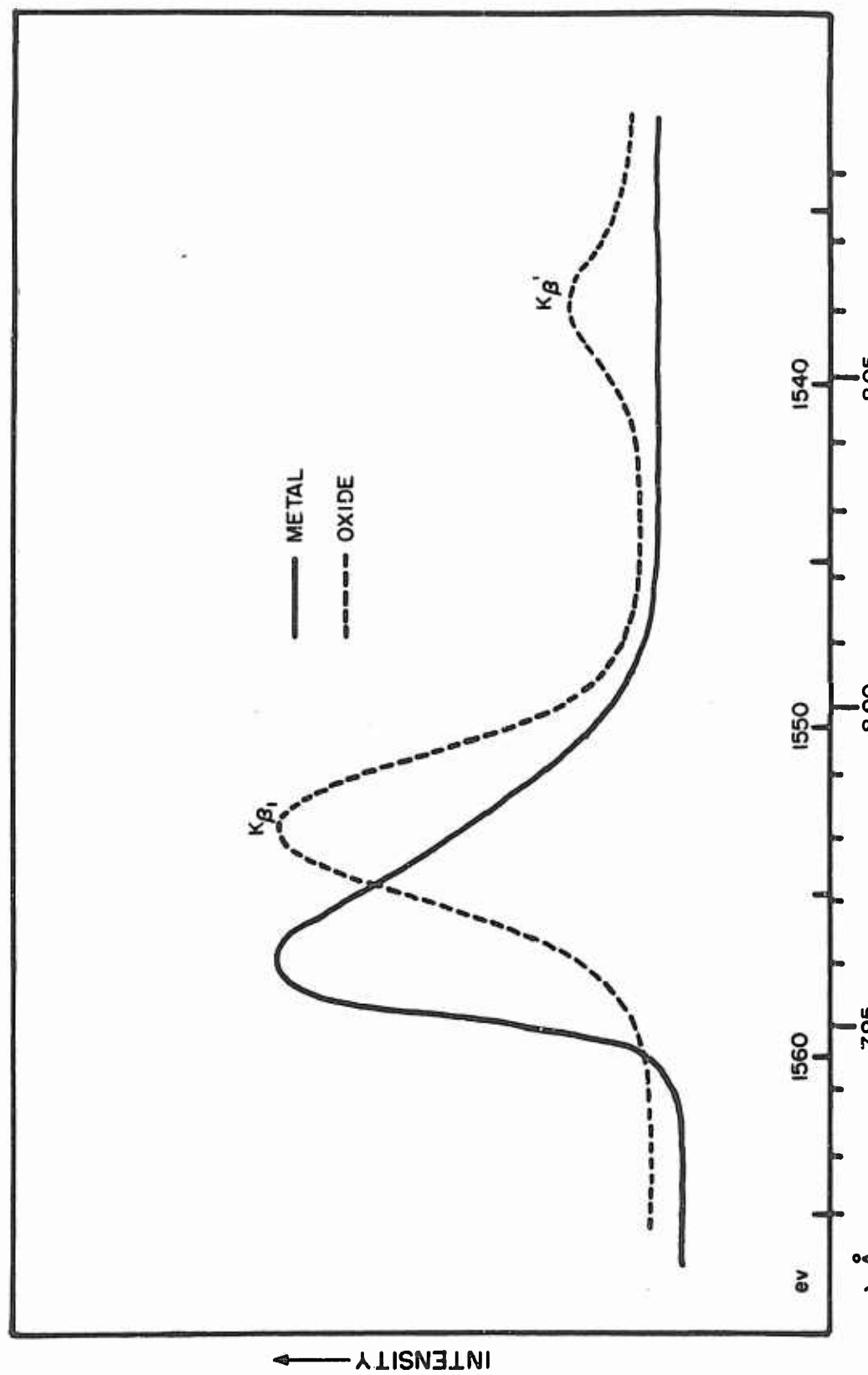


Figure 1. Aluminum K Emission Band from Pure Metal and Oxide (EDDT Crystal)

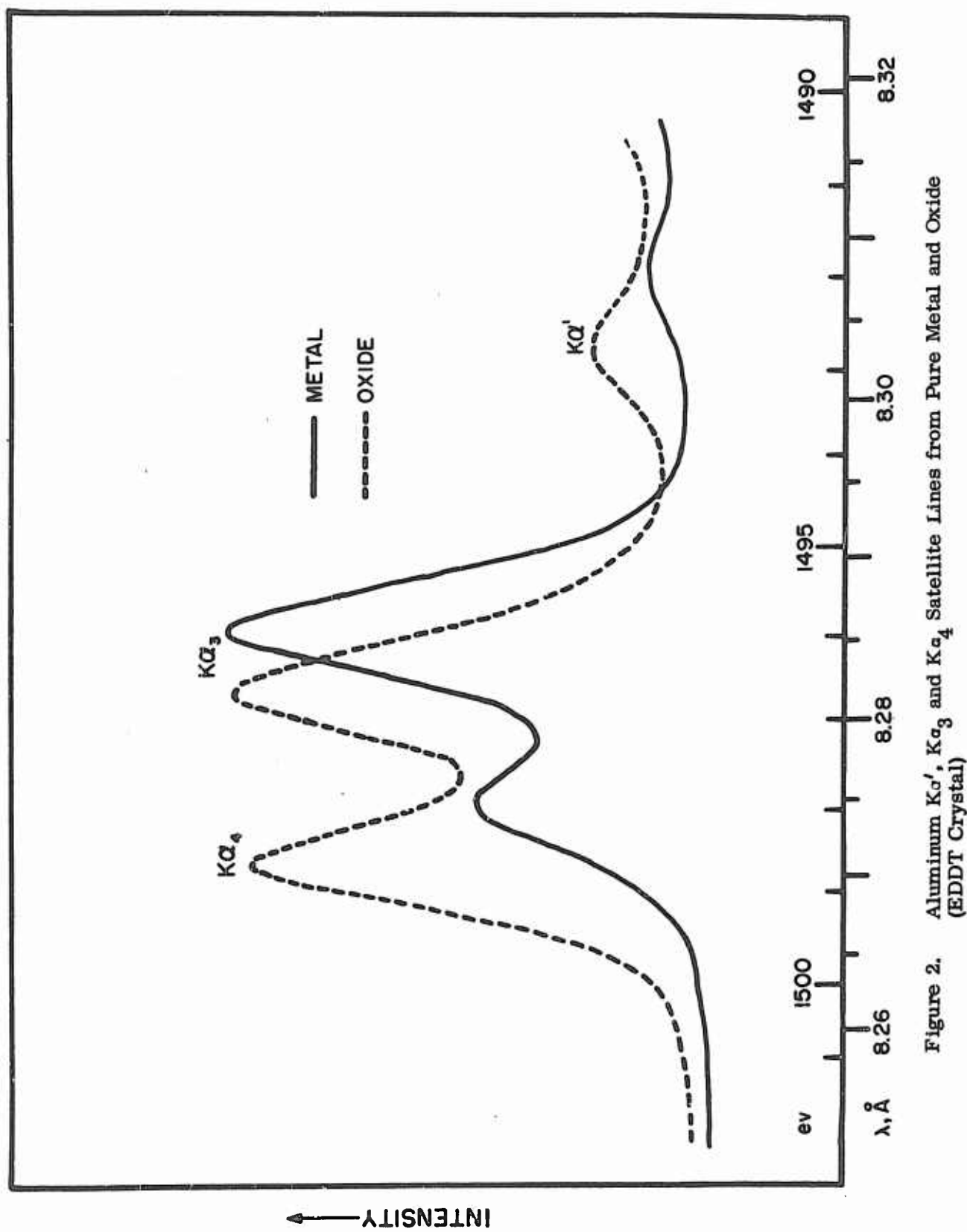


Figure 2. Aluminum $K\alpha'$, $K\alpha_3$ and $K\alpha_4$ Satellite Lines from Pure Metal and Oxide (EDDT Crystal)

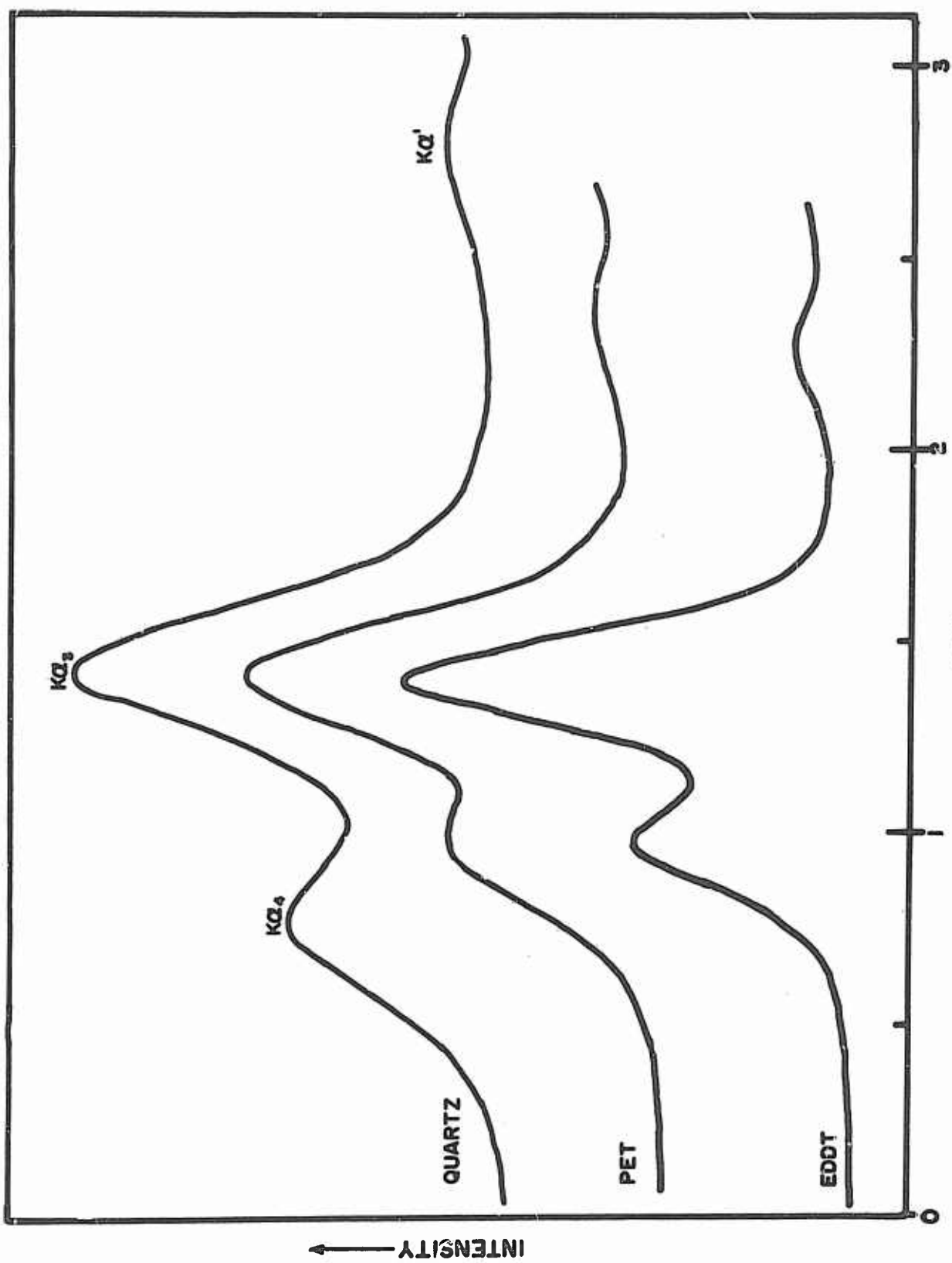


Figure 3. Aluminum $K\alpha'$, $K\alpha_3$ and $K\alpha_4$ Satellite Lines from Al Metal as Dispersed with EDDT, PET and Quartz Crystals

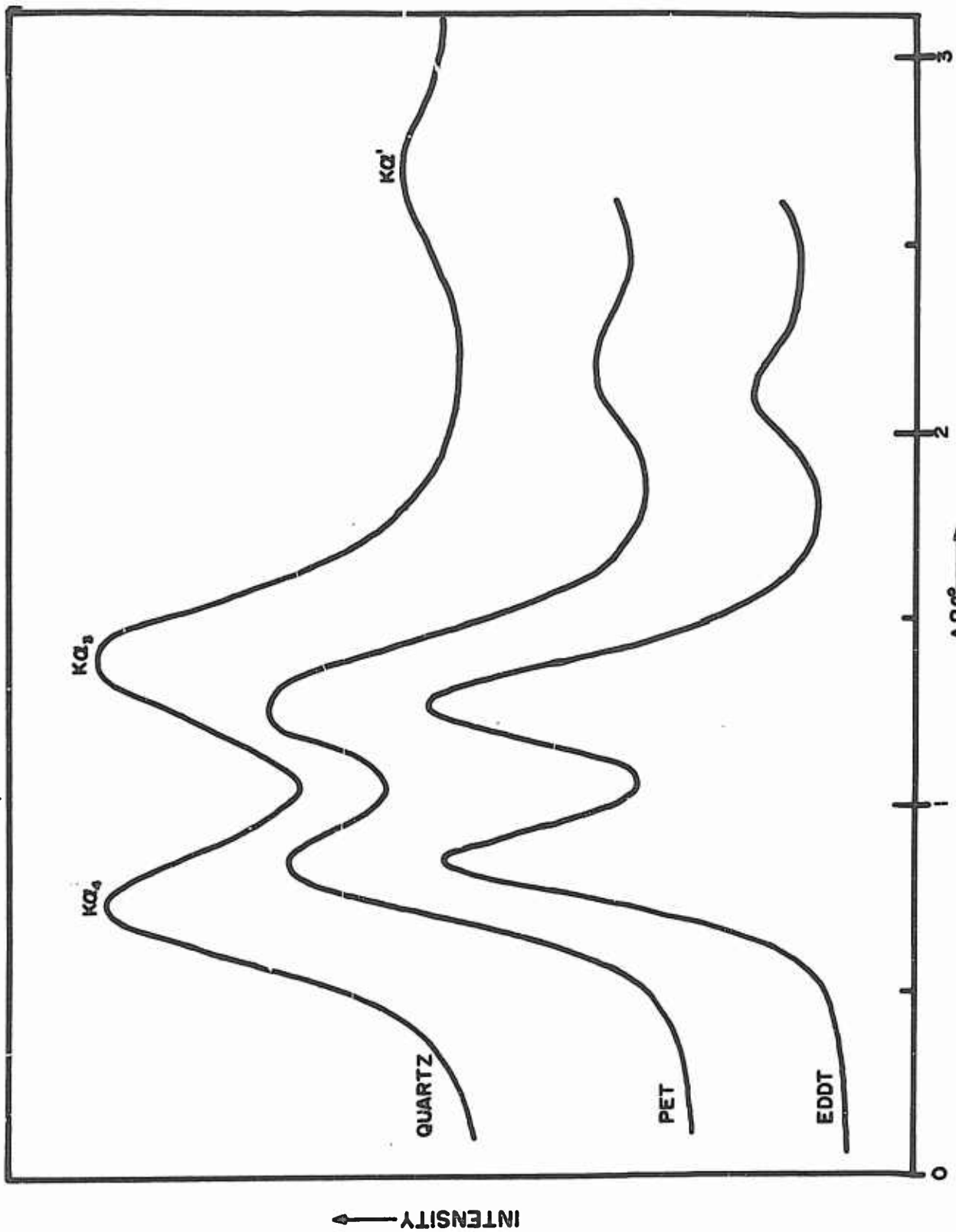


Figure 4. Aluminum $K\alpha'$, $K\alpha_3$ and $K\alpha_4$ Satellite Lines from Al_2O_3 as Dispersed with EDDT, PET and Quartz Crystals

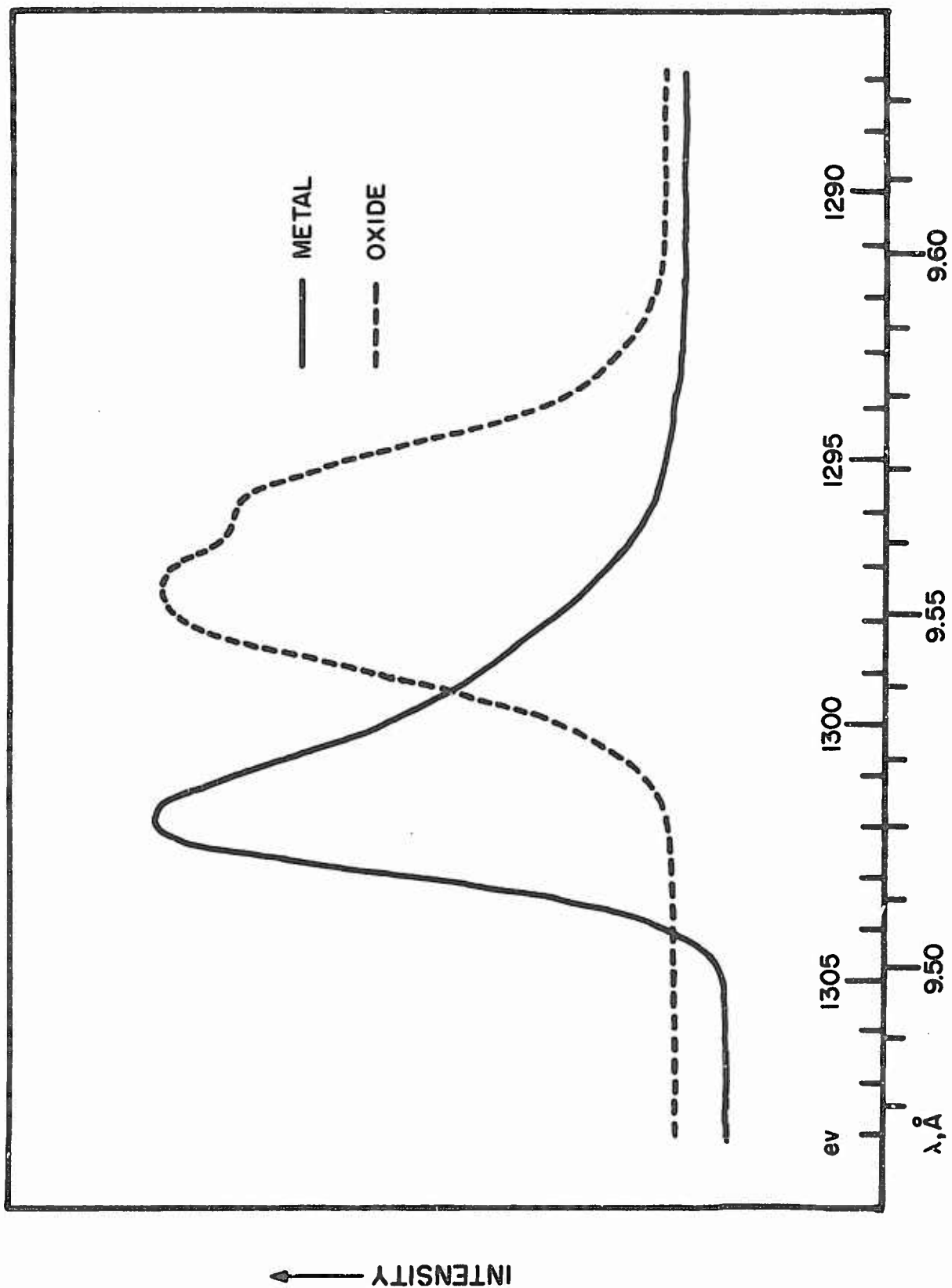


Figure 5. Magnesium K Emission Band from Pure Metal and Oxide (ADP Crystal)

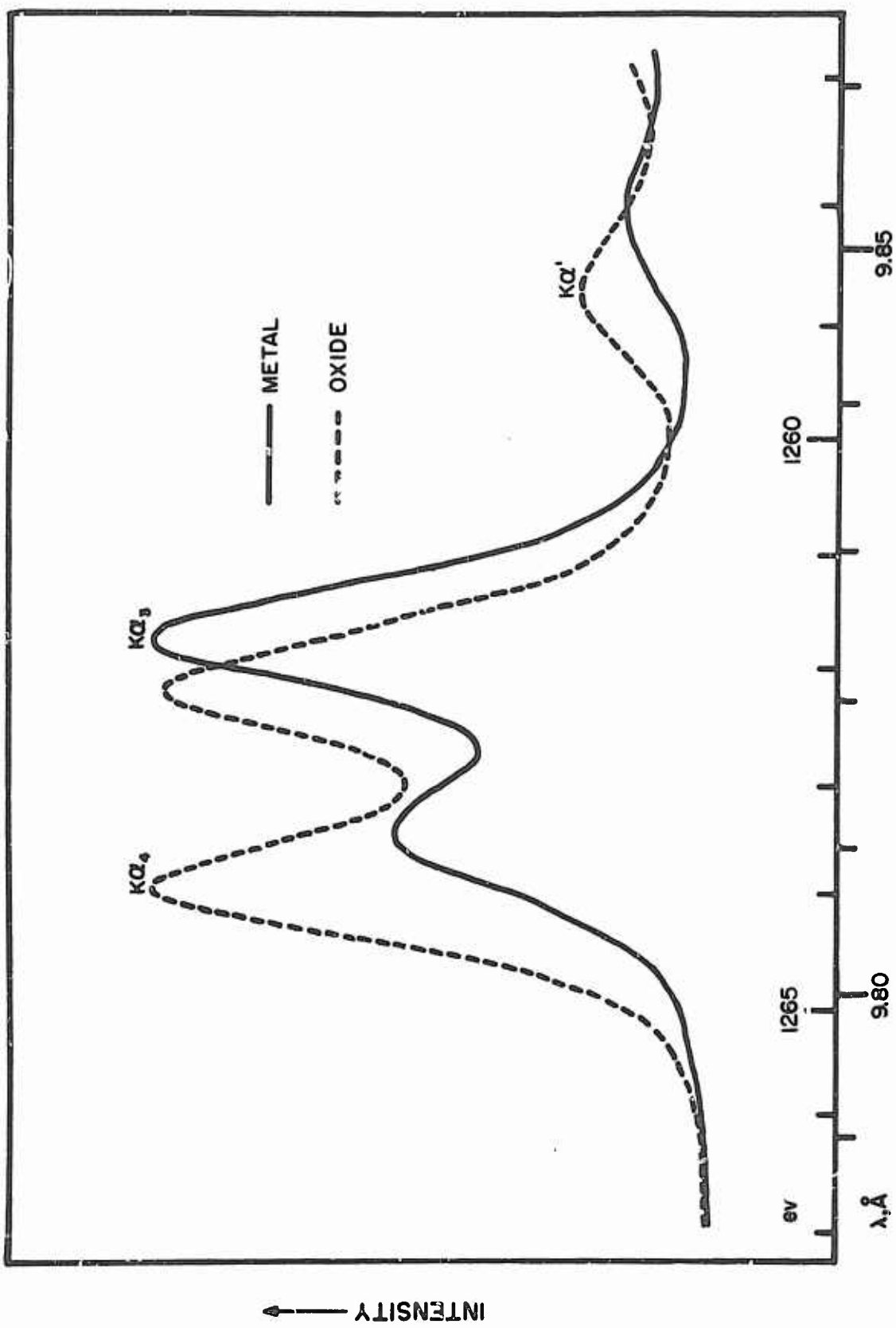


Figure 6. Magnesium $K\alpha'_1$, $K\alpha_3$ and $K\alpha'_4$ Satellite Lines from Pure Metal and Oxide (ADP Crystal)

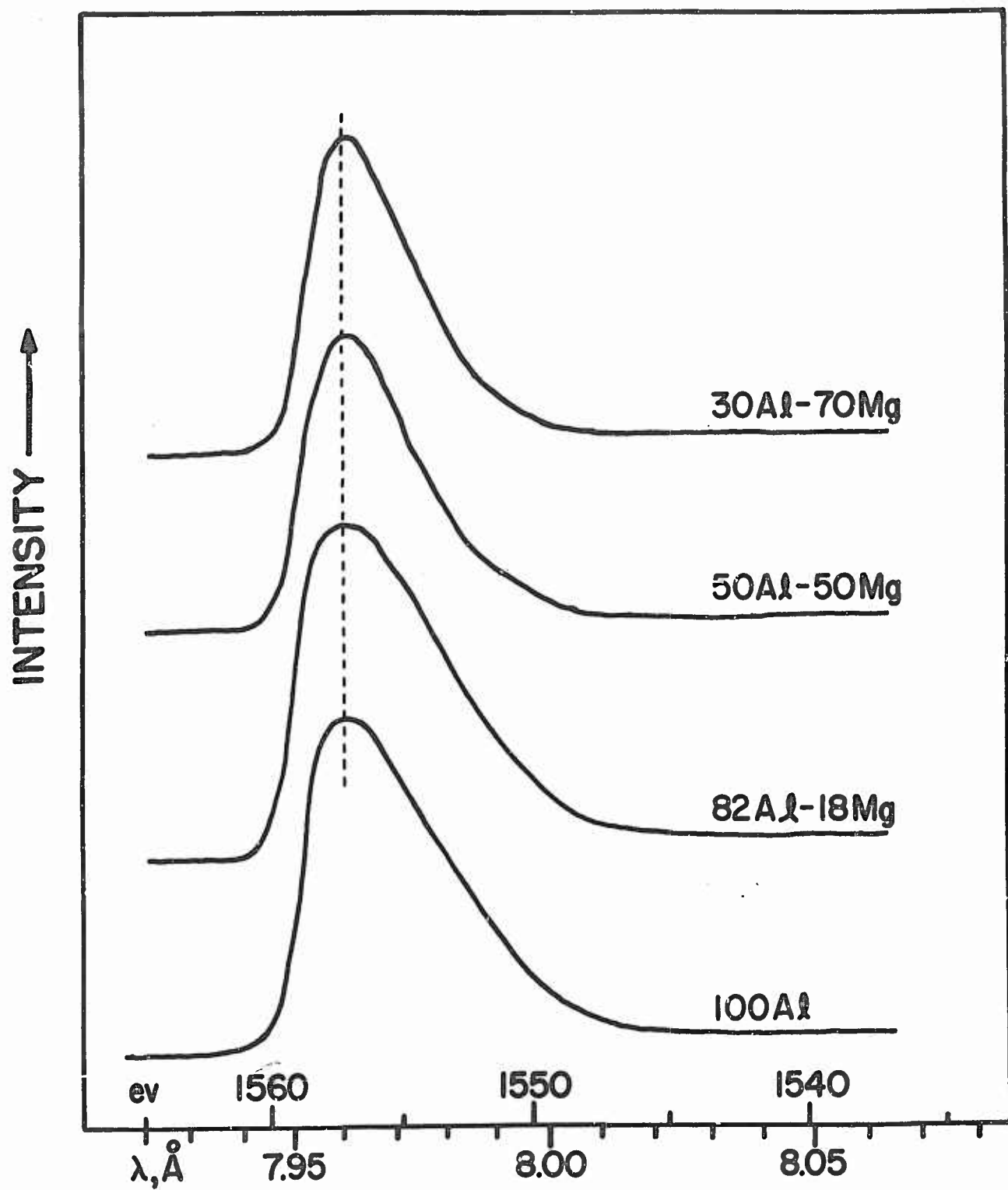


Figure 7. Aluminum K Emission Band from Some Al-Mg Alloys (EDDT Crystal)

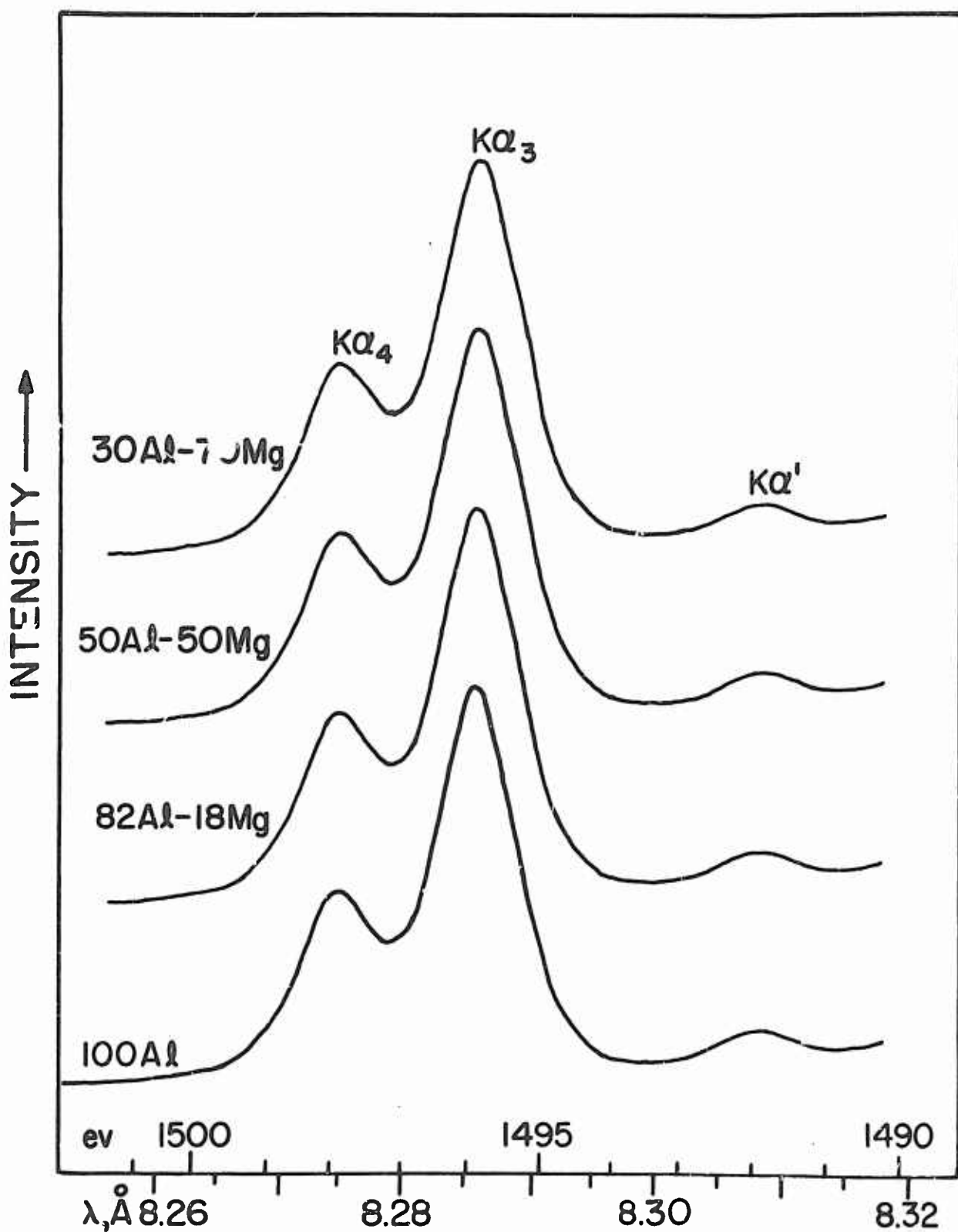


Figure 8. Aluminum $K\alpha'$, $K\alpha_3$ and $K\alpha_4$ Lines from Some Al-Mg Alloys (EDDT Crystal)

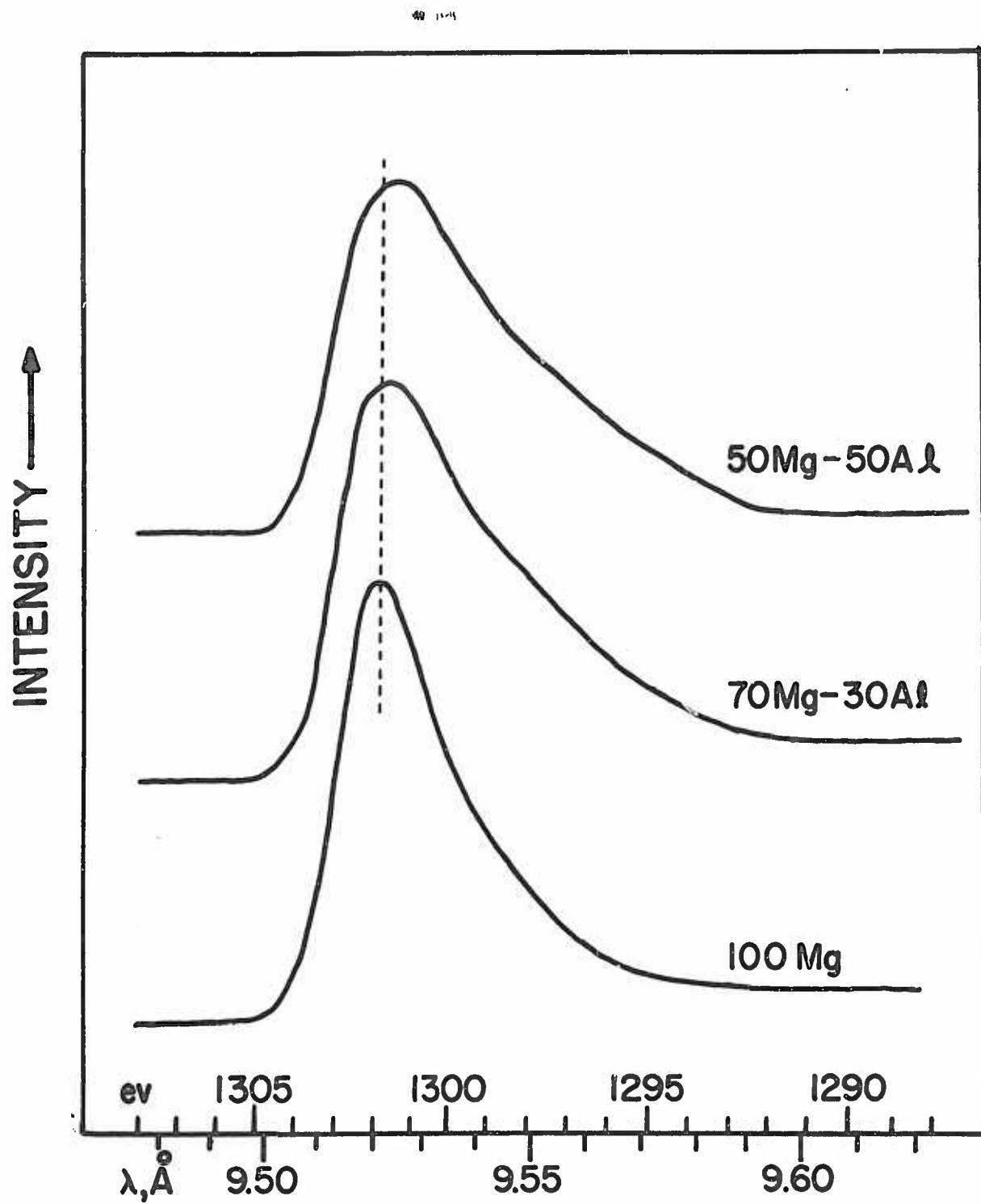


Figure 9. Magnesium K Emission Band from Some Al-Mg Alloys (ADP Crystal)

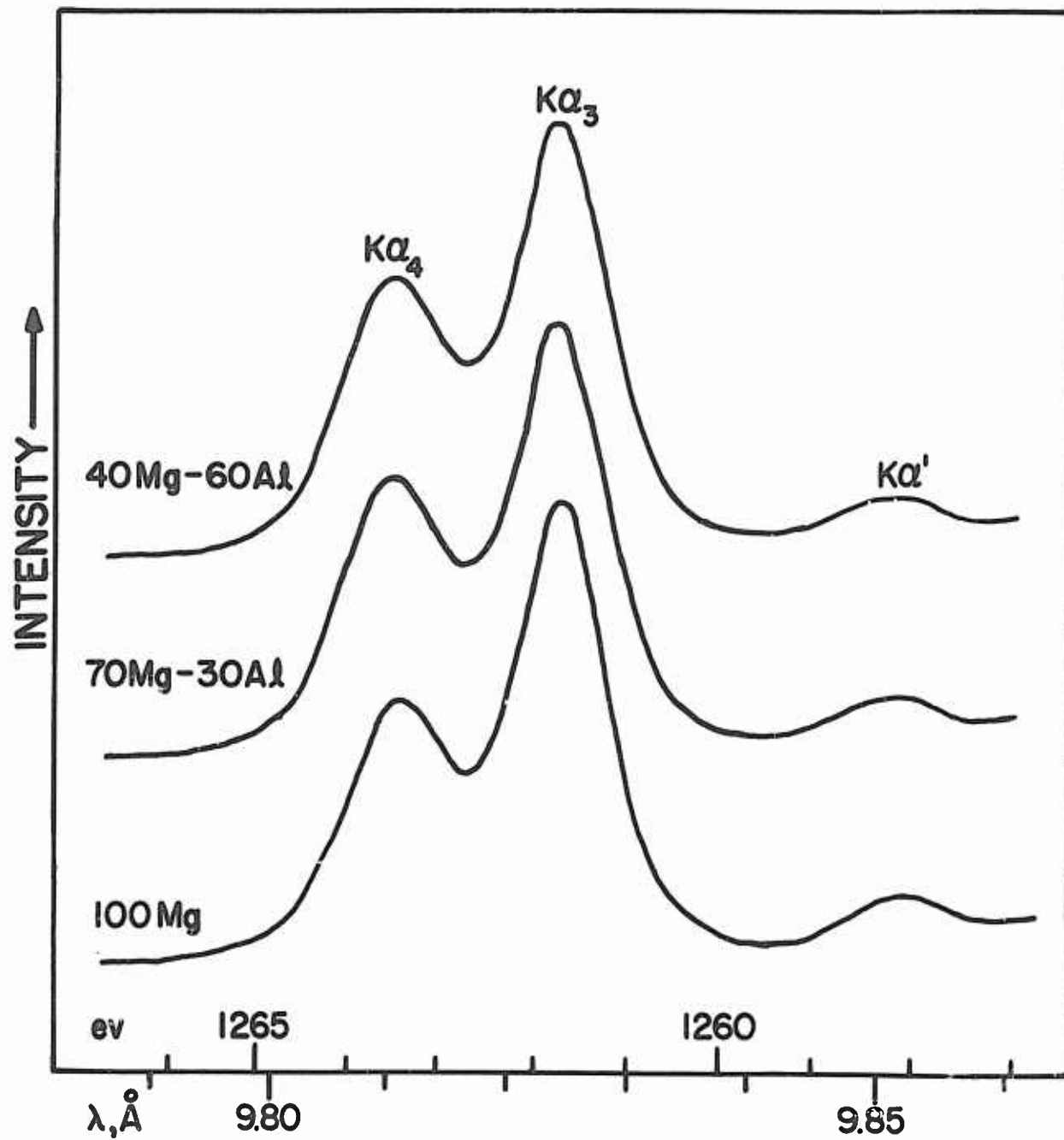


Figure 10. Magnesium $K\alpha'$, $K\alpha_3$ and $K\alpha_4$ Lines from Some Al-Mg Alloys (ADP Crystal)

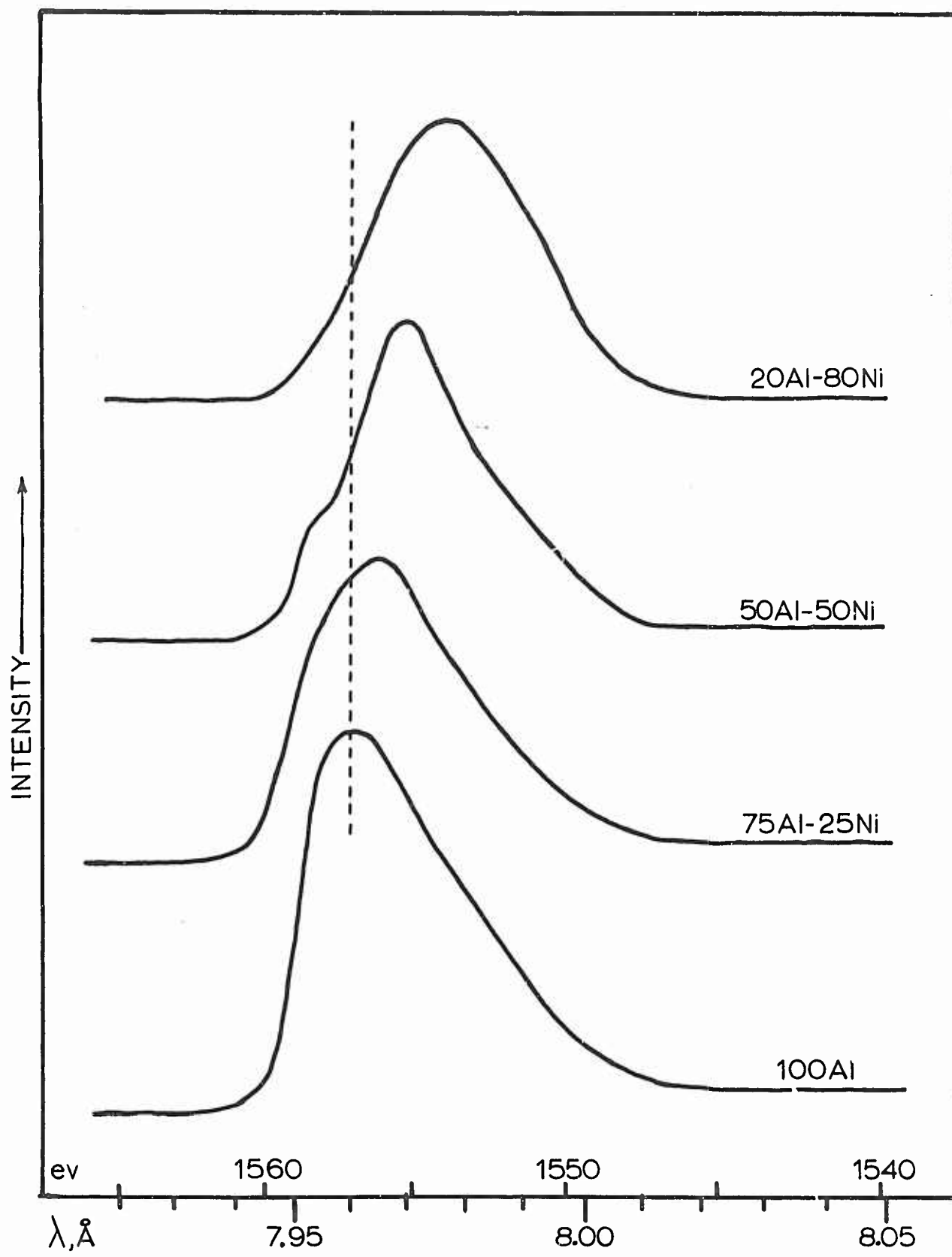


Figure 11. Aluminum K Emission Band from Some Al-Ni Alloys (EDDT Crystal)

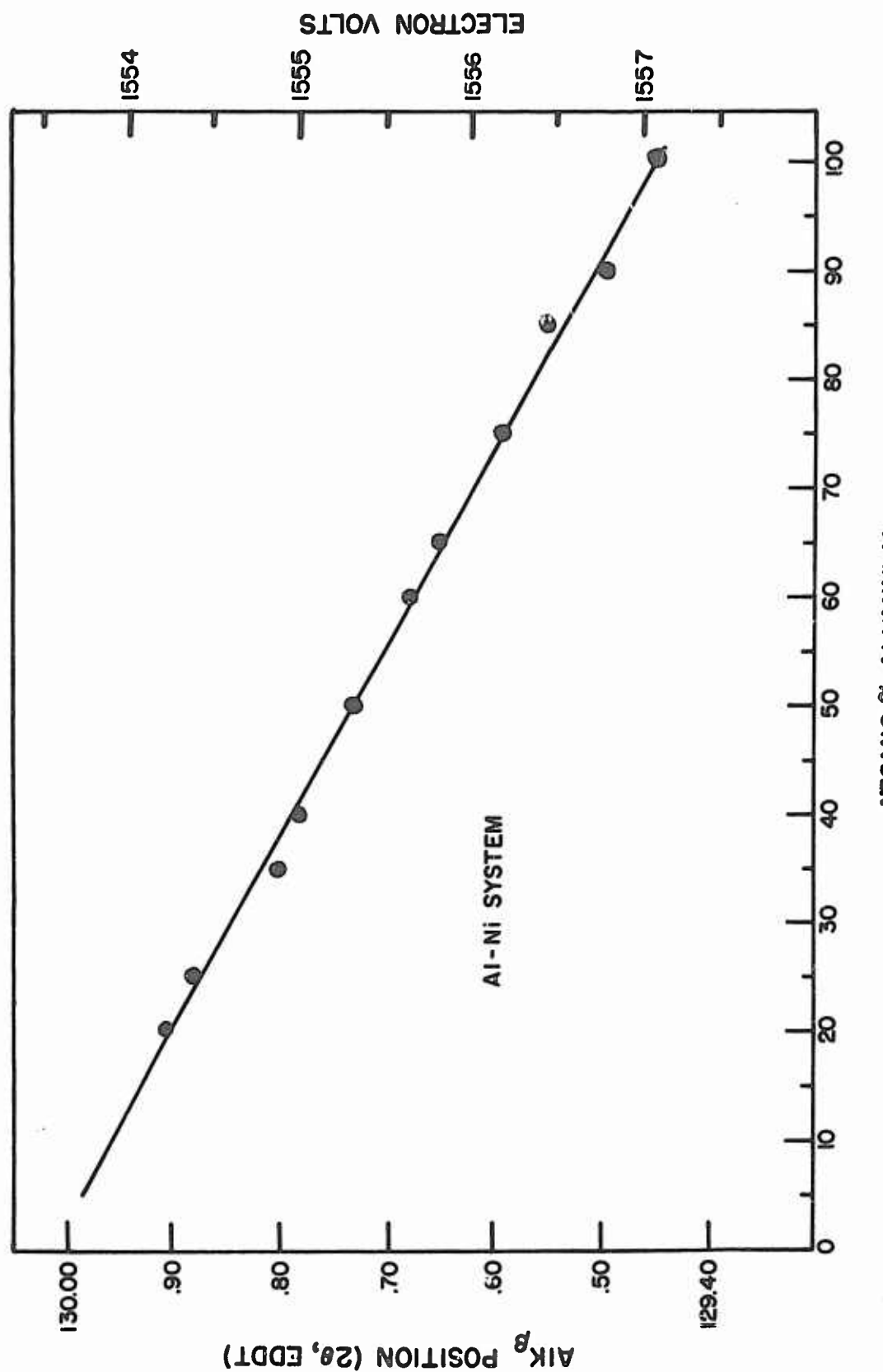


Figure 12. Al K Band Shift with Alloy Composition in Al-Ni System

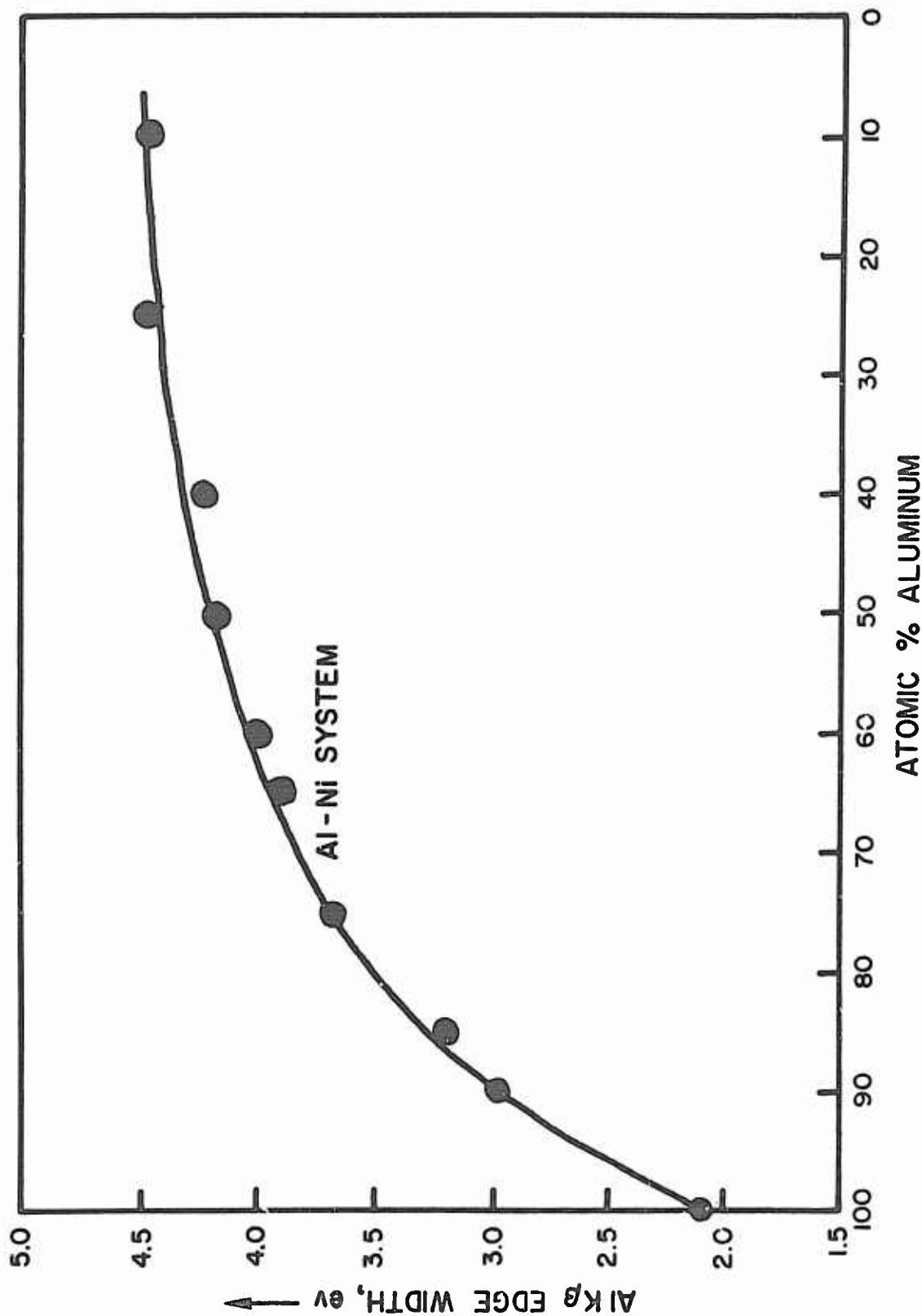


Figure 13. Variation in Uncorrected Emission Edge Width for Al K Band in Al-Ni System

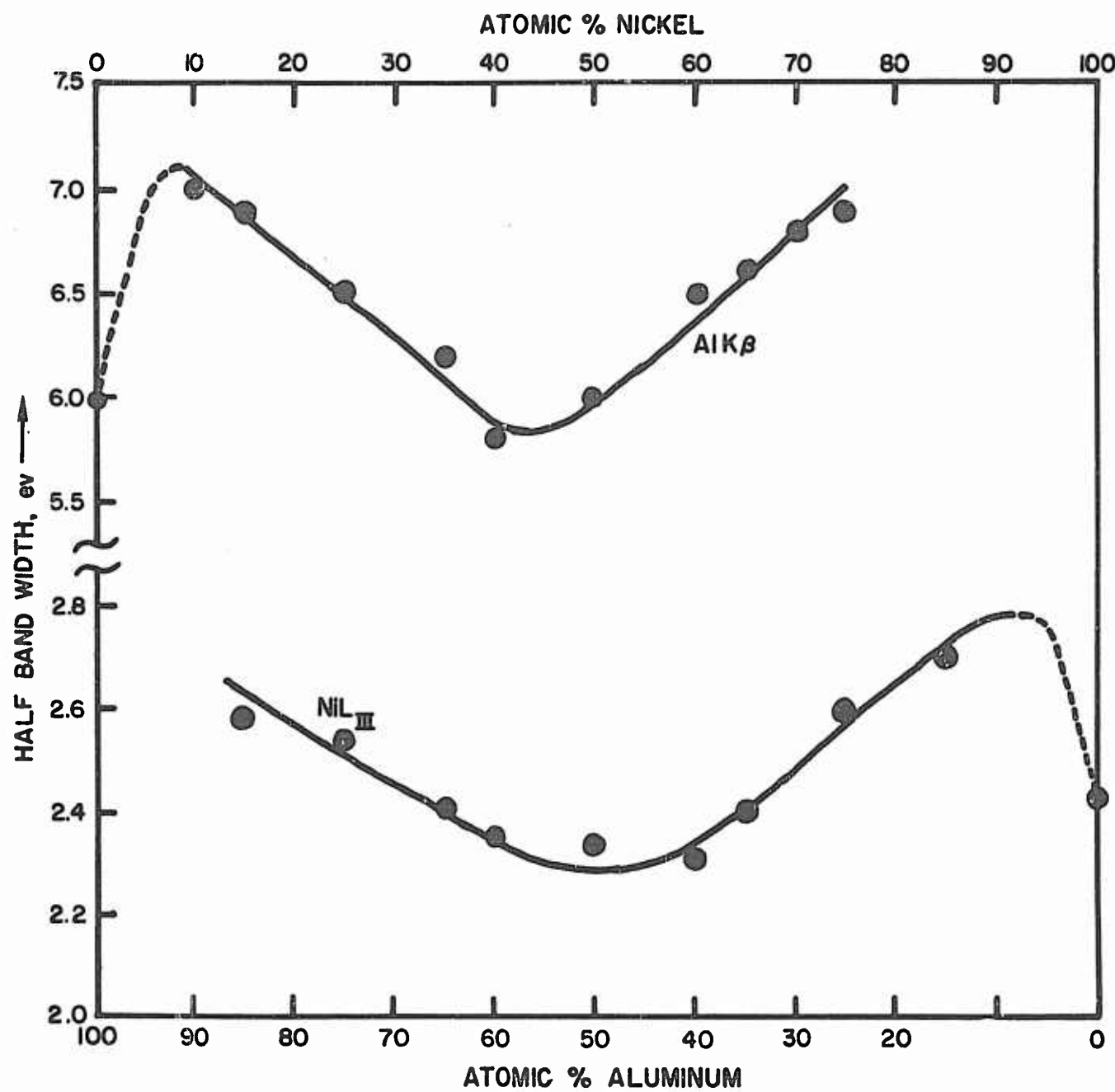


Figure 14. Variation in Uncorrected Half Band Width for Al K and NiL $_{\text{III}}$ Bands in Al-Ni System

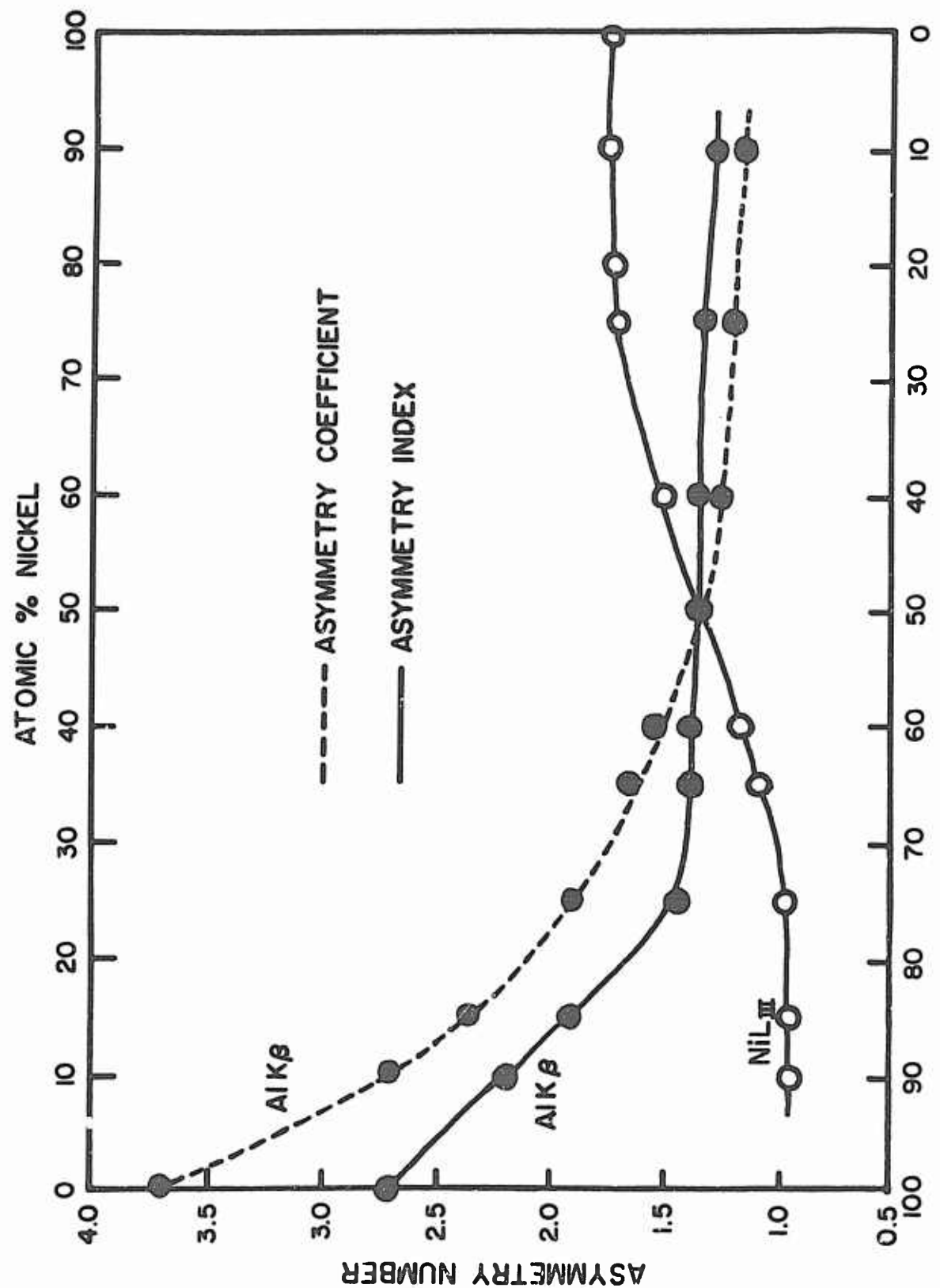


Figure 15. Change in Asymmetry Constants of Al K and Ni L β Bands with Alloy Composition in Al-Ni System

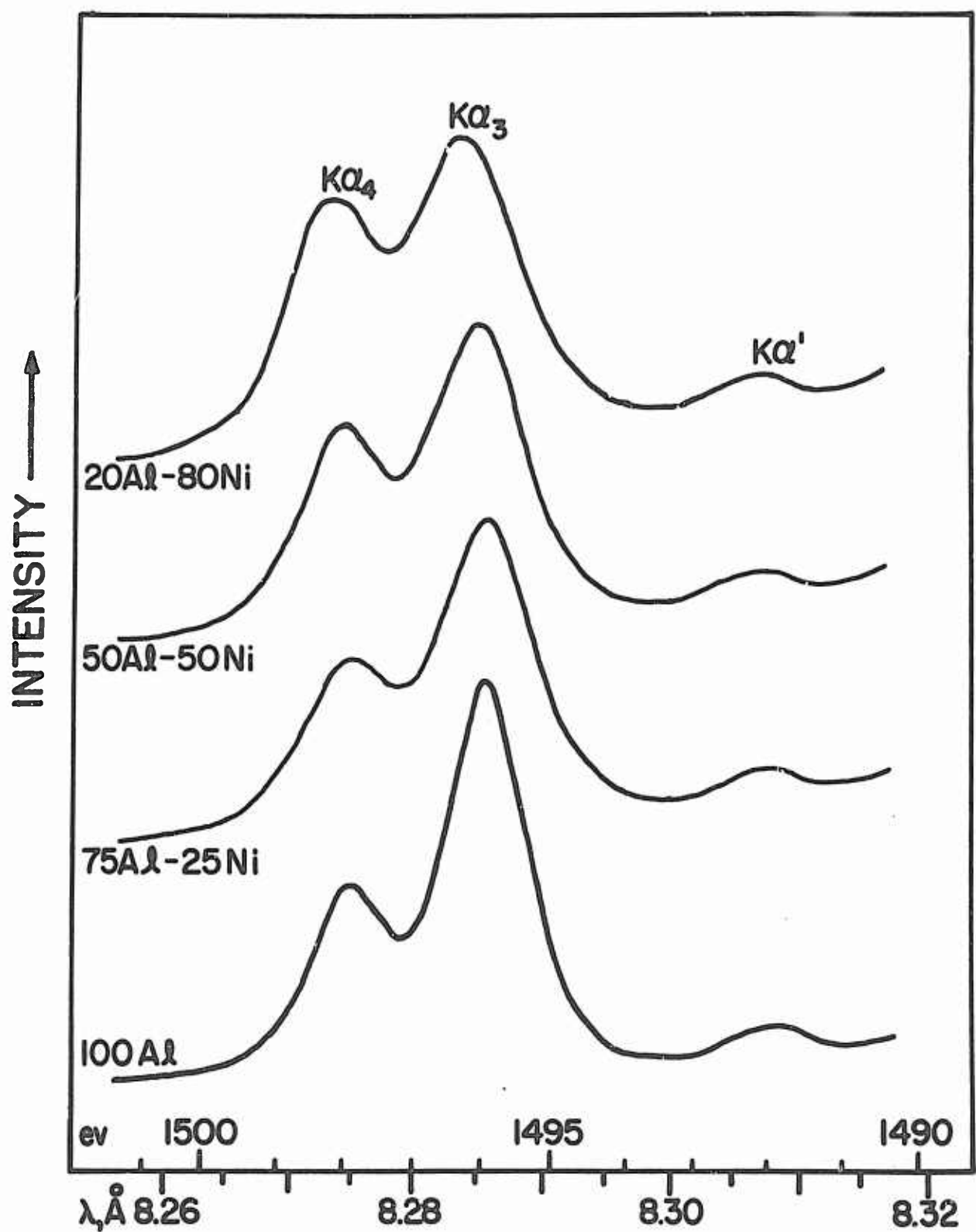


Figure 16. Aluminum Ka' , Ka_3 and Ka_4 Lines from Some Al-Ni Alloys (EDDT Crystal)

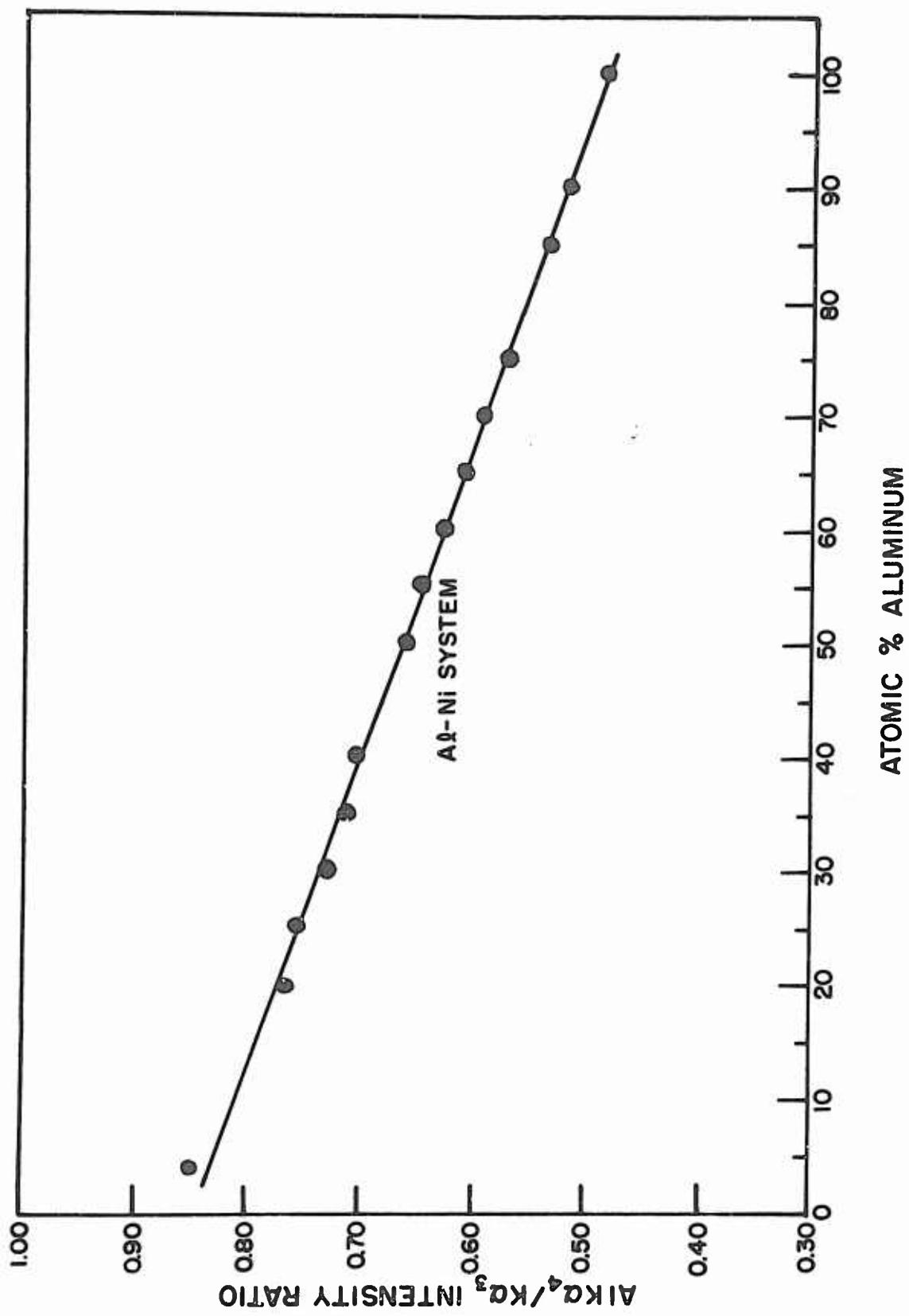


Figure 17. Variation in $Al K\alpha_4/K\alpha_3$ Intensity Ratio with Alloy Composition in Al-Ni System

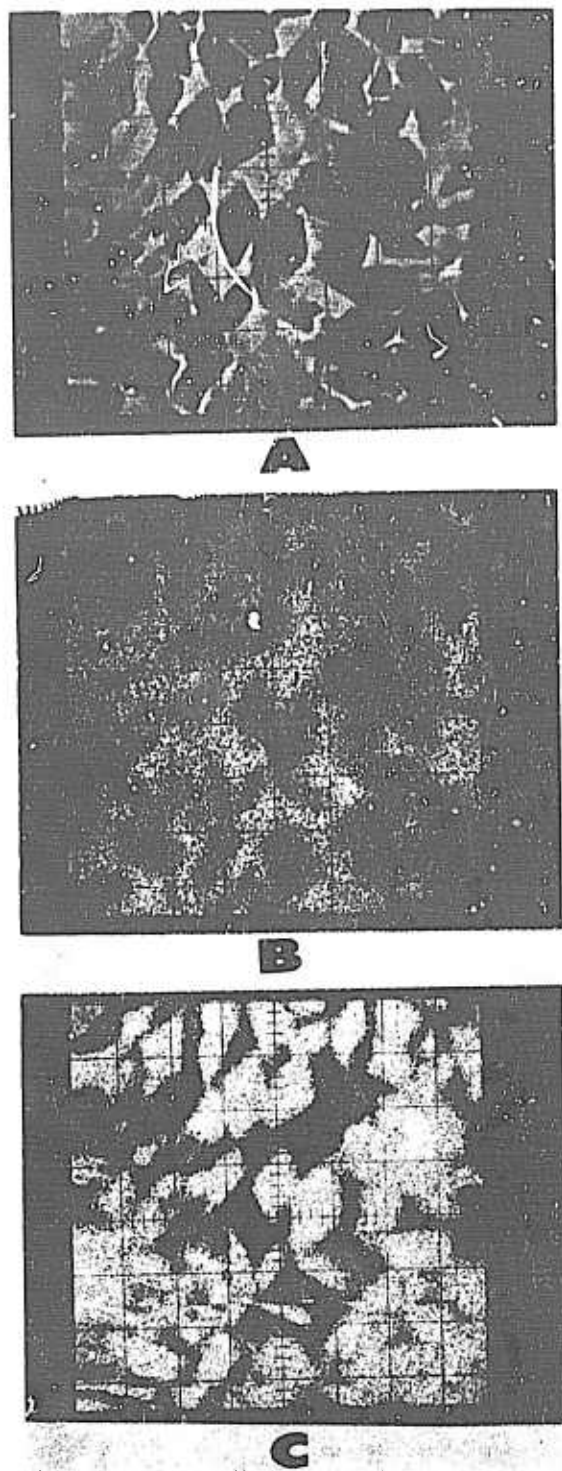


Figure 18. Microprobe Scan Images of 85Al-15Ni Alloy; (A) Beam Current Image at About 500X, (B) Al K X-ray Scan, (C) Ni K X-ray Scan

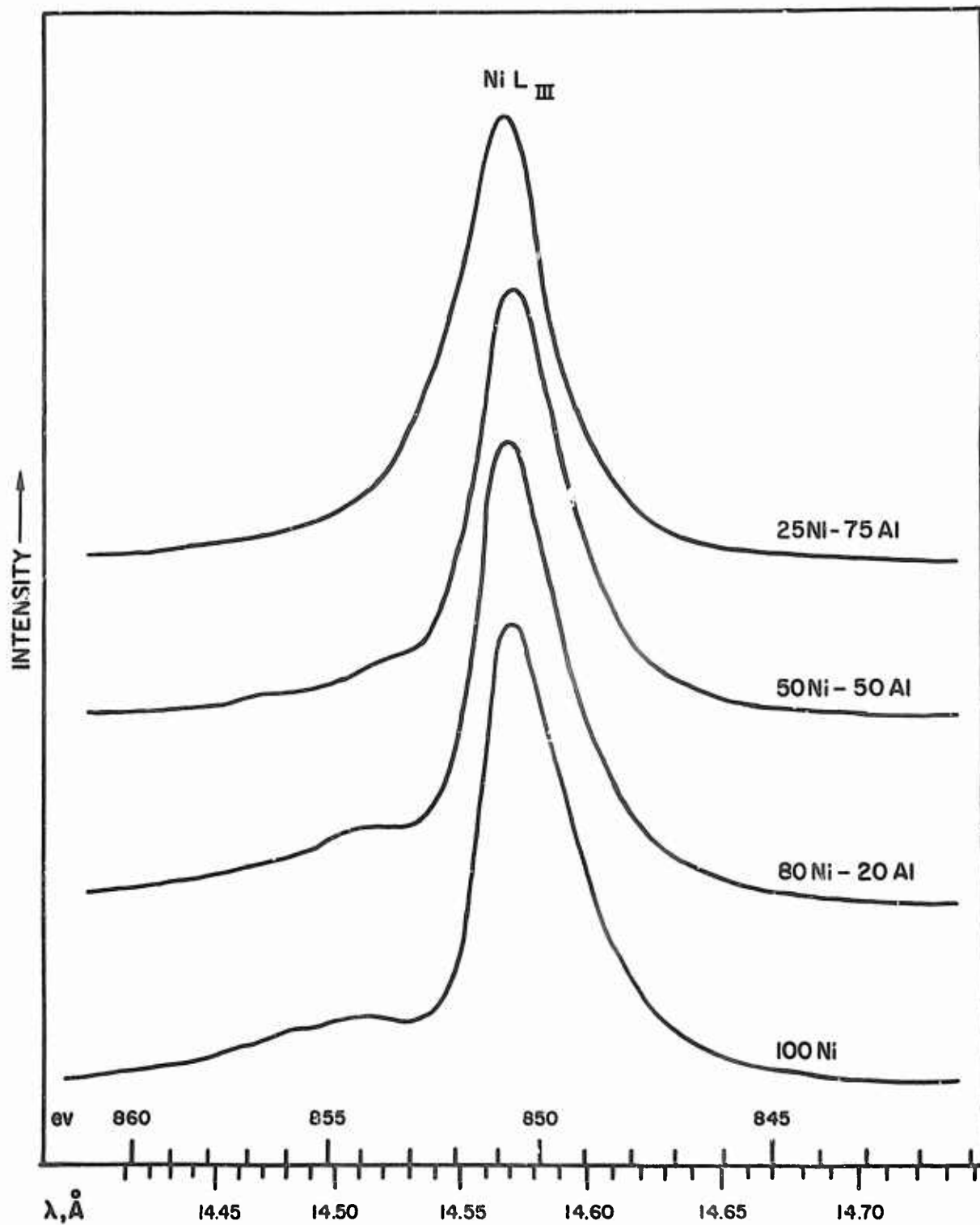


Figure 19. Ni L_{III} Emission Band from Some Al-Ni Alloys (Gypsum Crystal)

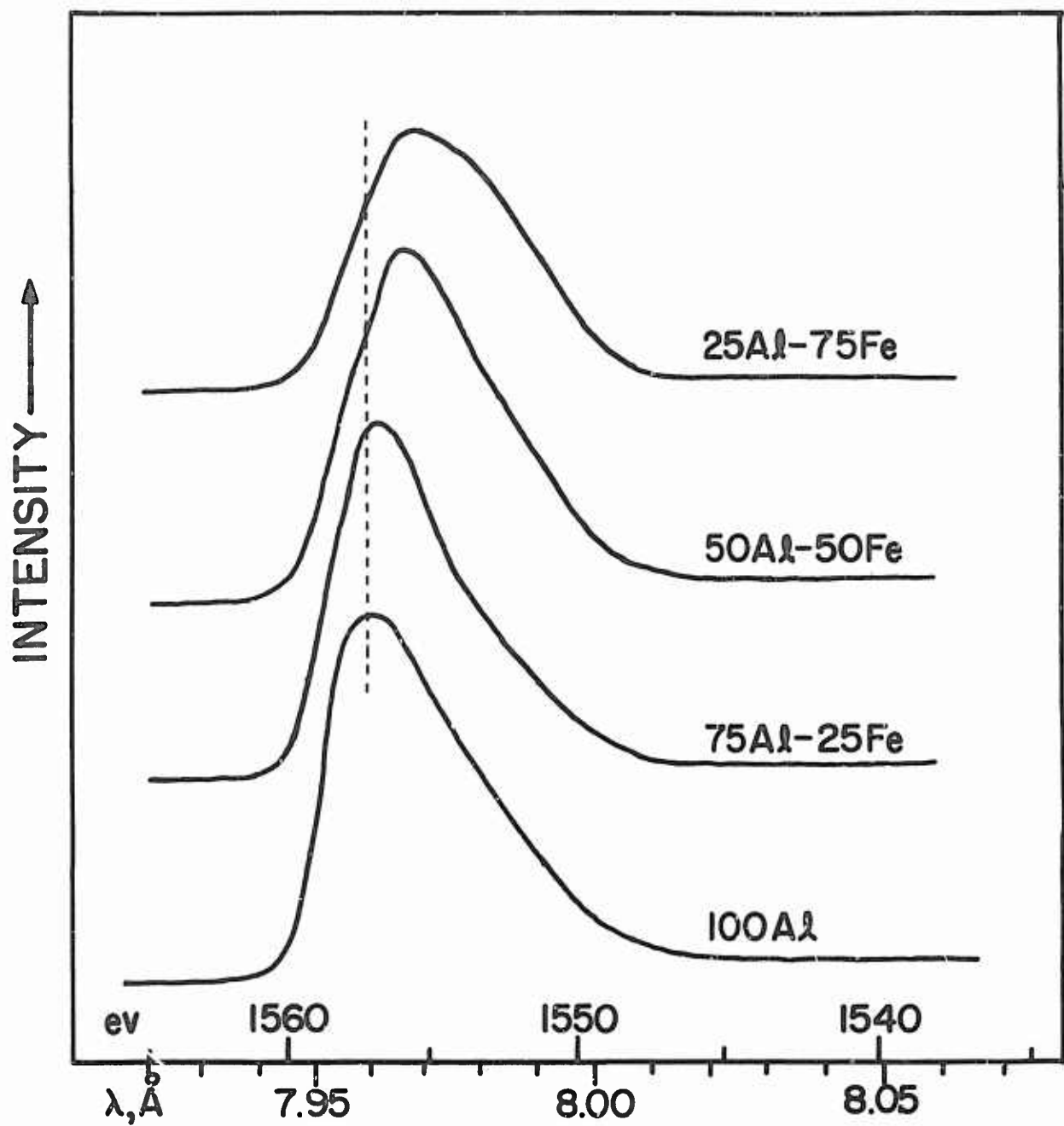


Figure 20. Aluminum K Emission Band from Some Al-Fe Alloys (EDDT Crystal)

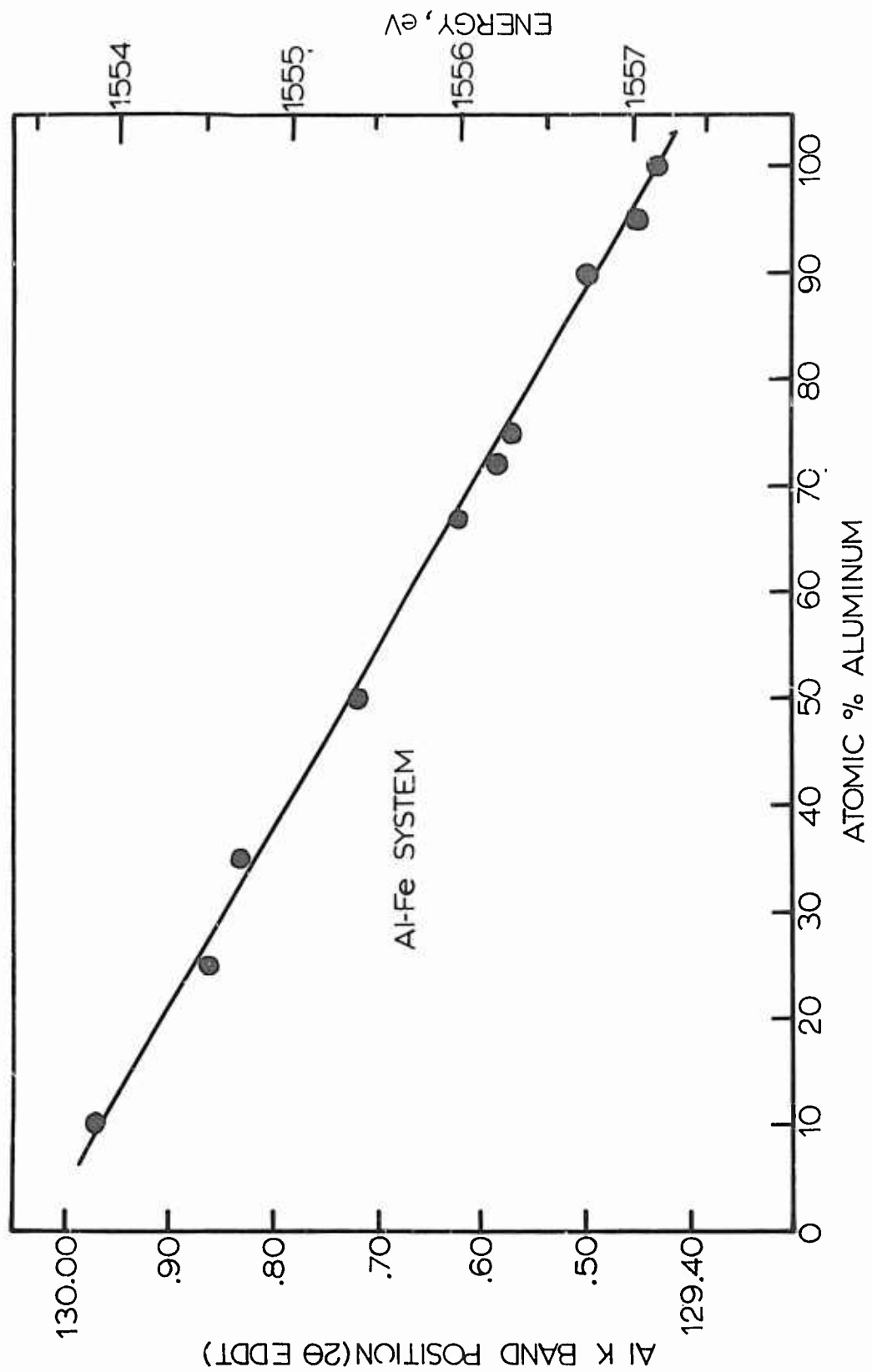


Figure 21. Al K Band Shift with Alloy Composition in Al-Fe System

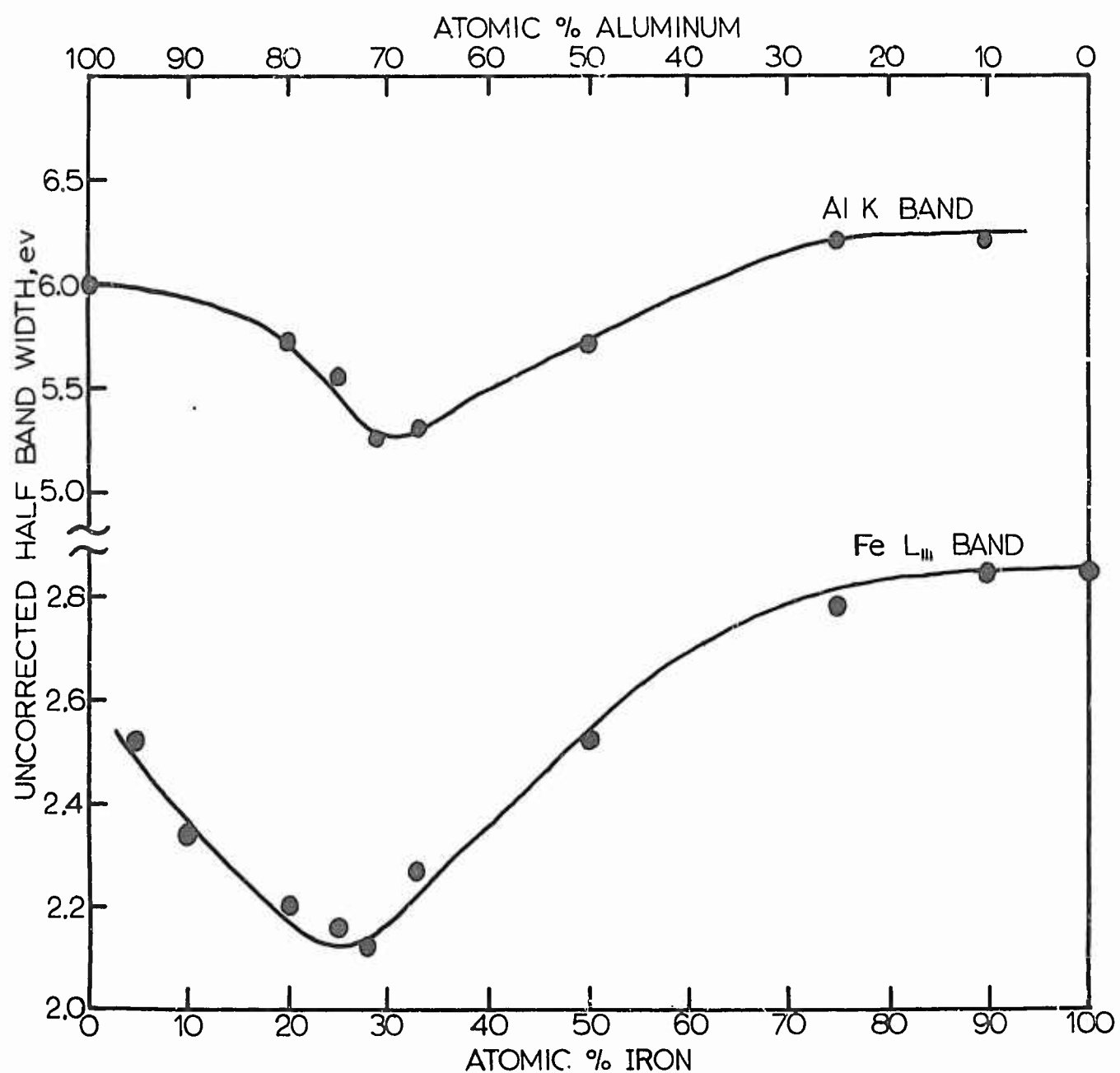


Figure 22. Variation in Uncorrected Half Band Width for Al K and Fe L_{III} Bands in Al-Fe System

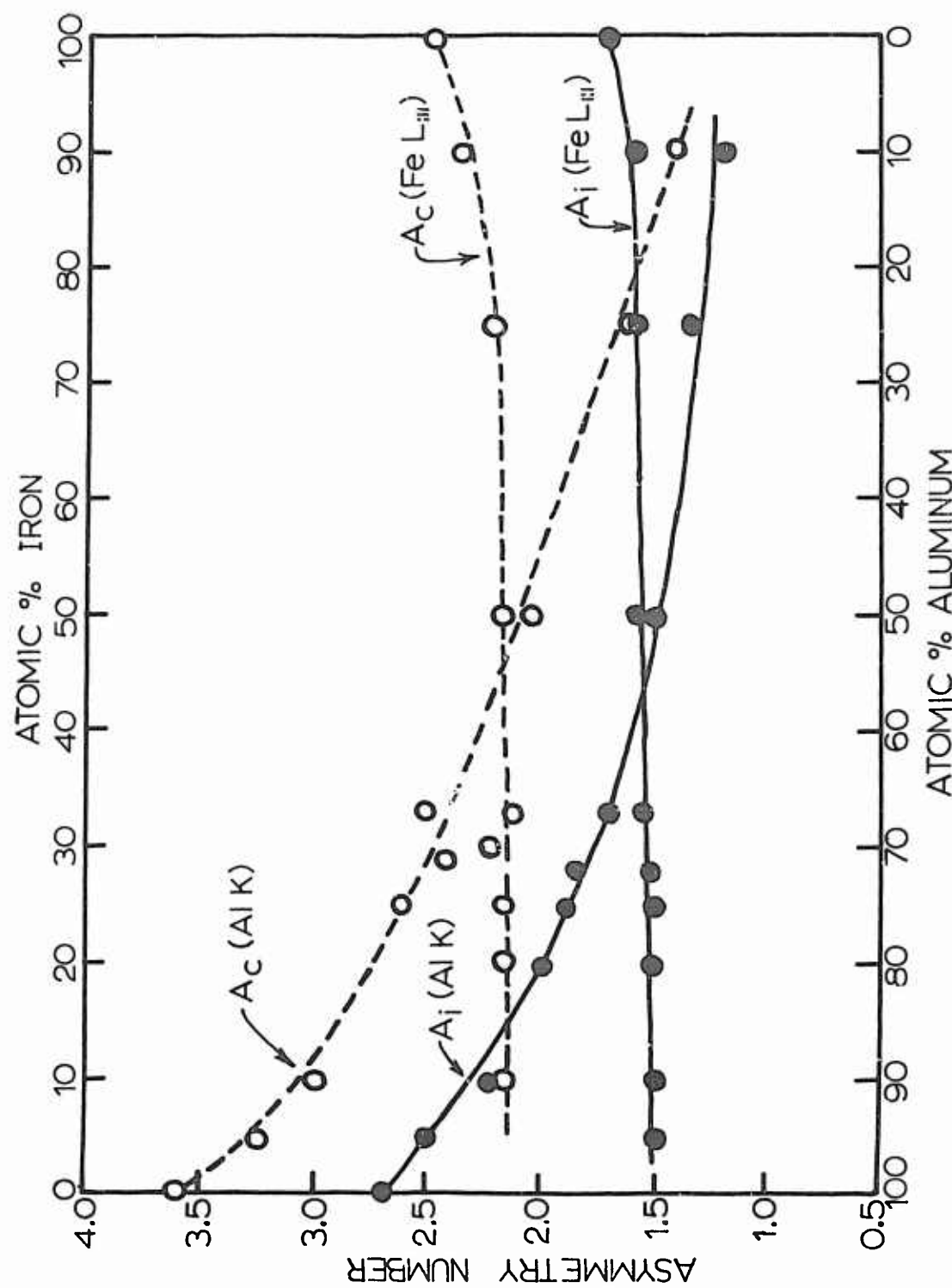


Figure 23. Change in Asymmetry Constants of Al K and FeL_{III} Bands with Alloy Composition in Al-Fe System

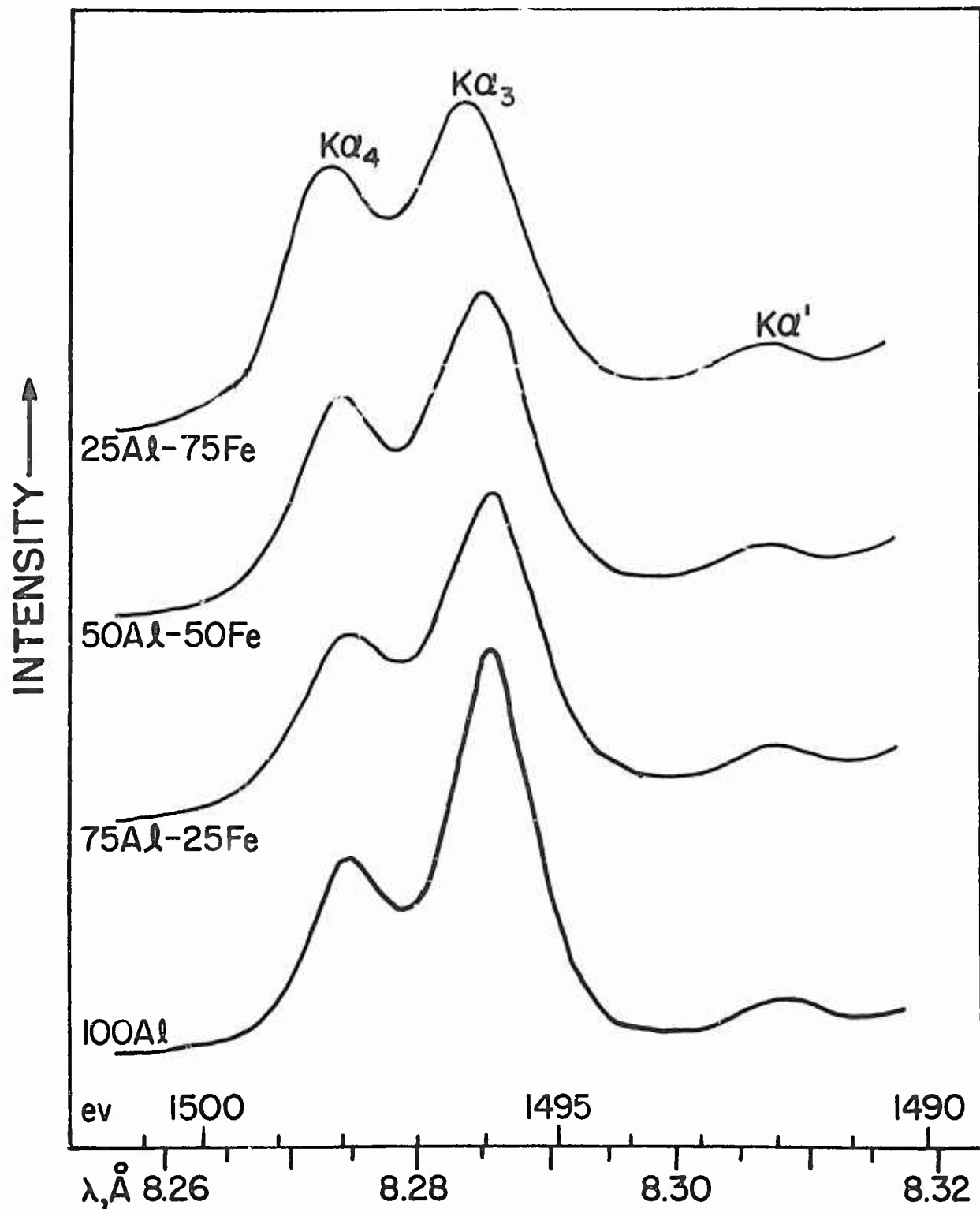


Figure 24. Aluminum Ka' , Ka_3 and Ka_4 Lines from Some Al-Fe Alloys (EDDT Crystal)

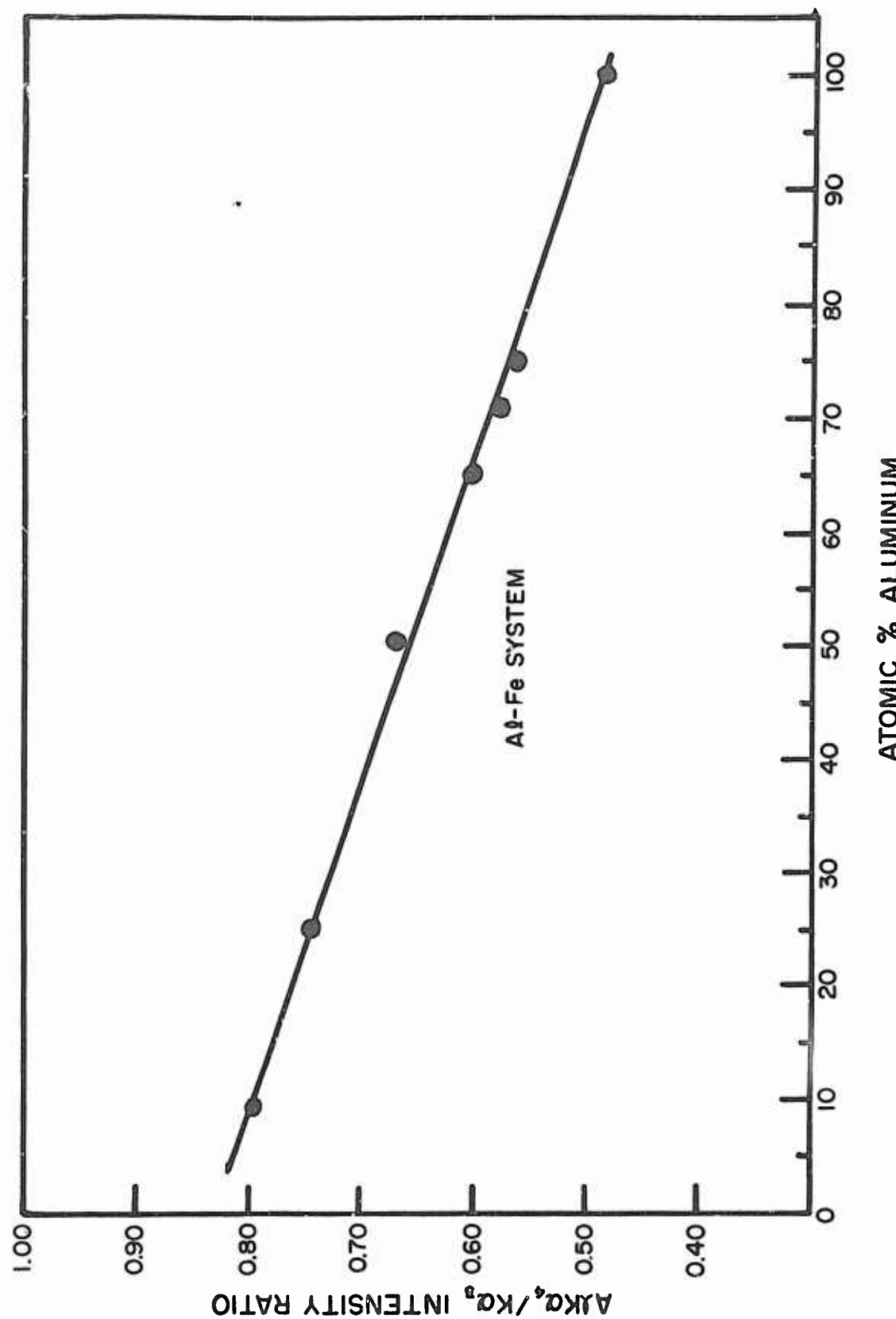


Figure 25. Variation in Al $K\alpha_4/K\alpha_3$ Intensity Ratio with Alloy Composition in Al-Fe System

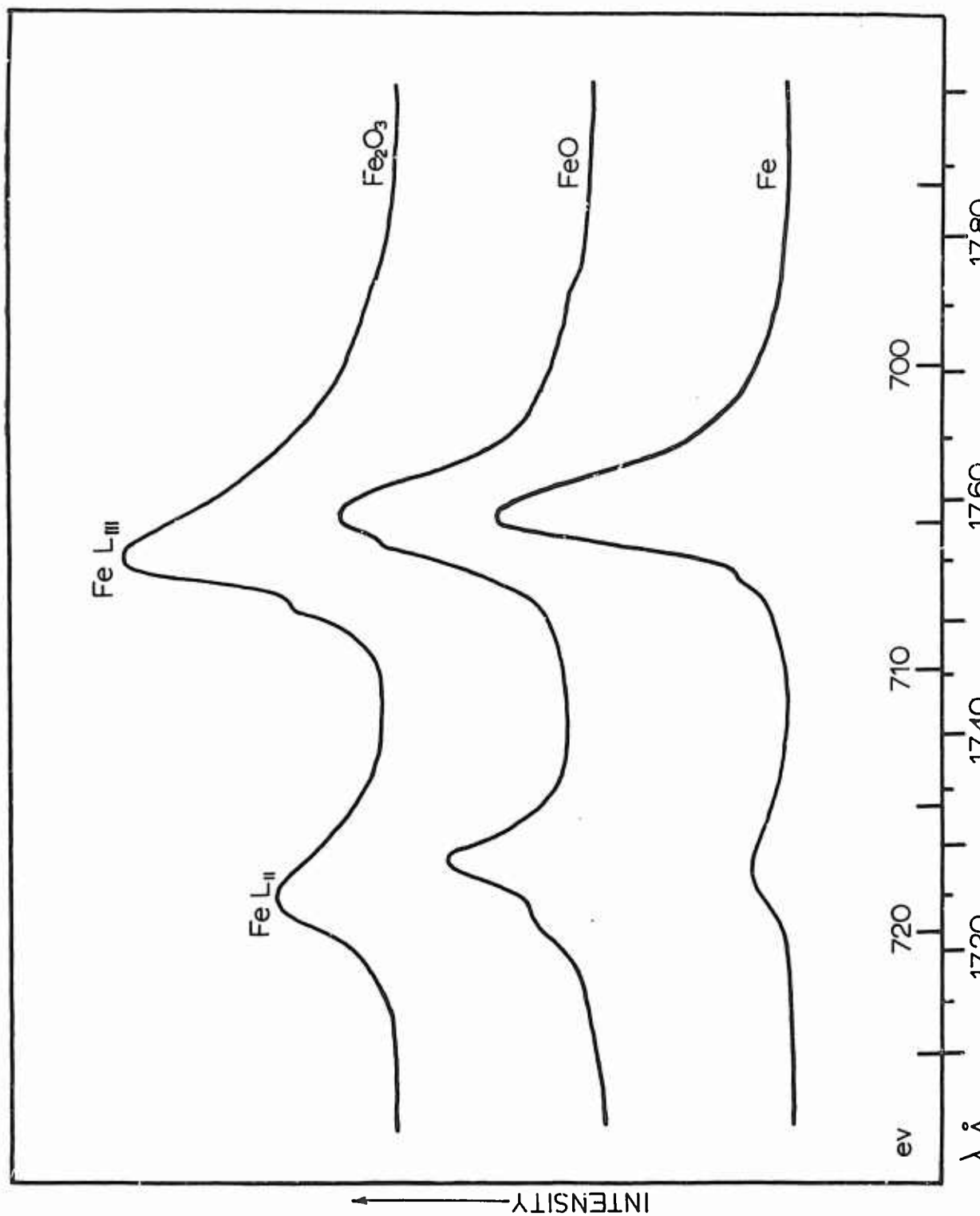


Figure 26. FeL_{II} and L_{III} Emission Bands from Fe , FeO and Fe_2O_3 (Itaconic Acid Crystal)

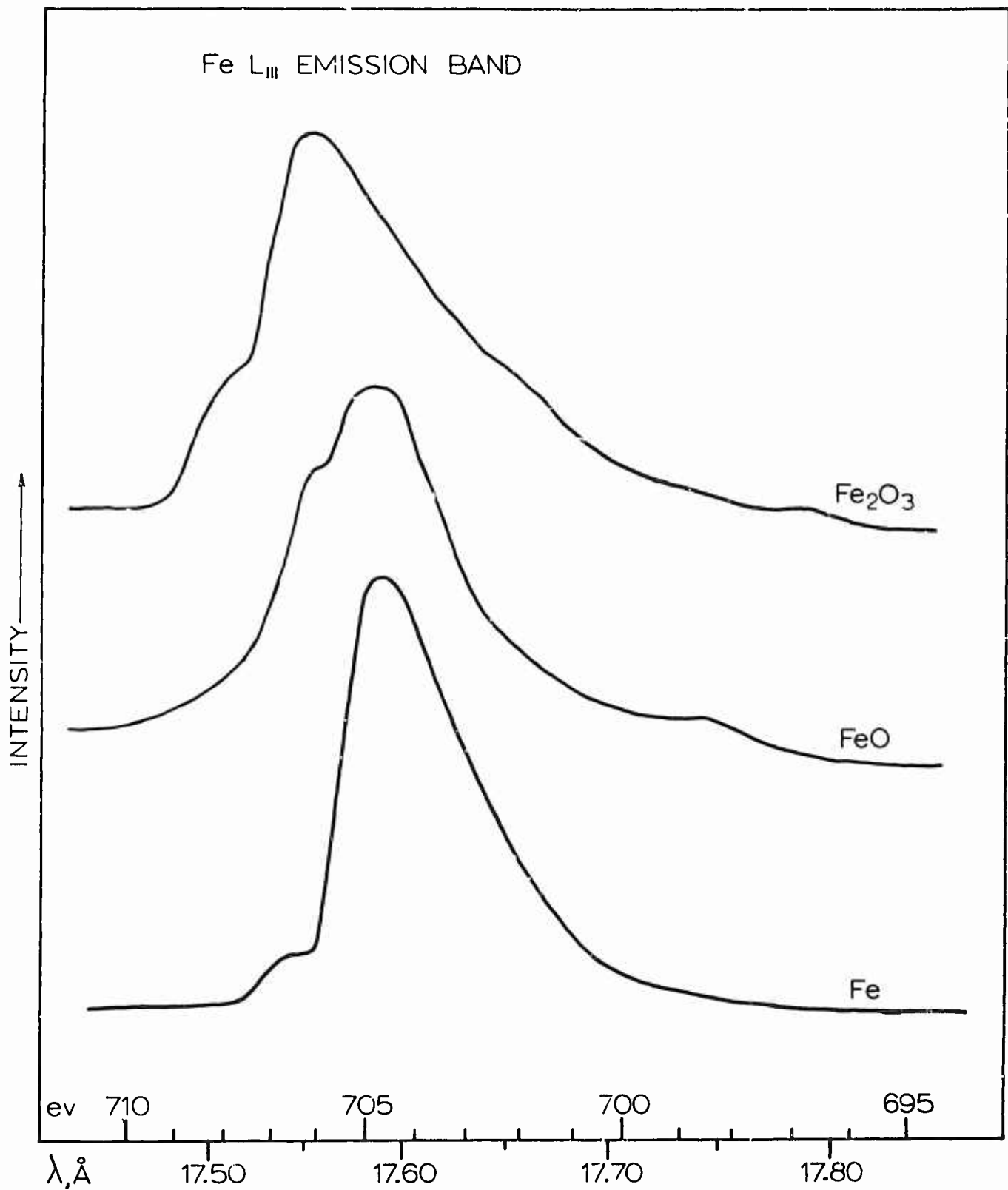


Figure 27. Fe L_{III} Emission Band from Fe, FeO and Fe₂O₃ (Itaconic Acid Crystal)

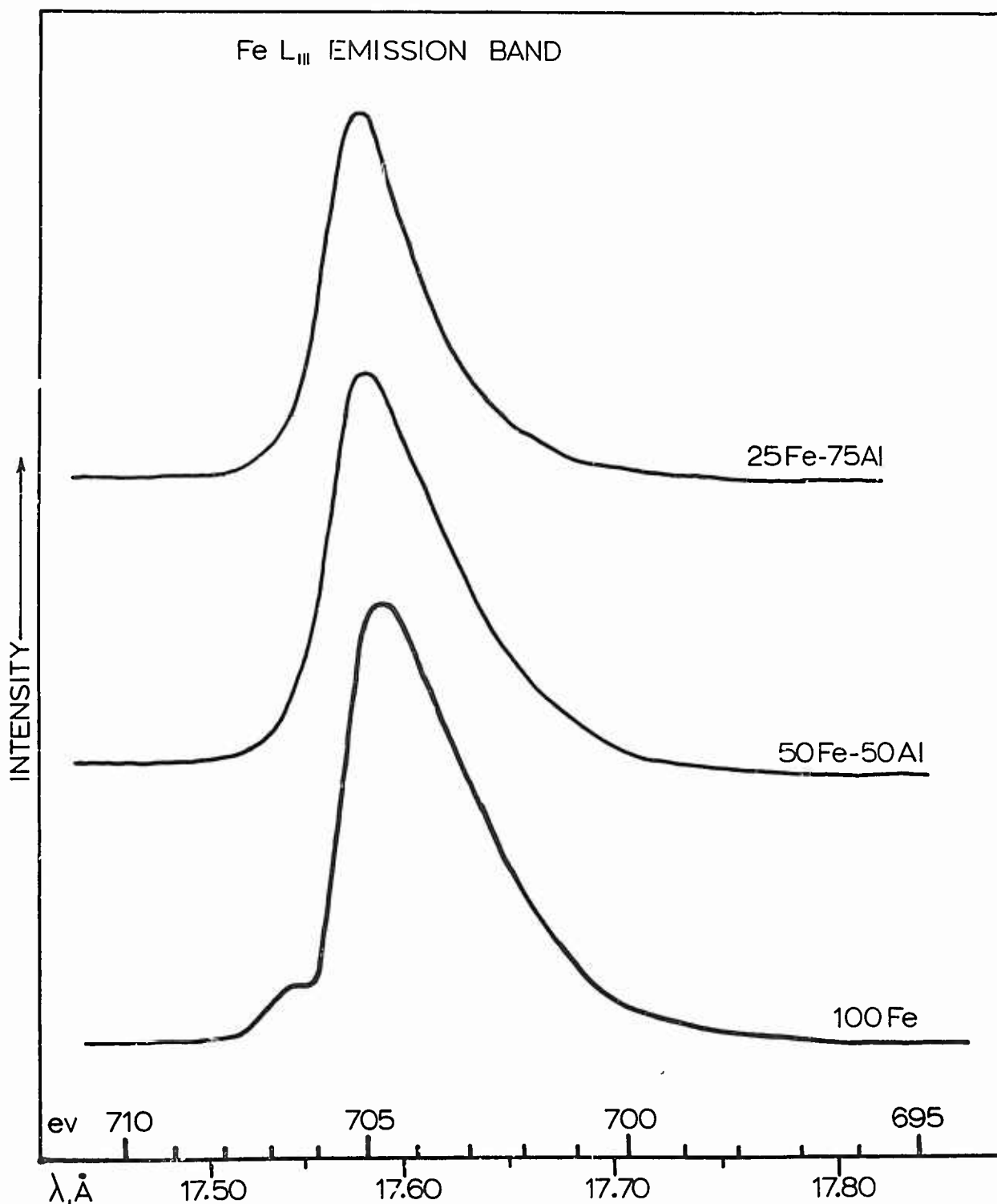


Figure 28. Fe L_{III} Emission Band from Some Al-Fe Alloys (Itaconic Acid Crystal)

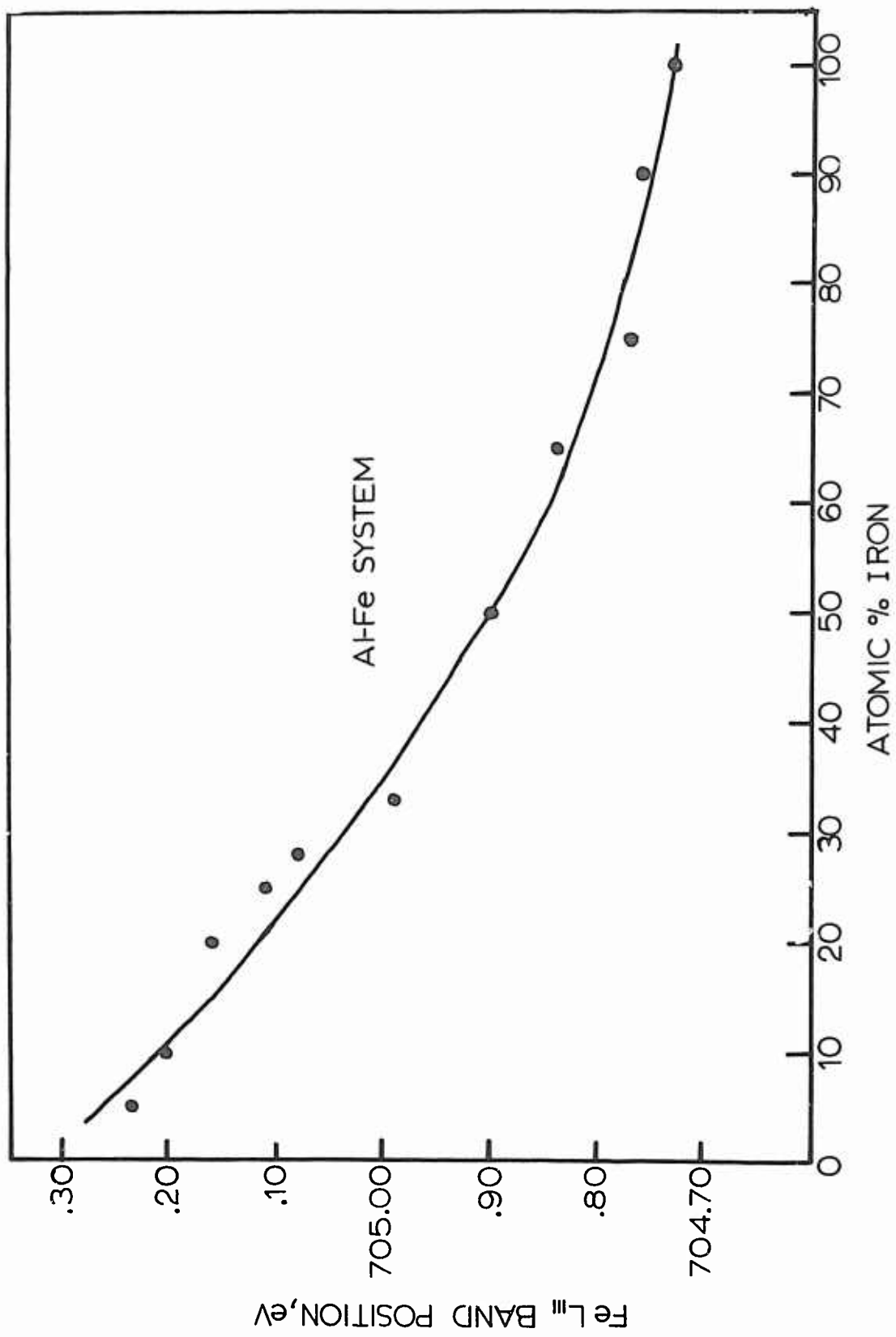


Figure 29. FeL_{III} Band Shift with Alloy Composition in Al-Fe System

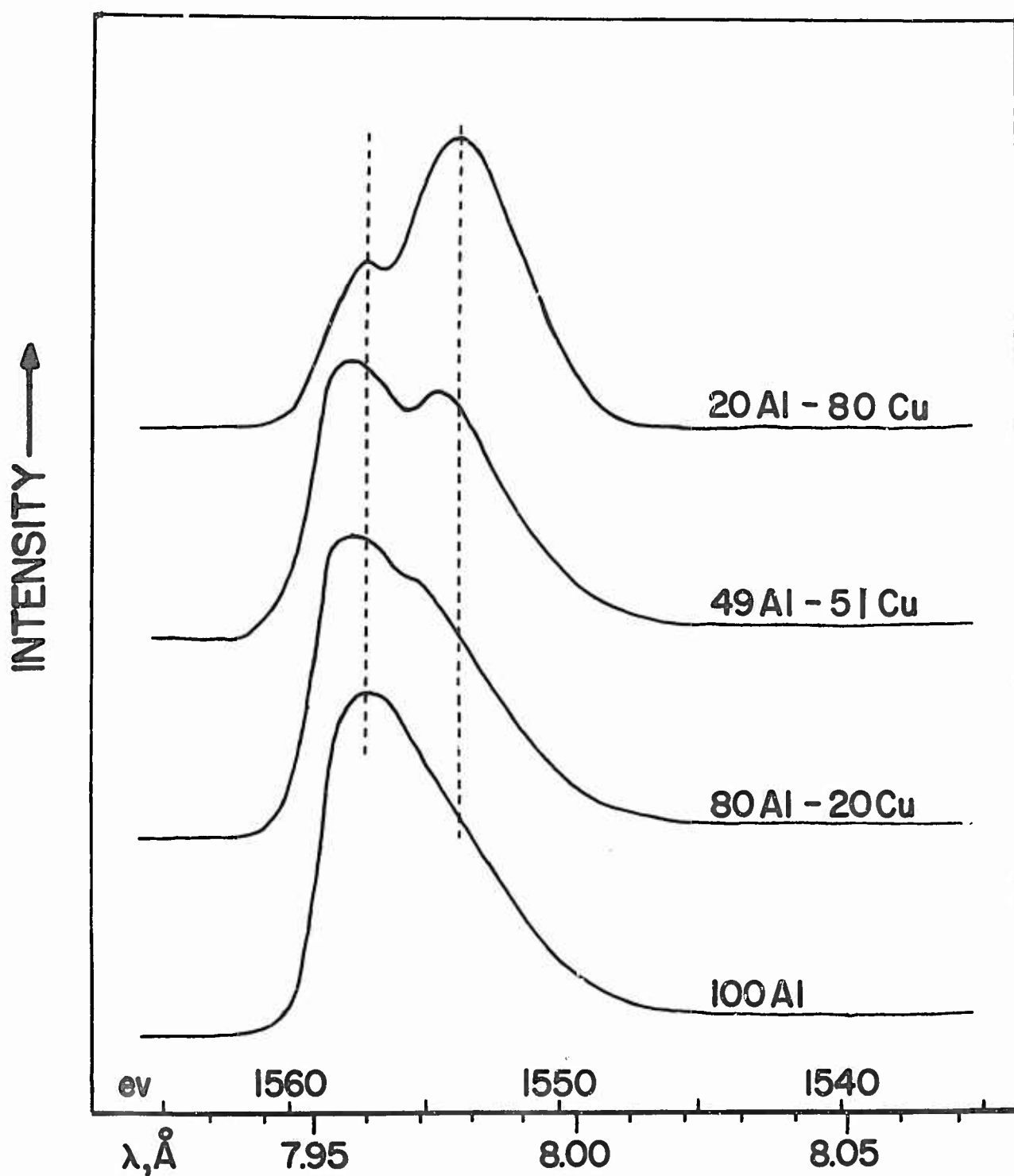


Figure 30. Aluminum K Emission Band from Some Al-Cu Alloys (EDDT Crystal)

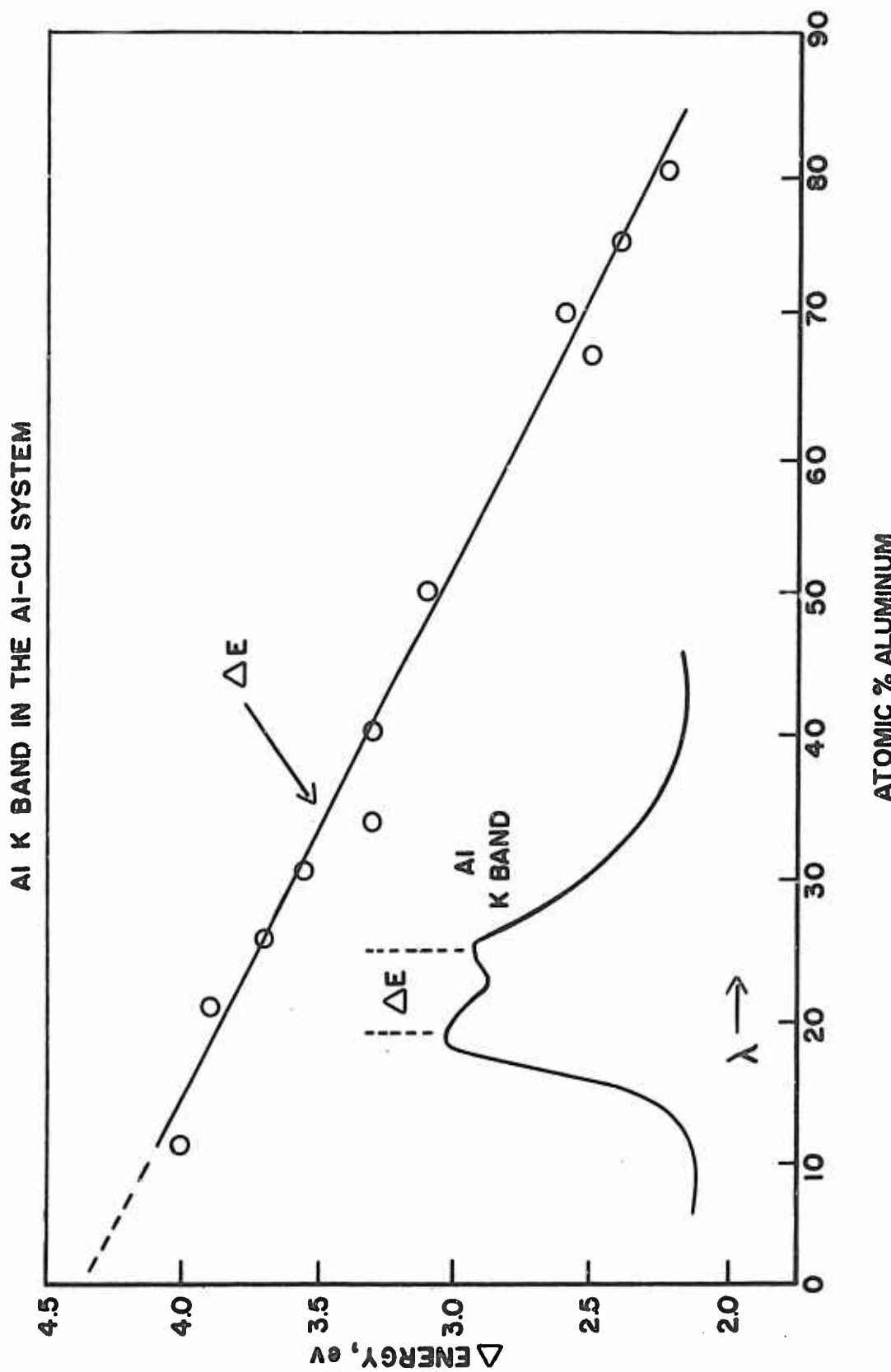


Figure 31. Variations in Energy Difference Between High and Low Energy Components of Al K Band with Alloy Composition in Al-Cu System

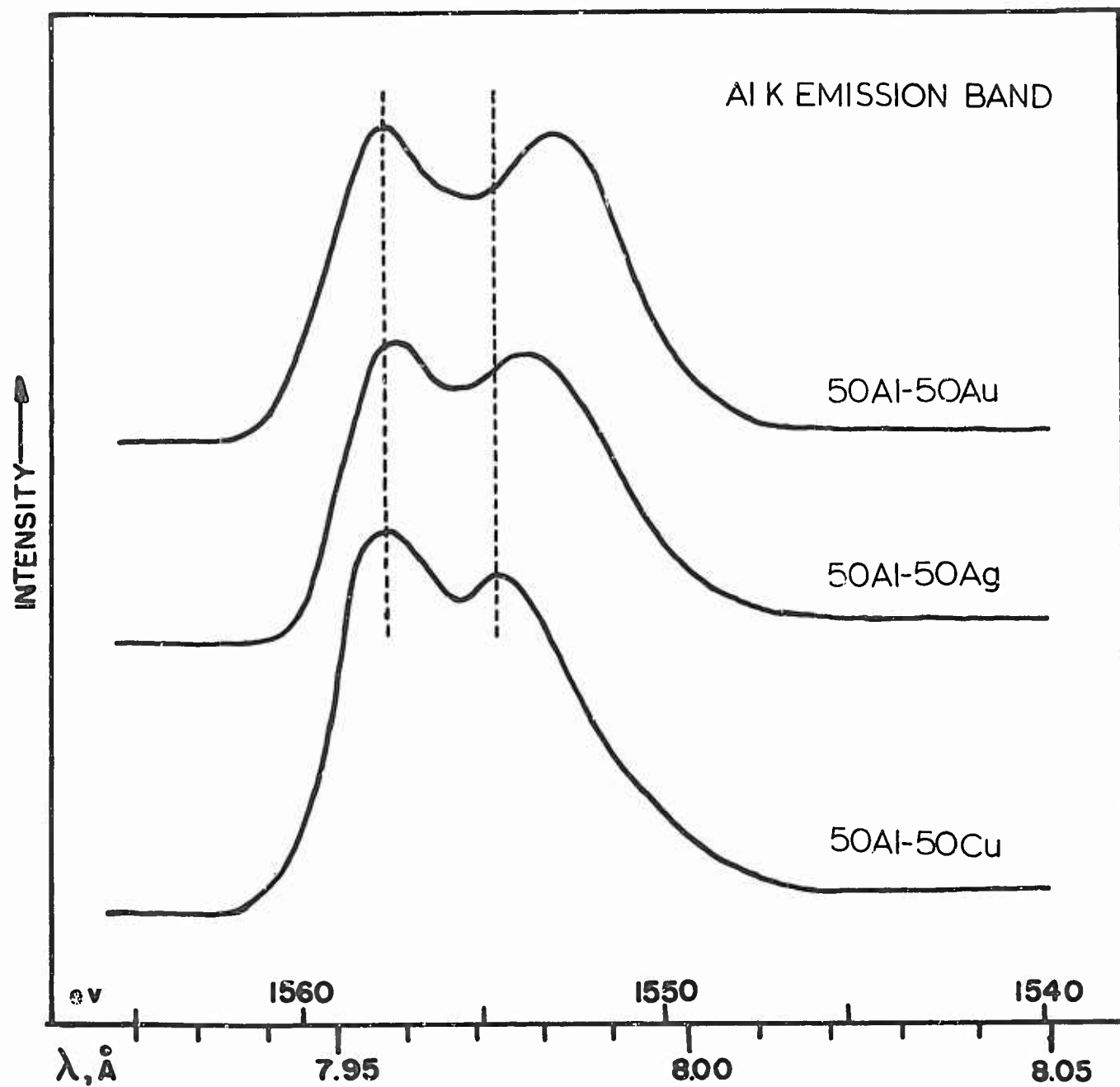


Figure 32. Aluminum K Emission Band from 1:1 Atomic Ratios of Al-Cu, Al-Ag, and Al-Au (EDDT Crystal)

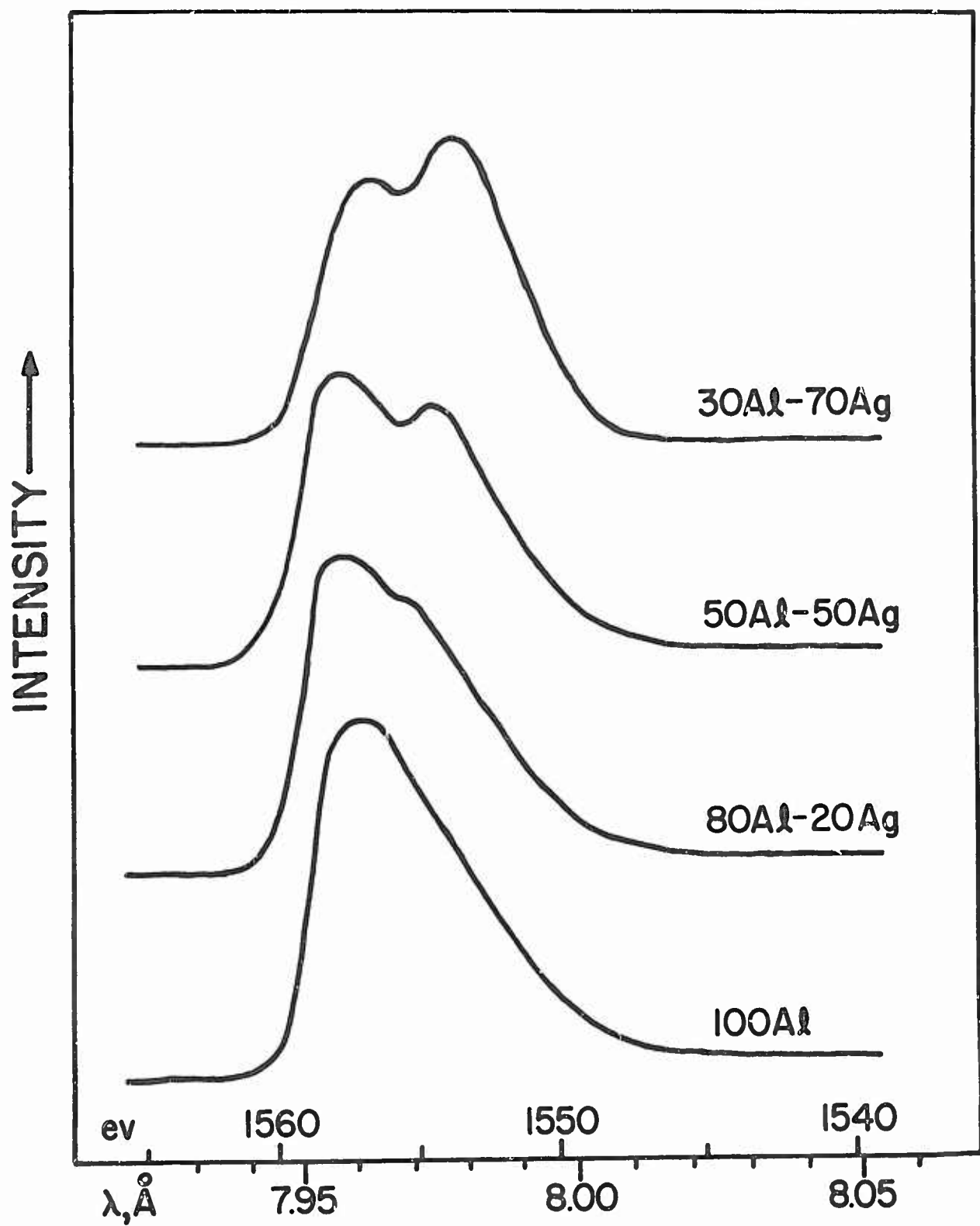


Figure 33. Aluminum K Emission Band from Some Al-Ag Alloys (EDDT Crystal)

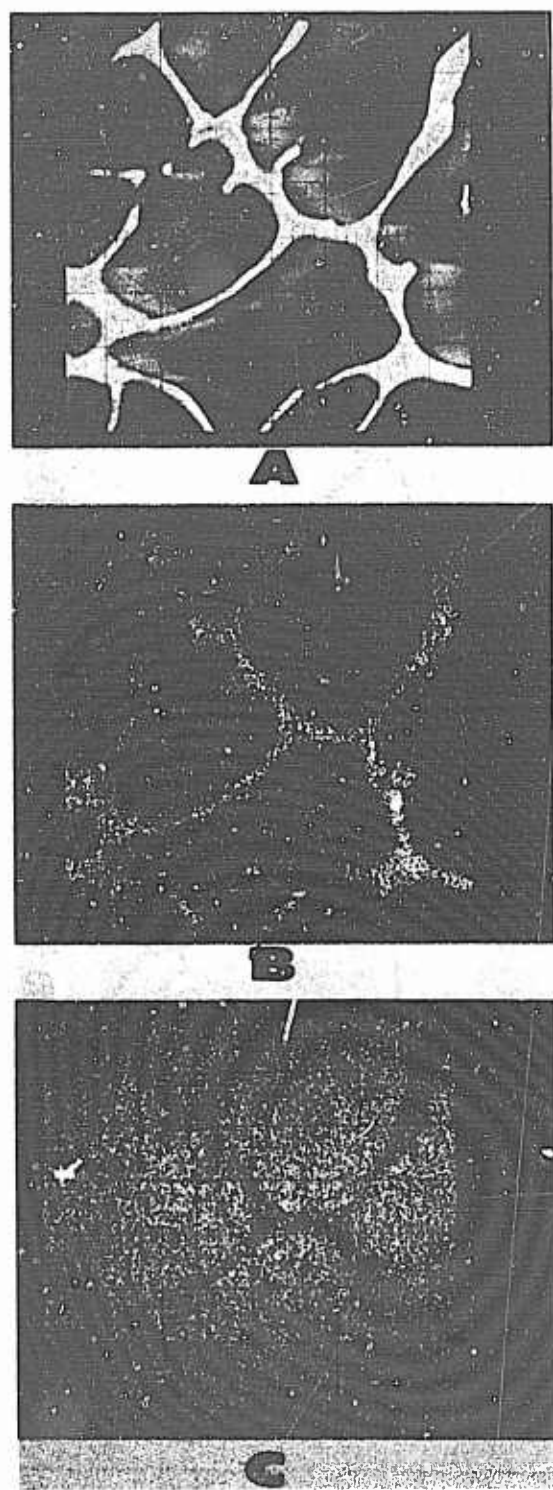
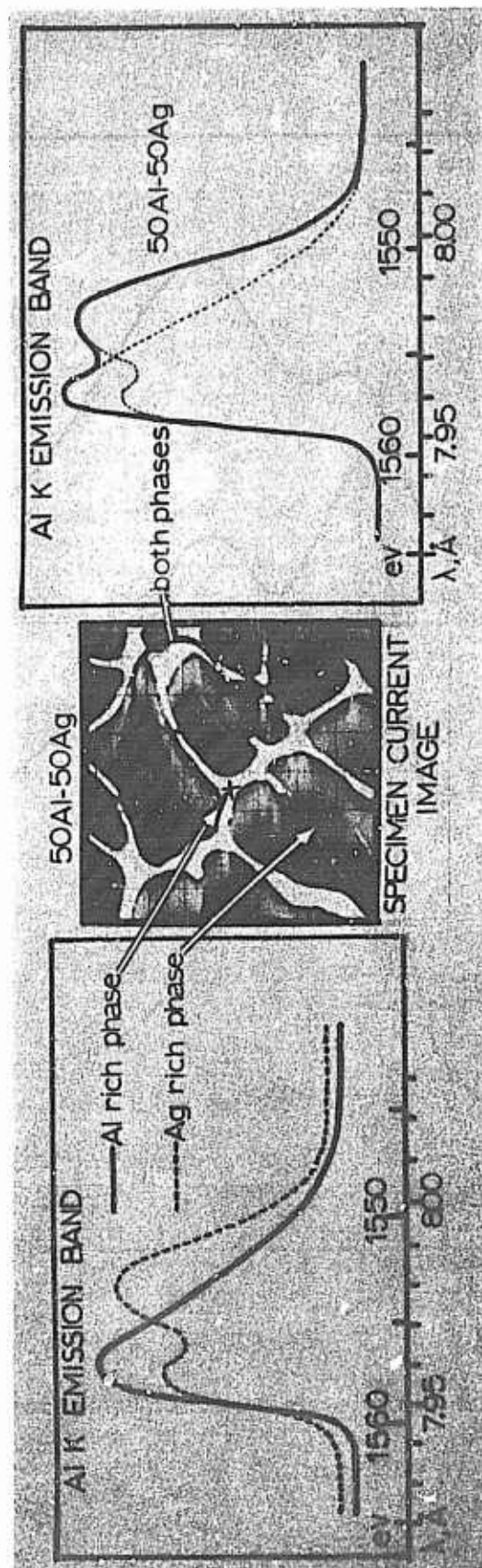


Figure 34. Microprobe Scan Images of 50Al-50Ag Alloy; (a) Specimen Current Image $\sim 500X$, (b) Al K X-ray Scan, (c) Ag K X-ray Scan



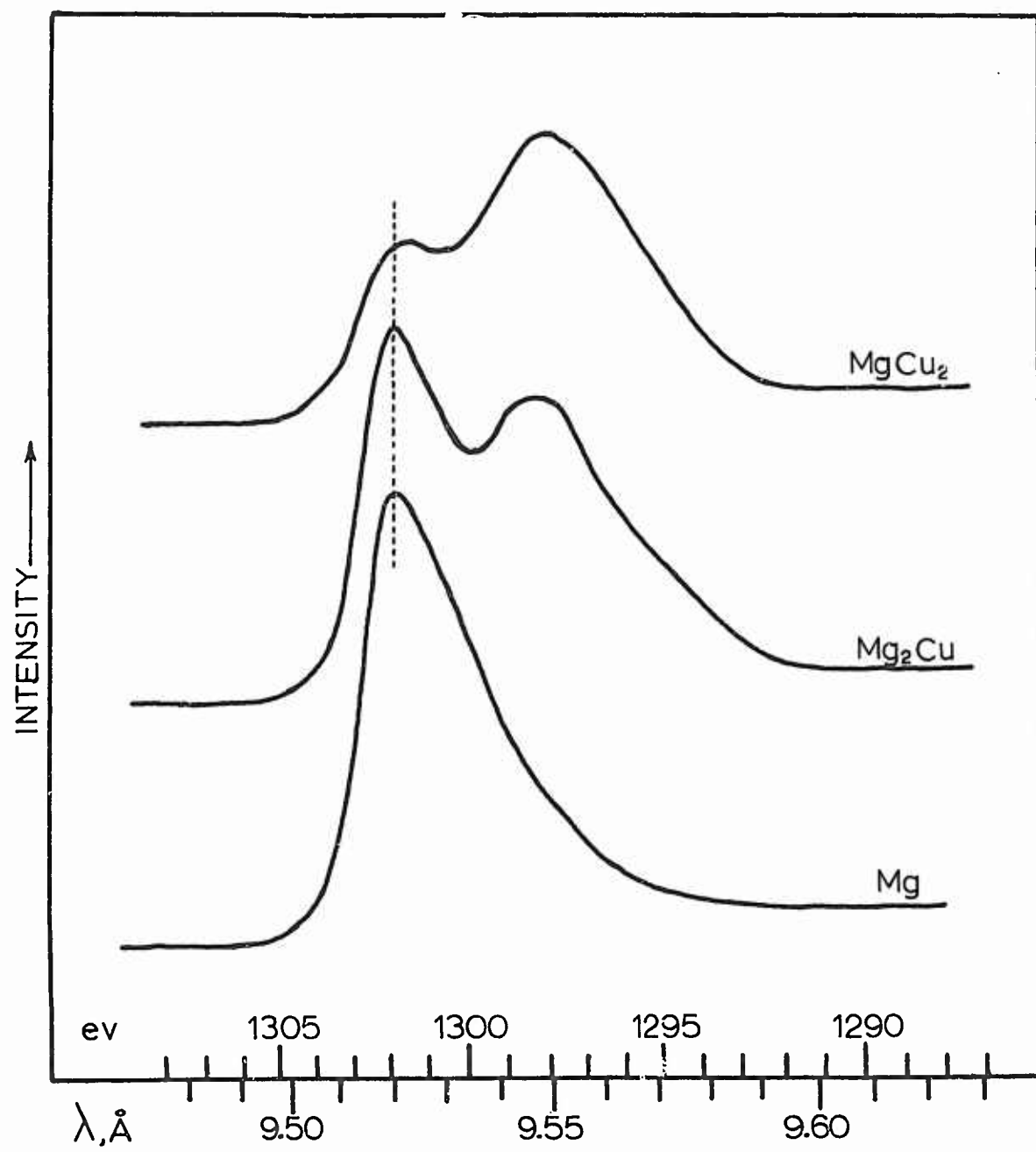


Figure 36. ¹Magnesium K Emission Band from Some Mg-Cu Alloys (ADP Crystal)

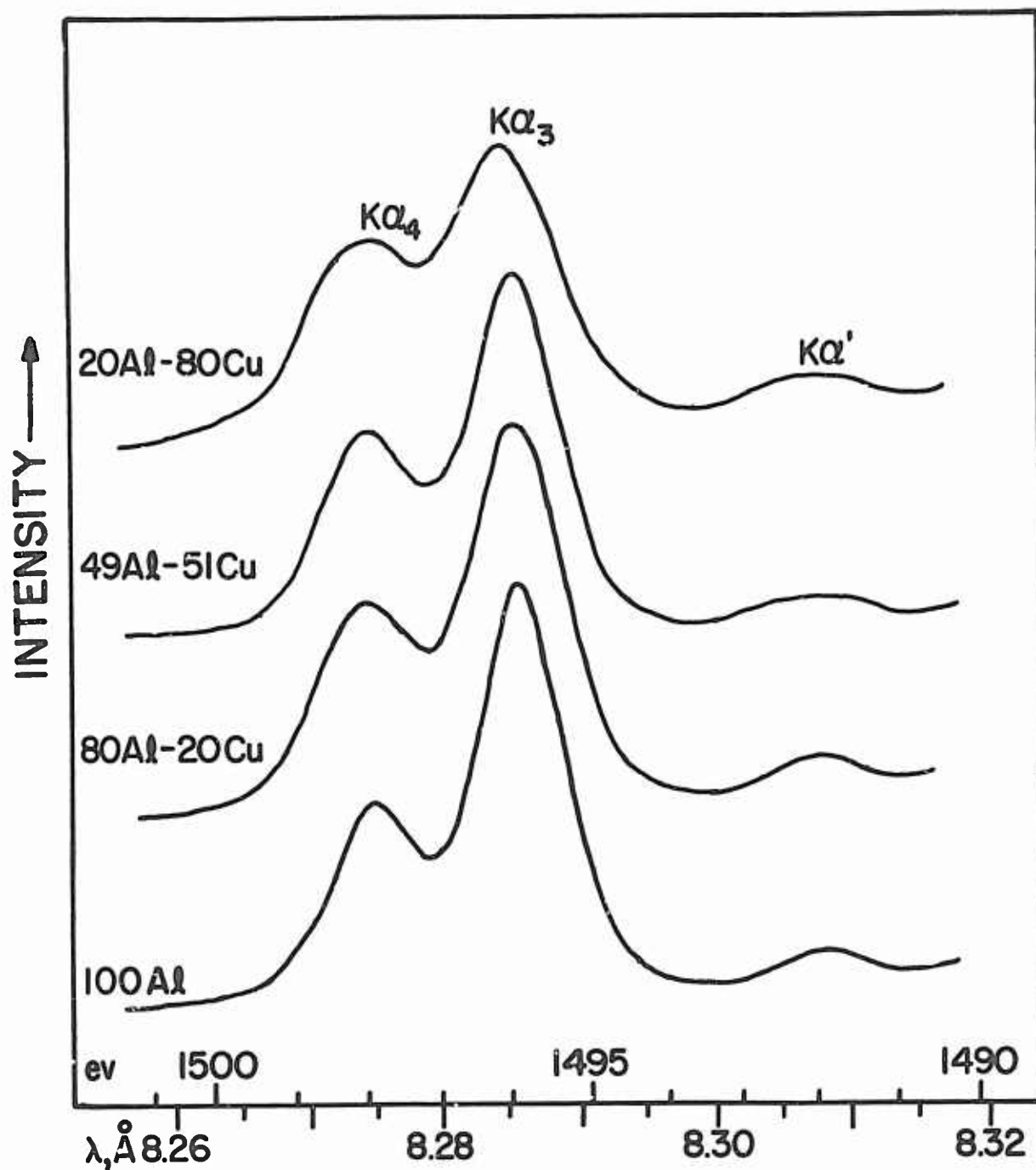


Figure 37. Aluminum $K\alpha'$, $K\alpha_3$ and $K\alpha_4$ Lines from Some Al-Cu Alloys (EDDT Crystal)

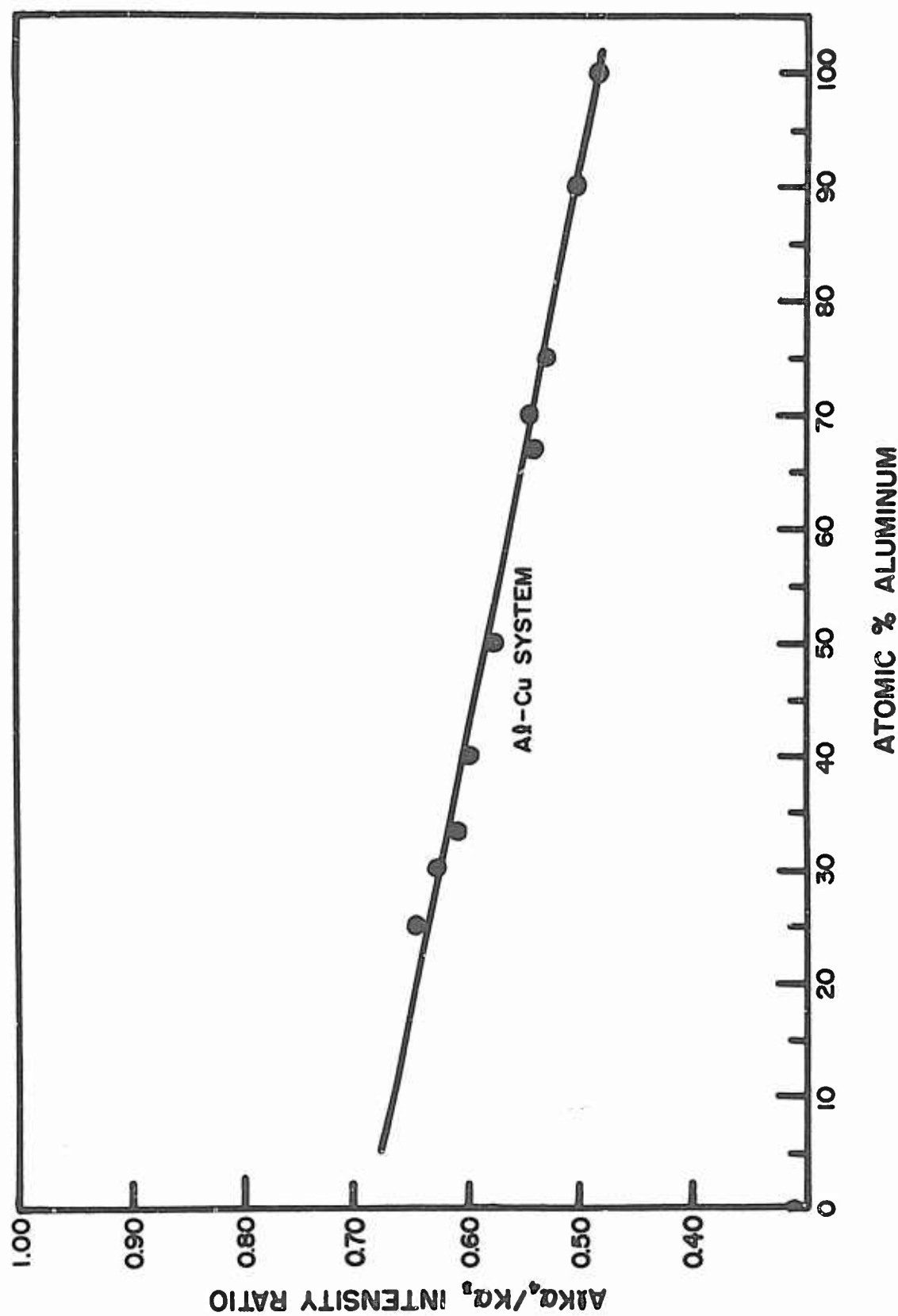


Figure 38. Variation in $\text{Al K}\alpha_2 / \text{K}\alpha_3$ Intensity Ratio with Alloy Composition in Al-Cu System

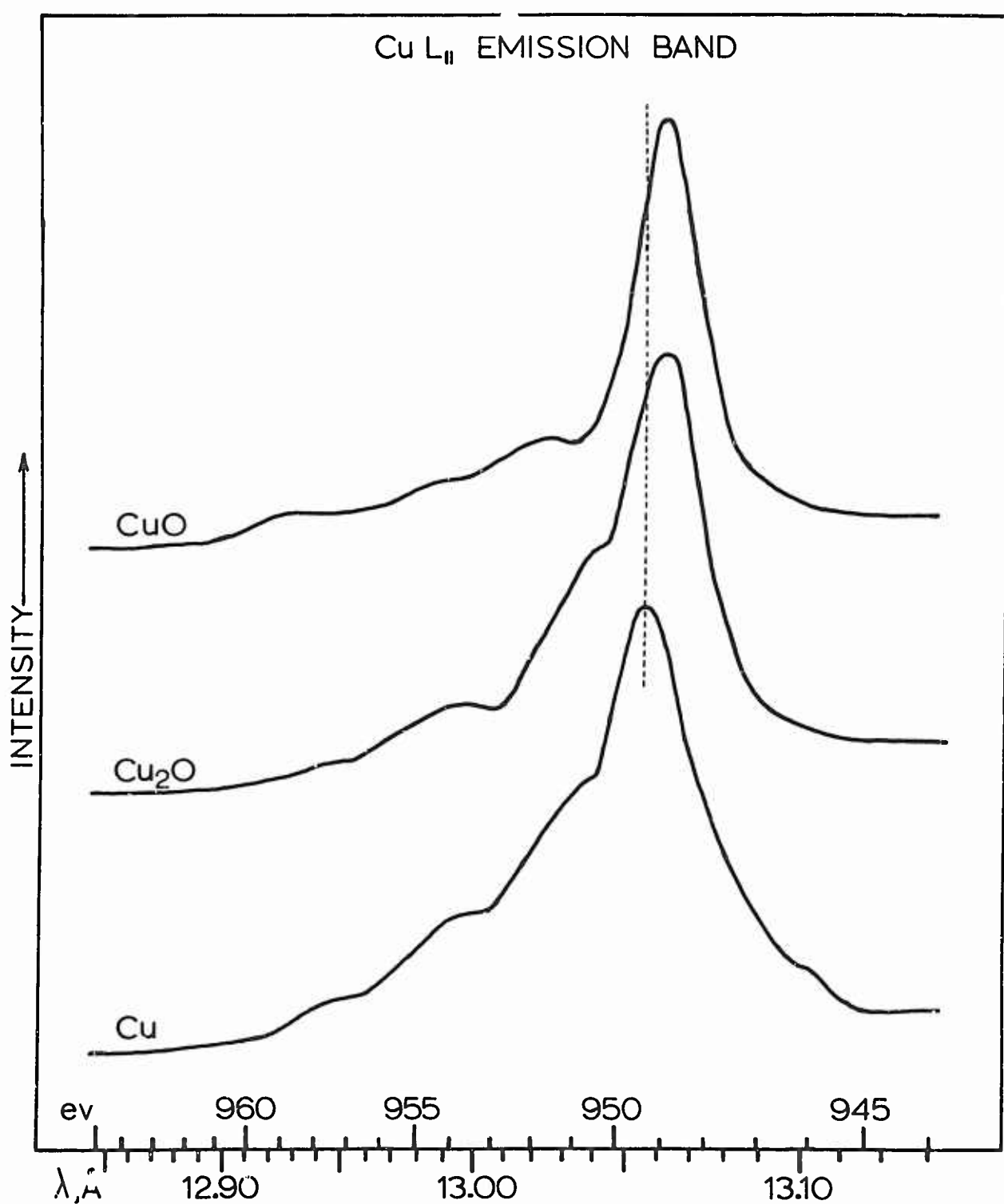


Figure 39. Copper L_{II} Emission Band from Metal and Oxides (NaAP Crystal)

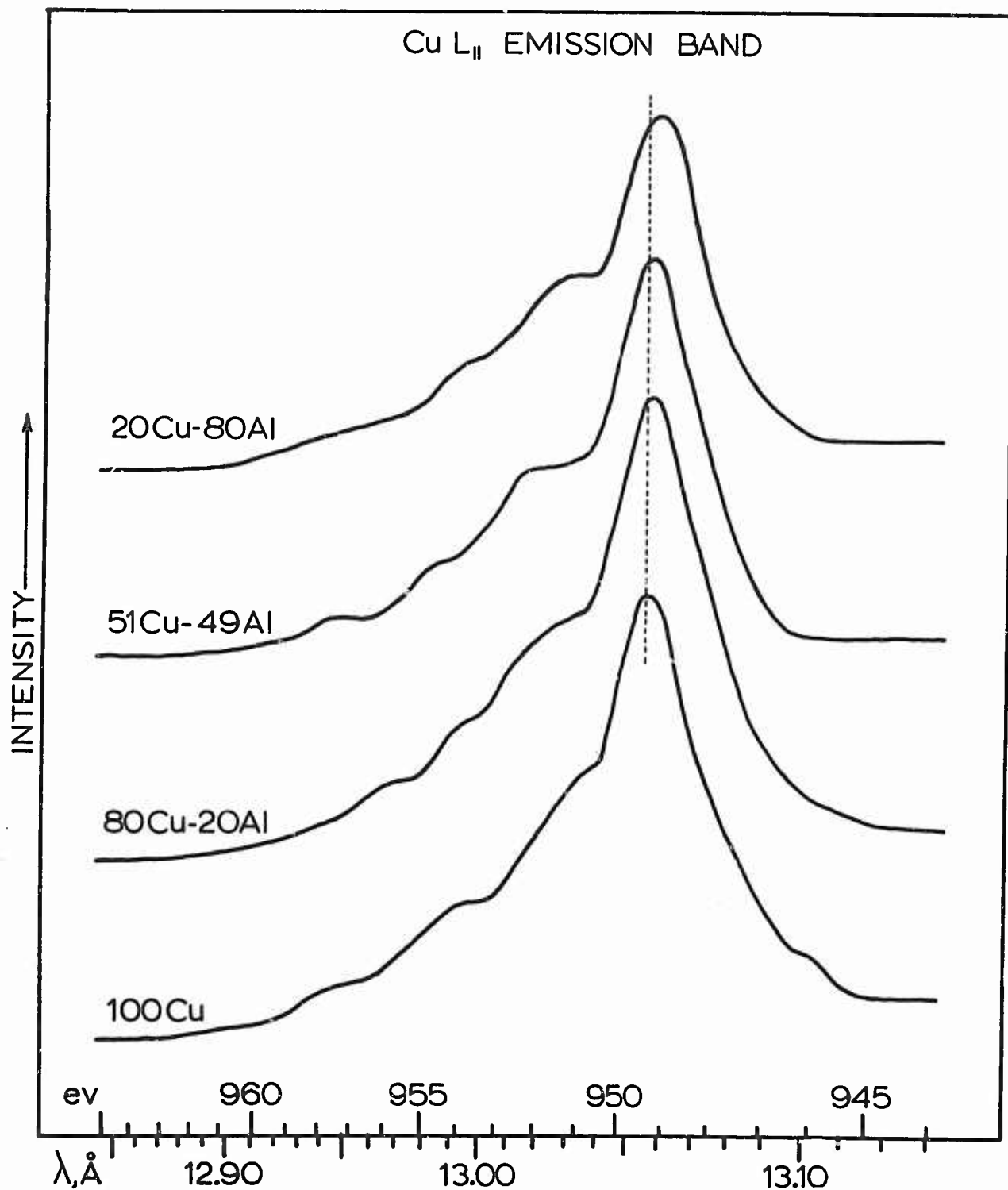
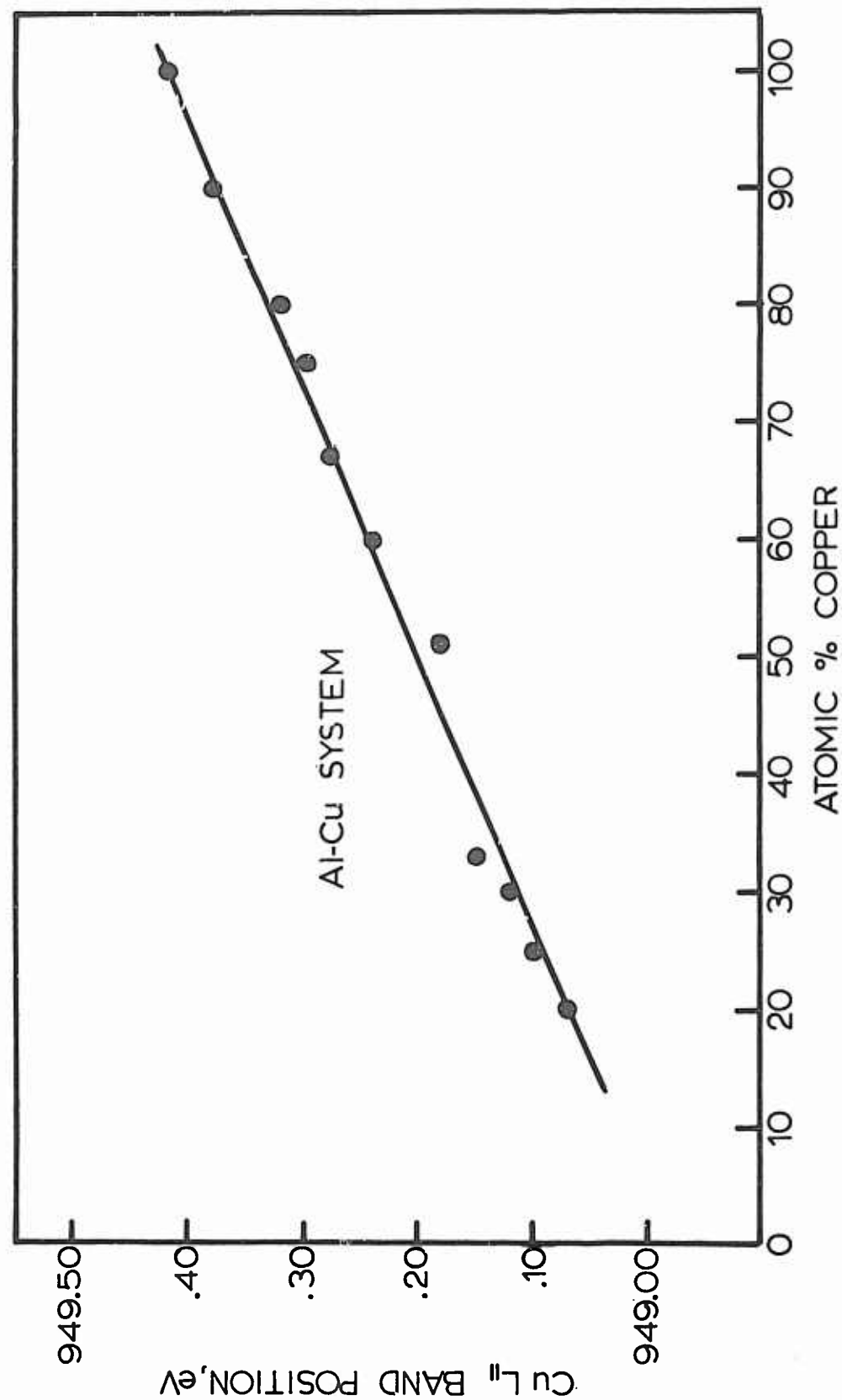


Figure 40. Copper L_{II} Emission Band from Some Cu-Al Alloys (NaAP Crystal)

Figure 41. Copper L_{II} Band Shift with Alloy Composition in Cu-Al System

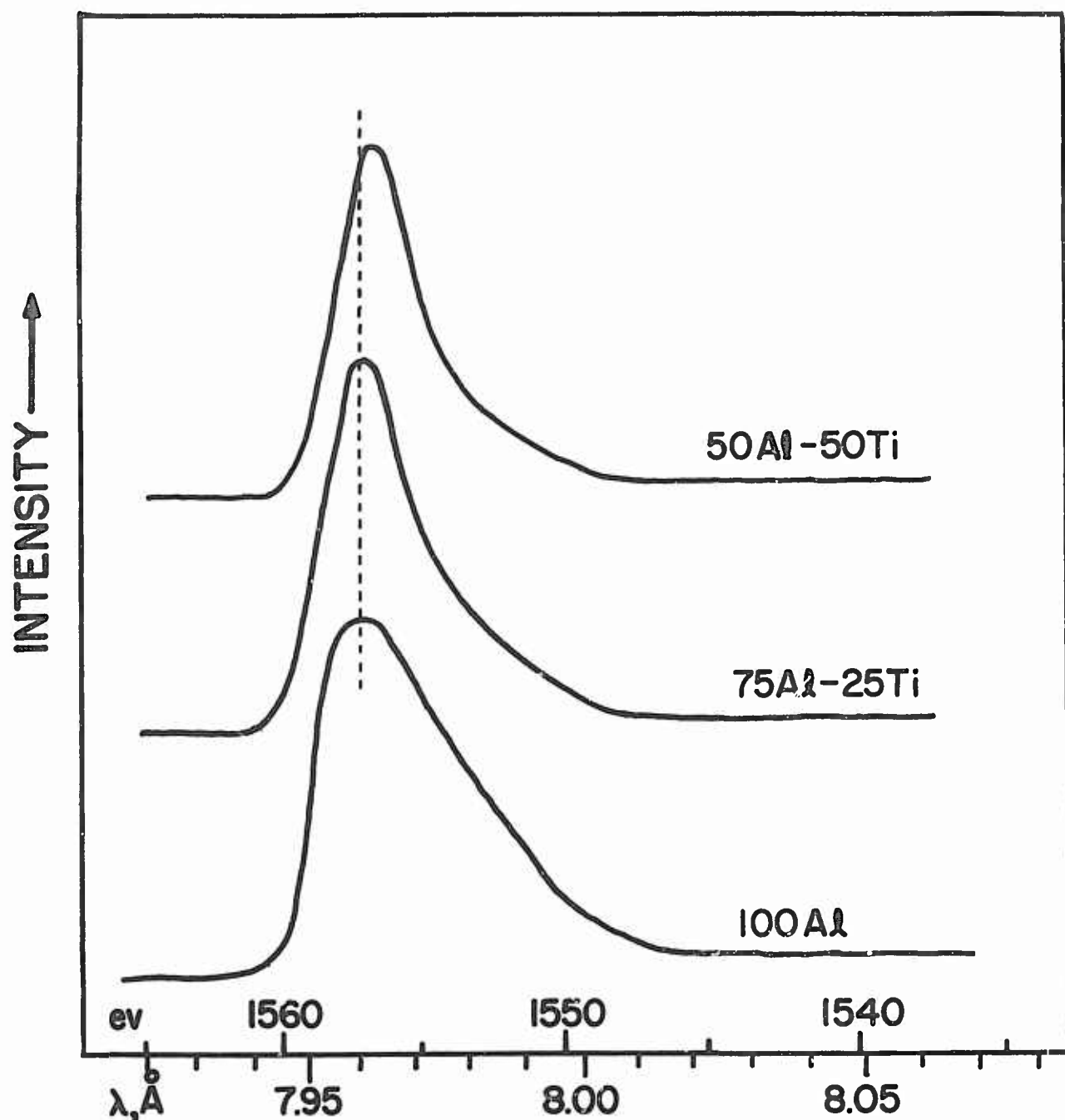


Figure 42. Aluminum K Emission Band from Some Al-Ti Alloys (EDDT Crystal)

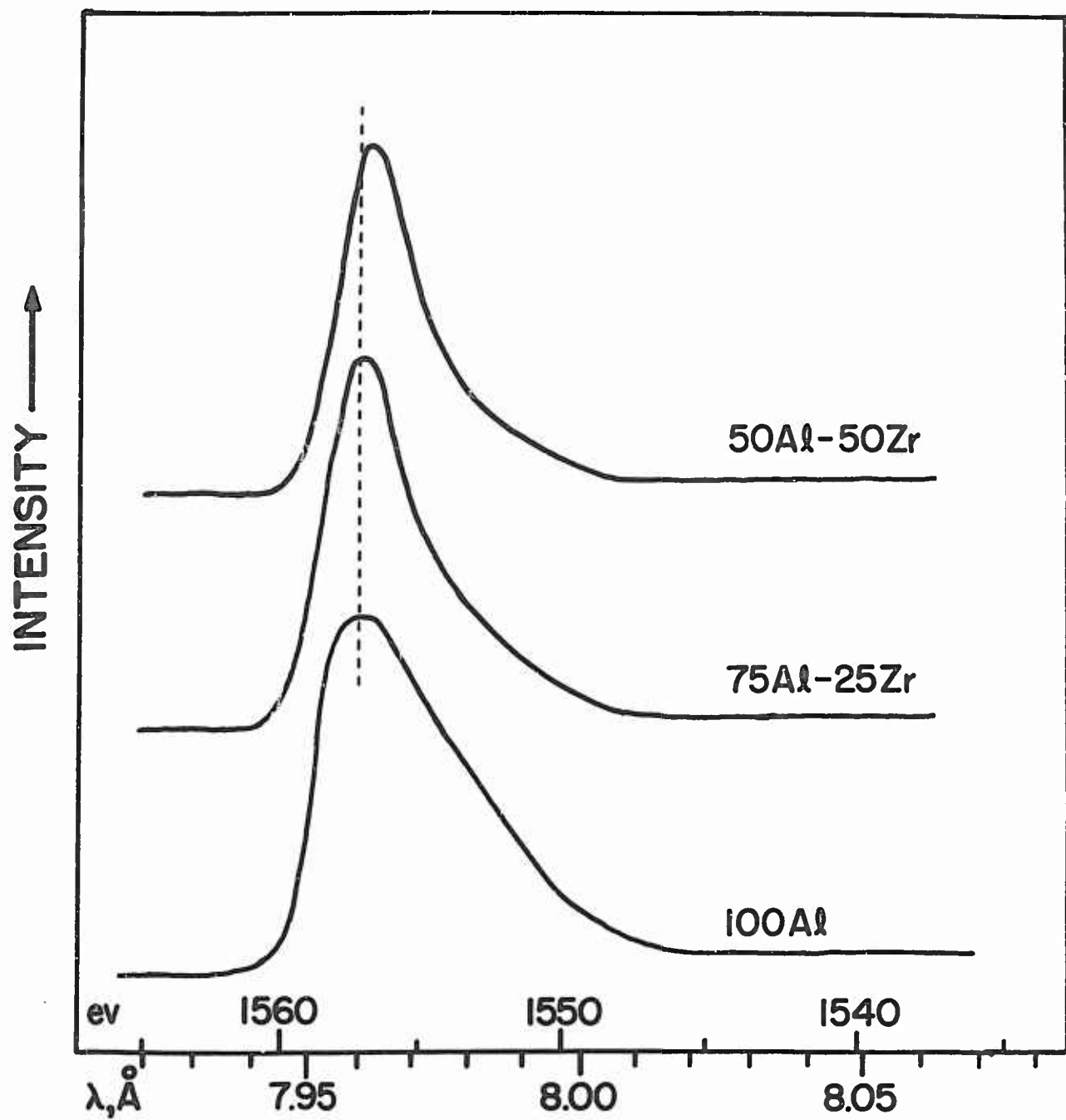


Figure 43. Aluminum K Emission Band from Some Al-Zr Alloys (EDDT Crystal)

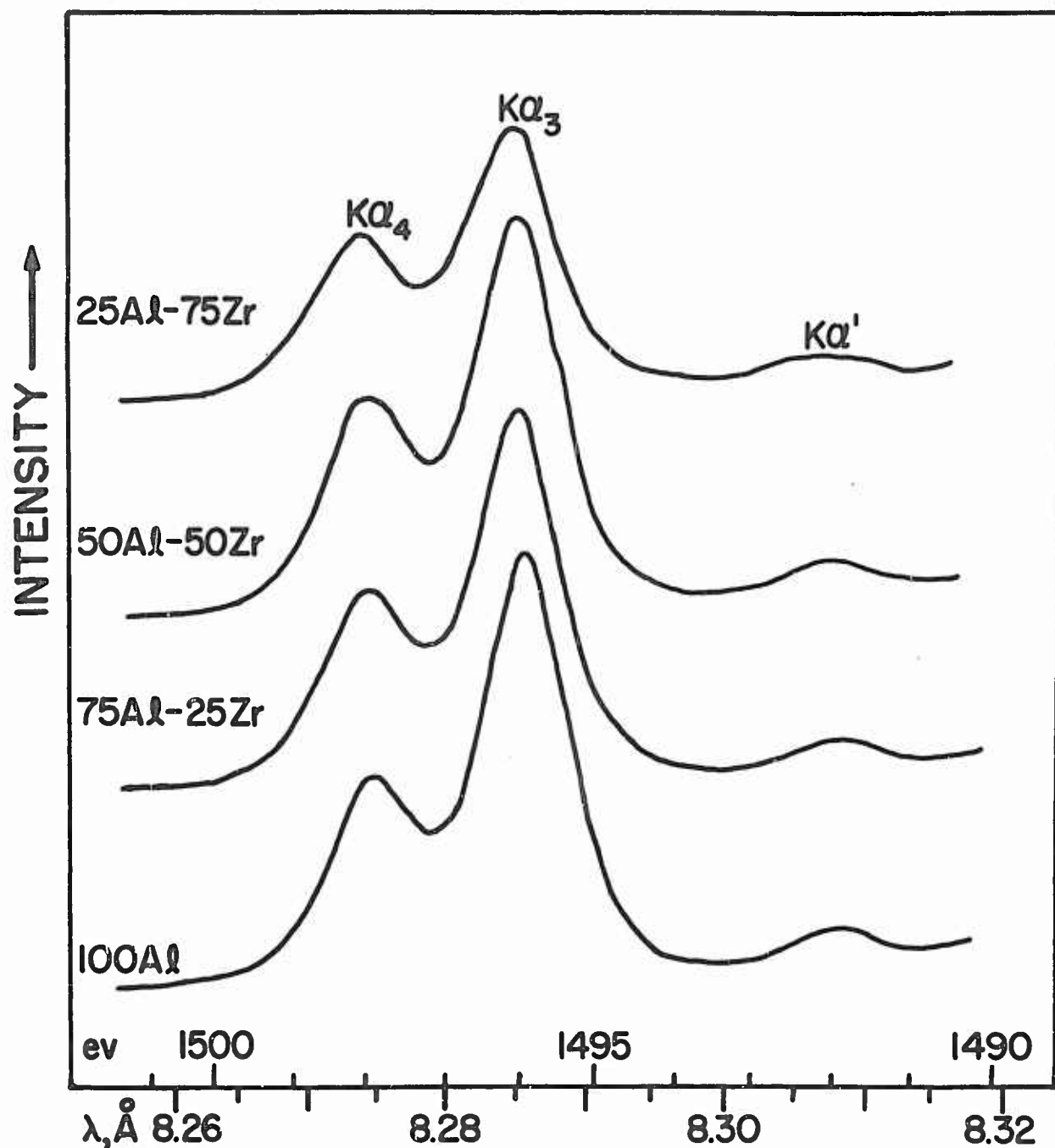


Figure 44. Aluminum $K\alpha'$, $K\alpha_3$ and $K\alpha_4$ Lines from Some Al-Zr Alloys (EDDT Crystal)

	IIA	IIIA	IVA	VA	VIA	VIIA
2		Mg	Al	P	S	
3	Ca	Ti	V	Cr	Mn	Fe
4					Co	Ni
5					Cu	Ag
6						Pt
						Au

Figure 45. Portion of the Periodic Table Showing the Elements with Which We Have Formed Aluminum Binary Compounds for X-Ray Emission Studies

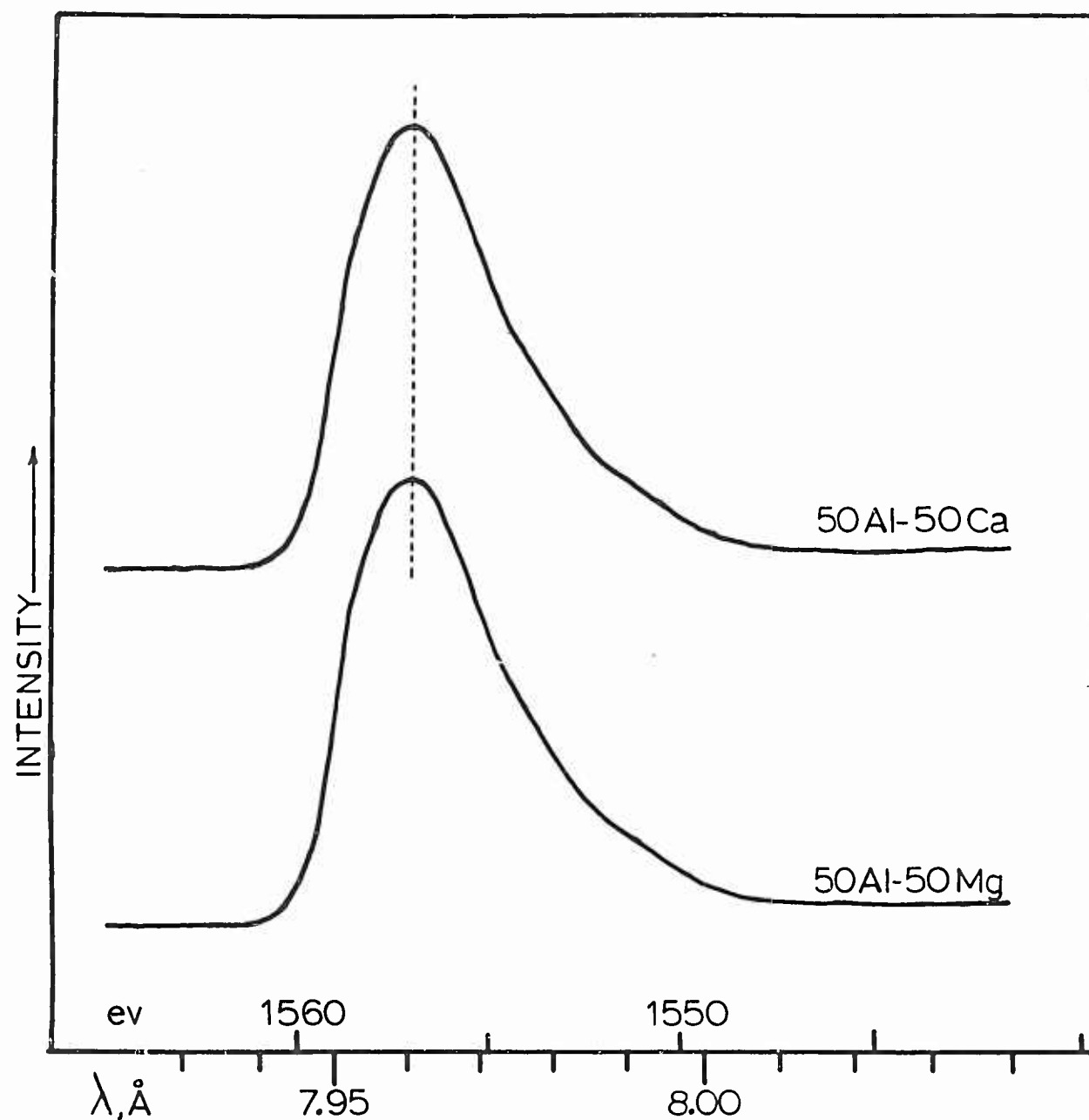


Figure 46. Aluminum K Emission Band From 1:1 Atomic Composition of Al-Mg and Al-Ca (EDDT Crystal)

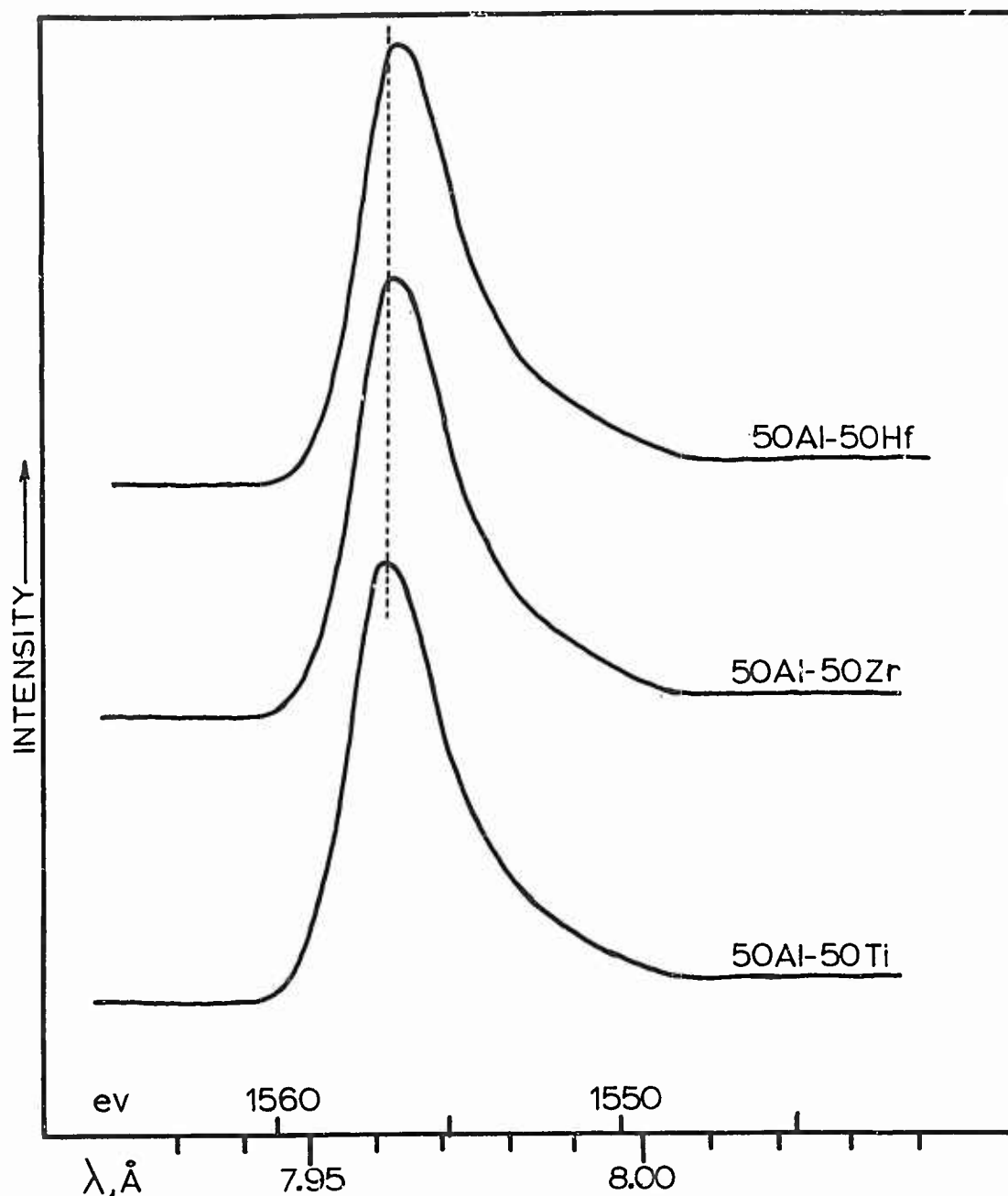


Figure 47. Aluminum K Emission Band From 1:1 Atomic Composition of Al-Ti, Al-Zr and Al-Hf (EDDT Crystal)

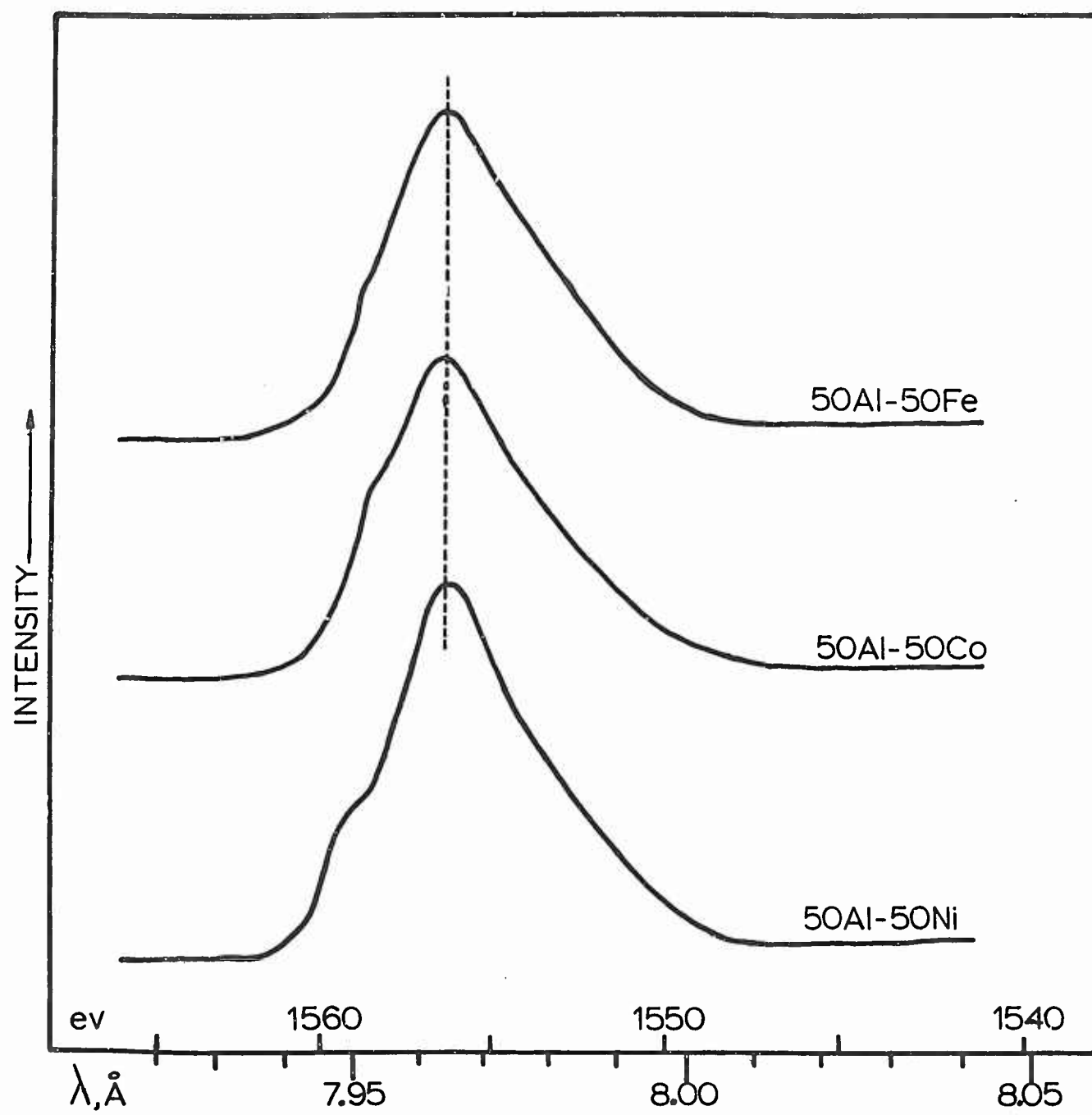


Figure 48. Aluminum K Emission Band From 1:1 Atomic Compositions of Al-Fe, Al-Co and Al-Ni (EDDT Crystal)

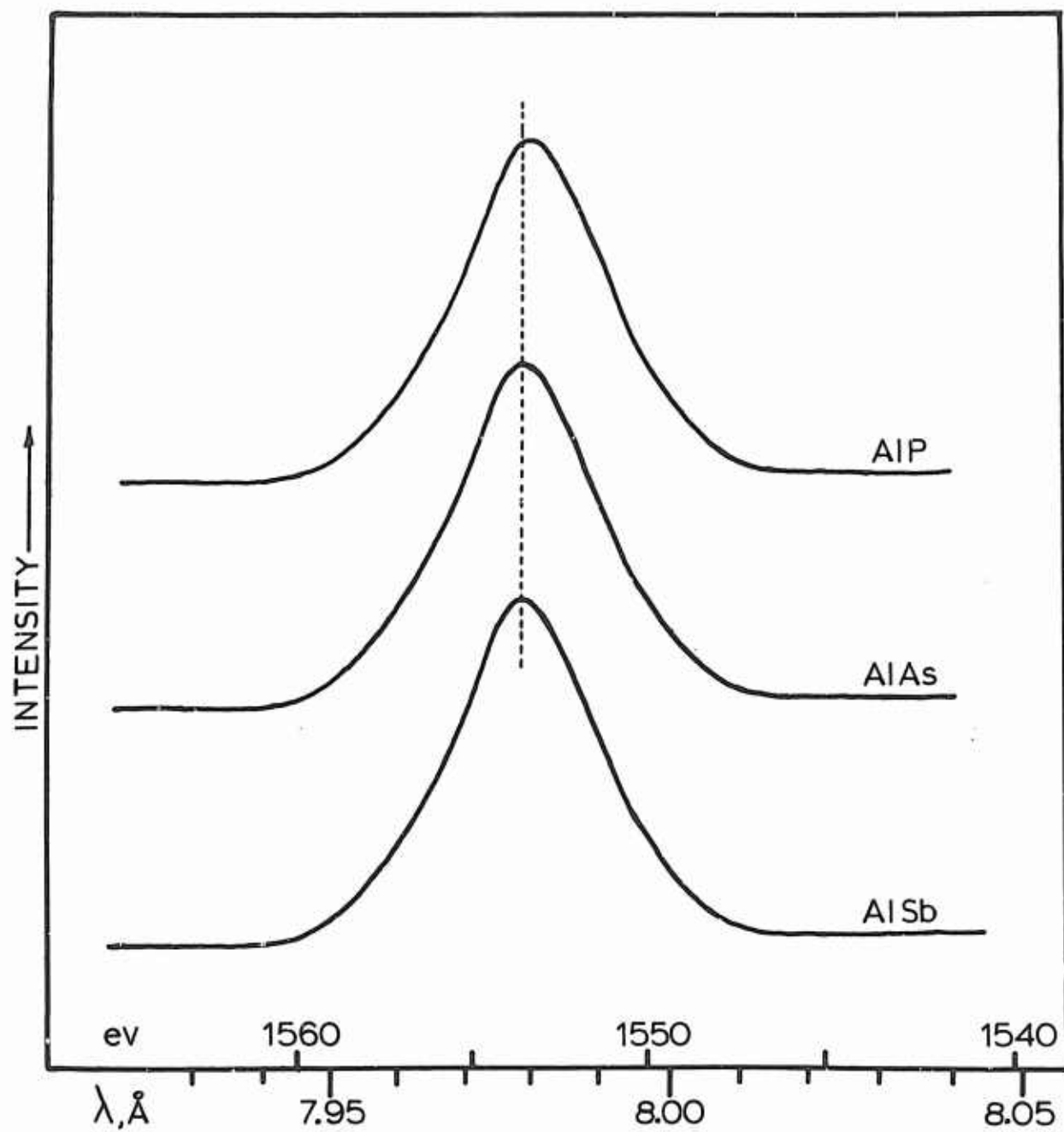


Figure 49. Aluminum K Emission Band from AlP, AlAs and AlSb (EDDT Crystal)

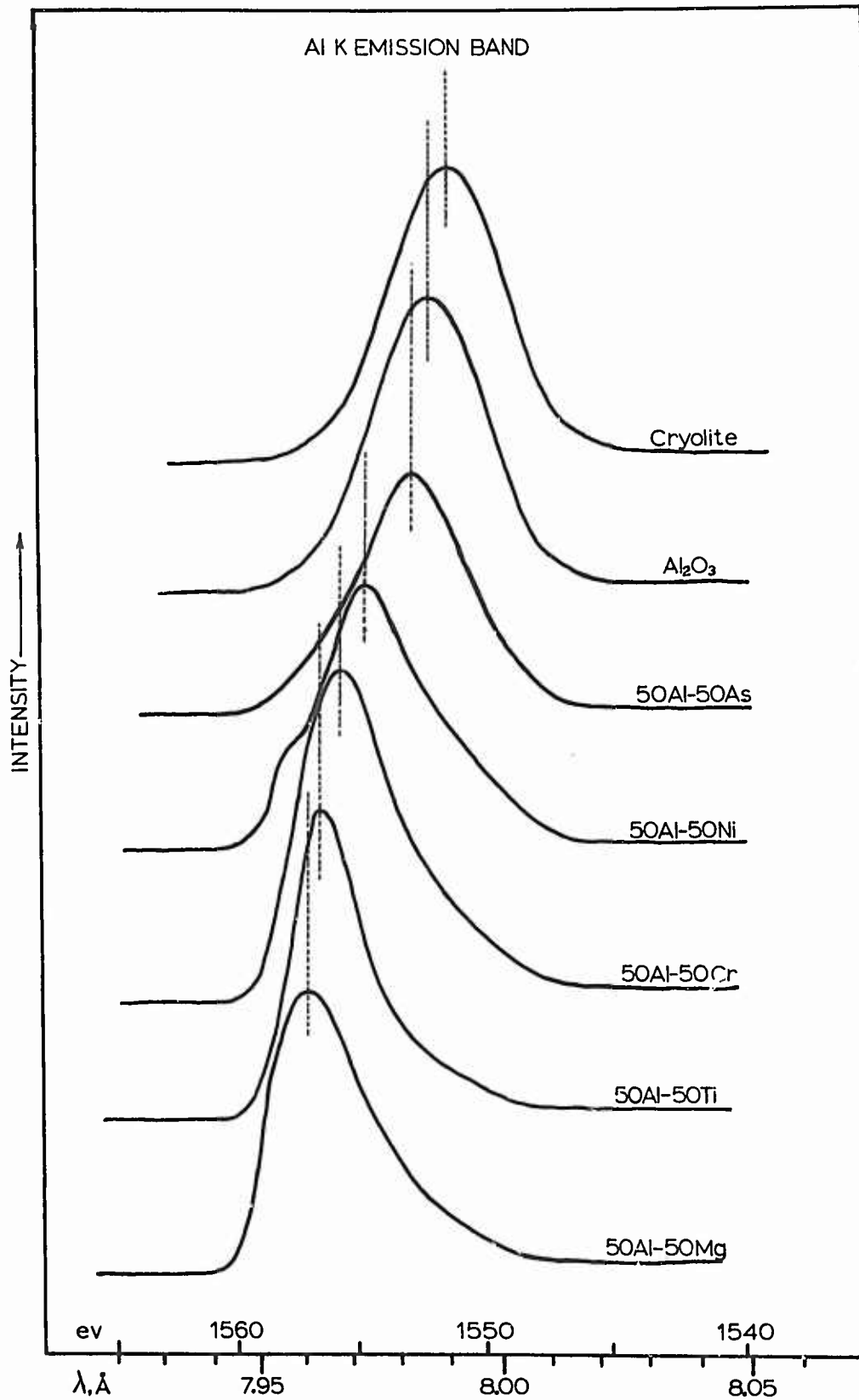


Figure 50. Aluminum K Emission Band from Various Binary Systems Where Second Components Fall Progressively from Left to Right Side of Periodic Table (EDDT Crystal)

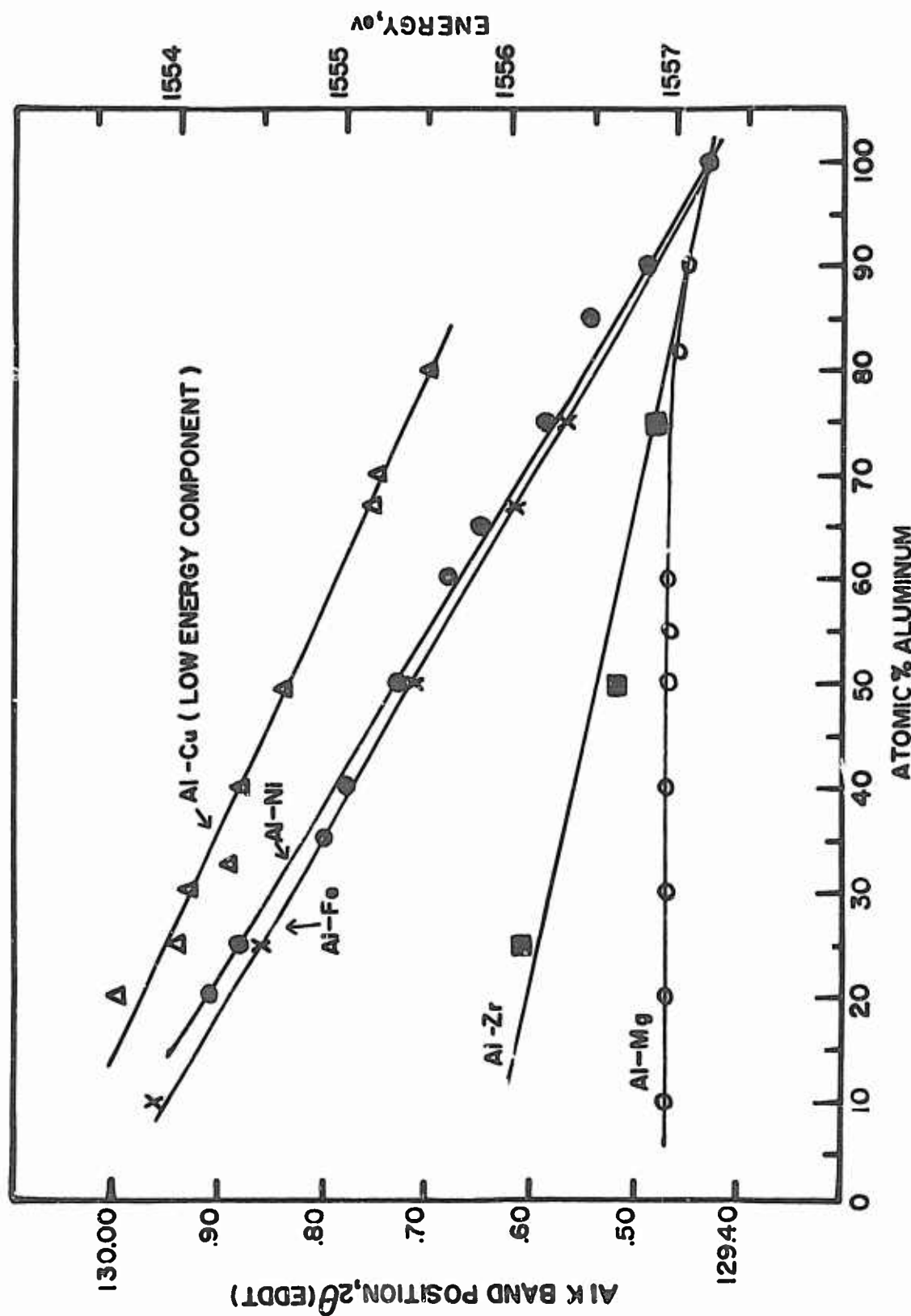


Figure 51. Relationship of Variation in Al K band Positions as a Function of Alloy Compositions for Several Binary Systems

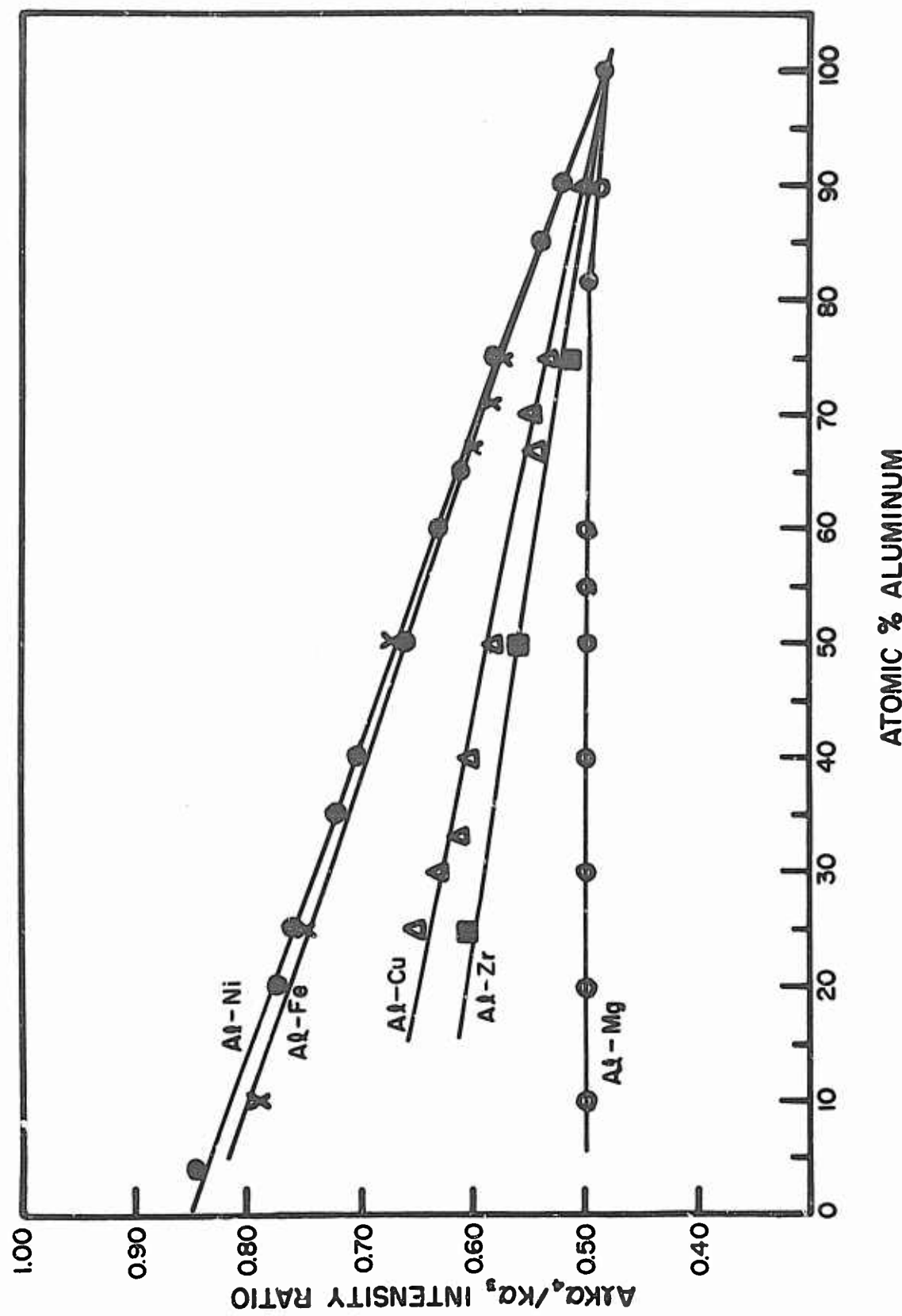


Figure 52. Relationship of Variation in Al $K\alpha_4/K\alpha_3$ Intensity Ratio as a Function of Alloy Composition for Several Binary Systems

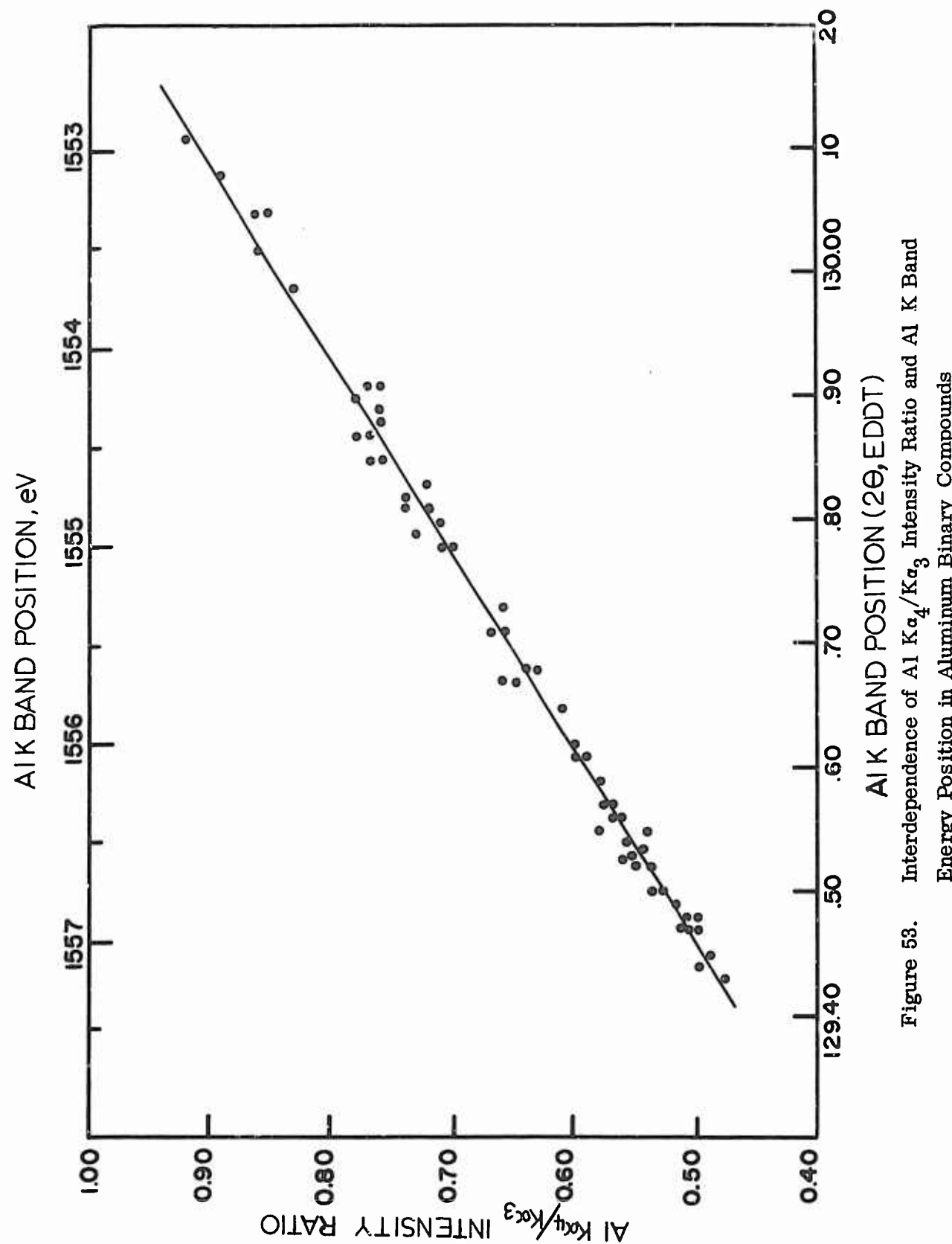


Figure 53. Interdependence of $Al\ K\alpha_4/K\alpha_3$ Intensity Ratio and Al K Band Energy Position in Aluminum Binary Compounds

UNCLASSIFIED

Security Classification

DOCUMENT CONTROL DATA - R&D

(Security classification of title, body of abstract and indexing annotation must be entered when the overall report is classified)

1. ORIGINATING ACTIVITY (Corporate author) Air Force Materials Laboratory Wright-Patterson Air Force Base, Ohio		2a. REPORT SECURITY CLASSIFICATION Unclassified
		2b. GROUP N/A
3. REPORT TITLE THE EFFECTS OF ELECTRONIC STRUCTURE AND INTERATOMIC BONDING ON THE SOFT X-RAY EMISSION SPECTRA FROM ALUMINUM BINARY SYSTEMS		
4. DESCRIPTIVE NOTES (Type of report and inclusive dates) Summary report covering work conducted between April 1965 and May 1966		
5. AUTHOR(S) (Last name, first name, initial) Fischer, David W. and Baun, William L		
6. REPORT DATE August 1966	7a. TOTAL NO. OF PAGES 96	7b. NO. OF REFS 26
8a. CONTRACT OR GRANT NO.	9a. ORIGINATOR'S REPORT NUMBER(S) AFML-TR-66-191	
b. PROJECT NO. 7367	9b. OTHER REPORT NO(S) (Any other numbers that may be assigned this report)	
c. Task No. 736702		
d.		
10. AVAILABILITY/LIMITATION NOTICES This document is subject to special export controls and each transmittal to foreign governments or foreign nationals may be made only with prior approval of AFML (MAYA), WPAFB, Ohio 45433		
11. SUPPLEMENTARY NOTES	12. SPONSORING MILITARY ACTIVITY Air Force Materials Laboratory Wright-Patterson AFB, Ohio 45433	
13. ABSTRACT <p>Aluminum, magnesium and some transition metal soft X-ray emission bands from a series of aluminum binary alloys and other aluminum binary compounds were investigated using 6 KV electron excitation and a flat crystal vacuum spectrometer. The overall shape of the valence electron emission band and its energy position as a function of alloy composition was determined. It appears from the data that the aluminum K band undergoes changes in shape and energy position which are dependent on the electronic configuration of the element with which the aluminum is chemically bonded. In the Al-Mg system the Al K band is not significantly changed for any composition. On the other hand, the group 1B metals (Cu, Ag and Au) cause the Al K band to split into two components. If the same atomic ratio of aluminum and another element is formed for each of the elements in a given period of the periodic table, it is found that the aluminum K band becomes lower in energy and somewhat more symmetrical in shape as we go from lower to higher atomic number in that period. Elements of the same sub-group appear to have virtually the same effect on the aluminum band but each different sub-group apparently has a different effect. The overall trend seems to indicate that the more electronegative the second component is, the greater effect it has on the aluminum spectrum.</p>		

DD FORM 1473
1 JAN 64**UNCLASSIFIED**
Security Classification

UNCLASSIFIED

Security Classification

14. KEY WORDS	LINK A		LINK B		LINK C	
	ROLE	WT	ROLE	WT	ROLE	WT
X-ray spectroscopy						
X-rays						
Spectra						
Aluminum						
Alloys						
INSTRUCTIONS						
1. ORIGINATING ACTIVITY: Enter the name and address of the contractor, subcontractor, grantees, Department of Defense activity or other organization (corporate author) issuing the report.	imposed by security classification, using standard statements such as:					
2a. REPORT SECURITY CLASSIFICATION: Enter the overall security classification of the report. Indicate whether "Restricted Data" is included. Marking is to be in accordance with appropriate security regulations.	<p>(1) "Qualified requesters may obtain copies of this report from DDC."</p> <p>(2) "Foreign announcement and dissemination of this report by DDC is not authorized."</p> <p>(3) "U. S. Government agencies may obtain copies of this report directly from DDC. Other qualified DDC users shall request through _____."</p> <p>(4) "U. S. military agencies may obtain copies of this report directly from DDC. Other qualified users shall request through _____."</p> <p>(5) "All distribution of this report is controlled. Qualified DDC users shall request through _____."</p>					
2b. GROUP: Automatic downgrading is specified in DoD Directive 5200.10 and Armed Forces Industrial Manual. Enter the group number. Also, when applicable, show that optional markings have been used for Group 3 and Group 4 as authorized.						
3. REPORT TITLE: Enter the complete report title in all capital letters. Titles in all cases should be unclassified. If a meaningful title cannot be selected without classification, show title classification in all capitals in parenthesis immediately following the title.	If the report has been furnished to the Office of Technical Services, Department of Commerce, for sale to the public, indicate this fact and enter the price, if known.					
4. DESCRIPTIVE NOTES: If appropriate, enter the type of report, e.g., interim, progress, summary, annual, or final. Give the inclusive dates when a specific reporting period is covered.	11. SUPPLEMENTARY NOTES: Use for additional explanatory notes.					
5. AUTHOR(S): Enter the name(s) of author(s) as shown on or in the report. Enter last name, first name, middle initial. If military, show rank and branch of service. The name of the principal author is an absolute minimum requirement.	12. SPONSORING MILITARY ACTIVITY: Enter the name of the departmental project office or laboratory sponsoring (<i>paying for</i>) the research and development. Include address.					
6. REPORT DATE: Enter the date of the report as day, month, year, or month, year. If more than one date appears on the report, use date of publication.	13. ABSTRACT: Enter an abstract giving a brief and factual summary of the document indicative of the report, even though it may also appear elsewhere in the body of the technical report. If additional space is required, a continuation sheet shall be attached.					
7a. TOTAL NUMBER OF PAGES: The total page count should follow normal pagination procedures, i.e., enter the number of pages containing information.	It is highly desirable that the abstract of classified reports be unclassified. Each paragraph of the abstract shall end with an indication of the military security classification of the information in the paragraph, represented as (TS), (S), (C), or (U).					
7b. NUMBER OF REFERENCES: Enter the total number of references cited in the report.	There is no limitation on the length of the abstract. However, the suggested length is from 150 to 225 words.					
8a. CONTRACT OR GRANT NUMBER: If appropriate, enter the applicable number of the contract or grant under which the report was written.	14. KEY WORDS: Key words are technically meaningful terms or short phrases that characterize a report and may be used as index entries for cataloging the report. Key words must be selected so that no security classification is required. Identifiers, such as equipment model designation, trade name, military project code name, geographic location, may be used as key words but will be followed by an indication of technical context. The assignment of links, rules, and weights is optional.					
8b, 8c, & 8d. PROJECT NUMBER: Enter the appropriate military department identification, such as project number, subproject number, system numbers, task number, etc.						
9a. ORIGINATOR'S REPORT NUMBER(S): Enter the official report number by which the document will be identified and controlled by the originating activity. This number must be unique to this report.						
9b. OTHER REPORT NUMBER(S): If the report has been assigned any other report numbers (<i>either by the originator or by the sponsor</i>), also enter this number(s).						
10. AVAILABILITY/LIMITATION NOTICES: Enter any limitations on further dissemination of the report, other than those						

UNCLASSIFIED

Security Classification